

UNIVERSITY OF BELGRADE
FACULTY OF BIOLOGY

Amal Abdussalam Ali A. Hmaid

**THE ROLE OF NO-SYNTHETIC PATHWAY IN
STRUCTURAL REMODELING OF RAT
MYOCARDIUM**

Doctoral dissertation

Belgrade, 2016.

UNIVERZITET U BEOGRADU
BIOLOŠKI FAKULTET

Amal Abdussalam Ali A. Hmaid

**ULOGA NO-SINTAZNOG PUTA U
STRUKTURNOM REMODELIRANJU MIOKARDA
PACOVA**

Doktorska disertacija

Beograd, 2016.

COMMITTEE MEMBERS:

dr Aleksandra Korać, Full Professor, supervisor
University of Belgrade-Faculty of Biology

dr Aleksandra Janković, Research Fellow, supervisor,
University of Belgrade-
Institute for biological research „Siniša Stanković“,

dr Bato Korać, Associate Professor
University of Belgrade-Faculty of Biology

dr Milica Markelić, Assistant Professor
University of Belgrade-Faculty of Biology

dr Milica Labudović-Borović, Assistant Professor
University of Belgrade-Faculty of Medicine

Belgrade, _____

ACKNOWLEDGEMENTS

The experimental work of the doctoral dissertation was done at the Institute of Zoology, Faculty of Biology, University of Belgrade, in cooperation with the Centre for Electron Microscopy, Faculty of Biology, University of Belgrade and at the Institute for biological research "Siniša Stanković", University of Belgrade within the project: "White and/or brown: the importance of adipose tissue in maintaining the overall redox dependent metabolic control of physiological and metabolic adaptations" #173055, of the Ministry of Education, Science and Technological Development of the Republic of Serbia. The author was financially supported by the Libyan Ministry of Higher Education and Scientific Research.

I thank my country Libya on this scholarship and the full support.

*My deepest gratitude is due to each of the members of the faculty and especially thank to **prof. dr Aleksandra Korać** for her valuable supervision, guidance and constructive advice throughout the present study.*

*My sincere gratefulness and appreciation are also extended to **dr Milica Markelić** for her guidance and continuous efforts done throughout the present.*

*Also my sincere thanks to **dr Aleksandra Janković**.*

*I am thankful to **prof. dr Bato Korać**.*

*With all the thanks and respect to **prof. dr Željko Tomanović**, Dean of Faculty of Biology.*

*Finally my deepest thanks are to my husband **Abdullah Abdulmajied Saghier** for supporting and encouragement during work on this dissertation and my **father Abdussalam**, **mother Salema** from them I have learnt the great deals of life; also I am grateful to my sister **Amany**.*

Researcher

Amal Abdussalam Ali A. Hmaid

THE ROLE OF NO-SYNTHETIC PATHWAY IN STRUCTURAL REMODELING OF RAT MYOCARDIUM

ABSTRACT

Nitric oxide (NO), endogenously synthesized by nitric oxide synthases (NOSs), generally acts to fine tune and optimise cardiac pump function. Several experimental studies have shown that low (submicromolar) doses of NO exert small positive inotropic effects, while at higher, but still physiological levels, NO enhances cardiomyocyte relaxation and diastolic function. It has been known that reduced NO bioavailability plays an important role in the development of heart failure, but the mechanisms are still uncovered. This thesis deals with structural remodeling of right ventricle (RV) myocardium of rats, induced by chronic modulation of NO-producing system and cold acclimation. In order to examine the possible effects of NO on myocardial structure and molecular basis of its remodeling at room temperature (22 ± 1 °C) or cold (4 ± 1 °C) acclimation, adult male rats (Mill Hill hybrid hooded, 2-month-old), were treated with L-arginine or N^ω-nitro-L-arginine methyl ester (L-NAME) for 45 days, respectively.

Our results demonstrated that cold acclimation *per se* does not significantly alter the volume densities of myocardial tissue components, but leads to a trend in cardiomyocyte hypertrophy followed by a downward trend in capillarity. Also, cold-acclimated control animals showed a significant decrease of proliferating cell nuclear antigen expression in comparison with room temperature-kept control animals. In all, these results do not indicate the cold-induced RV hypertrophy, at least at histological level. Results demonstrated that the structural alterations observed after the L-arginine treatment corresponded to physiologic cardiac hypertrophy, since no pathological changes in the myocardial structure (increased collagen deposition and/or myofibril distortion) after chronic L-arginine treatment were seen. Namely, L-arginine treatment in RT-acclimated rats led to cardiomyocyte hypertrophy which was followed by a simultaneous increase in capillarity and interstitial connective tissue in the myocardium, maintaining the relative ratio of tissue components unaltered. The most prominent effect of L-NAME on rat myocardia observed was fibrosis, demonstrated as

an increase in connective tissue volume density accompanied by increased collagen abundance in the interstitium. This effect was followed by cardiomyocyte hypertrophy, despite a decrease in their volume density. These alterations were observed in both L-NAME-treated groups, with additional enhancement of interstitial fibrosis after cold acclimation. The reduced size of cardiomyocytes' nuclei was detected in the cold-acclimated control group, and in all L-arginine- and L-NAME-treated groups. This nuclear alteration, as well as the increased occurrence of cardiomyocytes' binucleation seems to play an important role in the cardiomyocytes and myocardial hypertrophy. Described nuclear changes were the most evident after the chronic treatment with L-NAME. According to our evidence, this is the first demonstration of nuclear alterations in cardiomyocytes after chronic L-NAME treatment which indicate their role in the cardiomyocyte hypertrophy. Besides nuclear alterations, significant ultrastructural changes were observed in the cardiomyocytes mitochondrial population in all examined groups. Namely, decreased profile surface of all mitochondrial subpopulations was observed in L-arginine room temperature-acclimated group, while L-NAME *per se* did not affect mitochondrial size, compared to untreated group. Cold acclimation decreased profile size of cardiomyocytic perinuclear and intersarcomeral mitochondrial subpopulations. Cold-acclimated L-arginine-treated animals had increased mitochondrial profile size, compared to both, untreated cold-acclimated and L-arginine-treated room temperature-acclimated group. Also, L-NAME-treated animals acclimated to cold had increased profile surface of mitochondria in perinuclear and subsarcolemal region, while in intersarcolemal region mitochondrial profiles decreased, compared to L-NAME-treated room temperature-acclimated group. Regarding the cardiomyocytes synapses, protein level of connexin 43 declined after L-arginine and, to a lesser extent, after L-NAME treatment at room temperature. Neither the cold acclimation *per se*, nor drug treatments during cold acclimation affected the connexin 43 expression level in the RV of rats, indicating that there were no profound changes in cardiac electric coupling during the structural remodeling, at least at the level of gap junctions. To reveal the involvement of endogenous NO-synthesis in the observed structural RV remodeling the expression levels and the localisation of NOSs were examined. NO precursor, L-arginine, upregulates eNOS expression in rats myocardium, thus indicating the primary effects

of eNOS in the NO production, at least in the RV of rats. On the other hand, L-NAME, a potent non-selective inhibitor of NOSs acts also at the level of translation on constitutive NOS isoforms in RV, by decreasing the expression of nNOS and by maintaining the expression of eNOS at the control level. Since herein demonstrated cold-induced upregulation of eNOS expression and downregulation of nNOS expression are not shown to induce any structural signs of RV hypertrophy in rats, we can assume a protective role of eNOS during increased cardiac afterload.

In conclusion, chronic L-arginine supplementation induces low level RV hypertrophy in RT-acclimated rats and significantly augments ventricular hypertrophy in cold-acclimated animals. L-arginine-induced ventricular hypertrophy could be considered physiological, since no signs of myocardial fibrosis were observed. In contrast, chronic treatment with L-NAME, an inhibitor of NOSs, caused pathological right ventricular hypertrophy with signs of myocardial fibrosis, demonstrating the importance of NO depletion in the development of cardiovascular disease.

KEYWORDS: Nitric oxide, L-NAME, L-arginine, NOSs, cardiomyocytes hypertrophy

SPECIFIC FIELD: Biology

SPECIAL TOPICS: Cell and Tissue Biology

UDC NUMBER: 546.172.6:[616.12-007.61+616.123](043.3)

ULOGA NO-SINTAZNOG PUTA U STRUKTURNOM REMODELIRANJU MIOKARDA PACOVA

REZIME

Azot oksid (NO), endogeno sintetisan NO sintazama (NOS, *engl.* NO synthases) ima važnu ulogu u optimizaciji adaptivnog odgovora srca. Poznato je da NO pri fiziološkim koncentracijama ima pozitivno inotropno dejstvo, kao i da je hronično redukovana fiziološki nivo NO spregnut sa izmenjenom funkcijom srca i da stoga može doprineti razvoju srčane insuficijencije.

Polazeći od ovih osnova, cilj teze je bio da razjasni mehanizme remodeliranja miokarda desne komore srca pacova u odgovoru na nisku temperaturu, kao i da se ispita uloga NO, modulacijom NO-sintaznog puta. U tu svrhu pacovi *Mill Hill* soja, starosti 2 meseca izlagani su niskoj temperaturi (4 ± 1 °C) u vremenu od 45 dana i poređeni sa životinjama aklimiranim na sobnu temperaturu (22 ± 1 °C). Obe grupe životinja, aklimirane na sobnu i nisku temperaturu dodatno su podeljene u tri podgrupe: 1. netretirane; 2. životinje tretirane supstratom NO sintaza NOS - L-arginin•HCl (2.25%) u pijaćoj vodi; 3. životinje pojene inhibitorom NOSs, L-NAME•HCl (0.01%).

U poređenju sa kontrolnim, životinje aklimirane na hladnoću imaju značajno nižu ekspresiju transkripcionog faktora proliferacije ćelija. Mada se beleži trend hipertrofije kardiomiocita i smanjenje kapilarnosti, volumenska gustina komponenti miokarda desne komore se ne menja kod pacova aklimiranih na hladnoću, u poređenju sa životinjama aklimiranim na sobnu temperaturu. Zajedno, rezultati ne pokazuju značajnu hipertrofiju desne komore prouzrokovane hladnoćom, barem ne na histološkom nivou. Rezultati pokazuju da strukturne promene nakon L-arginin tretmana odgovaraju fiziološkoj srčanoj hipertrofiji. Naime, L-arginin tretman pacova aklimiranih na sobnu temperaturu, u poređenju sa kontrolama vodi hipertrofiji kardiomiocita, praćeno istovremenim povećanjem kapilarnosti i vezivnog tkiva. Međutim, relativni odnos komponenti miokarda, količina kolagena i strukturna organizacija miofibrila se ne menja nakon L-arginin tretmana, u poređenju sa kontrolnim životinjama.

Sa druge strane, inhibicija enzimske sinteze NO L-NAME tretmanom rezultira pojavom fibroze, odnosno povećanjem volumenske gustine vezivnog tkiva uz povećano deponovanje kolagena u intersticijumu. Pored toga, uprkos smanjenju volumenske gustine, očigledna je hipertofija kardiomiocita. Opisane promene su prisutne u L-NAME-tretiranim grupama, na sobnoj i niskoj temperaturi. U okviru L-NAME-tretiranih grupa, fibrozna je izraženija u grupi pacova aklimiranih na hladnoću. Smanjena veličina nukleusa kardiomiocita je detektovana u netretiranoj grupi pacova aklimiranih na hladnoću, kao i nakon L-arginin- i L-NAME- tretmana. Rezultati teze ukazuju da povećanje binuklearnosti, zajedno sa opisanim smanjenjem veličine nukleusa imaju bitnu ulogu u hipertrofiji kardiomiocita, kao i samog miokardijuma. Značajno je da su opisane nukleusne promene najizrazitije u L-NAME-tretiranim grupama. Podaci koji se odnose na nukleusne promene i njihovu ulogu u hipertrofiji kardiomiocita nakon hroničnog L-NAME tretmana po prvi put su istaknuti u ovoj tezi, te su kao takvi jedinstveni u literaturi. Osim nukleusnih, značajne ultrastrukturne promene uočene su na nivou mitohondrijalnih populacija u svim ispitivanim grupama; u poređenju sa netretiranom grupom, smanjen površinski profil svih mitohondrijalnih subpopulacija je zabeležen u L-arginin-tretiranoj grupi pacova aklimiranih na sobnu temperaturu. Takođe, u poređenju sa kontrolom, smanjen površinski profil perinukleusnih i intersarkomeralnih mitohondrijalnih subpopulacija je zabeležen u grupi životinja aklimiranih na hladnoću. Međutim, L-arginin-tretirana grupa pacova aklimirana na hladnoću je imala veći površinski profil mitohondrija u poređenju sa netretiranom grupom sa hladnoće, kao i u poređenju sa L-arginin-tretiranom grupom koja je boravila na sobnoj temperaturi. Slično, povećan površinski profil mitohondrija u perinukleusnom i subsarkolemalnom kompartmentu, odnosno smanjen u intersarkomeralnom regionu zabeležen je u L-NAME-tretiranoj grupi životinja aklimiranih na hladnoću, u poređenju sa istim tretmanom na sobnoj temperaturi. Pored toga, ispitivanje ekspresije koneksina 43, jednog od koneksina električnih sinapsi interkalarnih diskova, je pokazalo da se ekspresija koneksina 43 značajno smanjuje nakon primenjenih tretmana u poređenju sa netretiranom grupom na sobnoj temperaturi. Sa druge strane, u miokardu pacova aklimiranih na hladnoću nema značajnih promena u ekspresiji koneksina 43 u poređenju sa kontrolnim pacovima, kao ni nakon primenjenih tretmana na hladnoći, u poređenju sa

netretiranom grupom sa hladnoće. Na osnovu toga se može zaključiti da nema izrazitih promena u kapacitetu za prenos akcionog potencijala u miokardu desne komore, barem ne kod grupa pacova aklimiranih na hladnoću. U cilju pojašnjavanja uloge endogene sinteze NO u pokazanom strukturnom remodeliranju miokarda desne komore srca pacova ispitivane su ekspresija i lokalizacija NOS. Rezultati pokazuju da L-arginin povećava ekspresiju endotelijalne NOS (eNOS), ukazujući da ova izoforma posreduje u produkciji NO u desnoj komori srca pacova. Sa druge strane, L-NAME, pored toga što deluje kao nespecifični inhibitor NOS, deluje i na translacioni nivo konstitutivnih izoformi, smanjujući proteinsku ekspresiju nNOS i održavajući nivo eNOS na kontrolnom nivou. Obzirom da aklimacija na hladnoću povećava eNOS, a suprimira ekspresiju nNOS, može se zaključiti da eNOS ima protektivnu ulogu u srčanom *afterload*-u i posledičnom razvoju hipertrofije desne komore srca.

Na osnovu dobijenih rezultata može se zaključiti da hronični L-arginin tretman indukuje umerenu hipertofiju desne komore srca pacova na sobnoj temperaturi i značajno je povećava u uslovima hronične stimulacije na hladnoći. L-argininom-indukovana ventrikularna hipertofija se može smatrati fiziološkom, obzirom na odsustvo fibroze. Sa druge strane, hronična inhibicija NOS, posredovana L-NAME je asocirana sa patološkom hipertrofijom miokarda desne komore sa karakterističnim znacima fibroze, ističući značaj deplecije NO u razvoju kardiovaskularne bolesti.

Ključne reči: Azot oksid, L-NAME, L-arginin, NOS, hipertofija kardiomiocita

NAUČNA OBLAST: Biologija

UŽA NAUČNA OBLAST: Biologija ćelija i tkiva

UDK BROJ: 546.172.6:[616.12-007.61+616.123](043.3)

Table of Contents

1. INTRODUCTION.....	1
1.1 <i>Myocardial structure and function</i>	1
1.1.1 Ventricular structure and function	1
1.1.2 Cardiomyocyte structure and function	4
1.1.3 Cardiac hypertrophy	6
1.1.4 Cellular and molecular mechanisms of cardiomyopathy	7
1.2 <i>Nitric oxide (NO)-producing system</i>	9
1.2.1 Physiological functions of NO in the heart	9
1.2.2 Nitric oxide synthase (NOS) isoforms in the heart	12
1.2.3 NOS system in heart during pathological conditions	13
1.3 <i>Effects of cold on heart</i>	13
1.4 <i>Right heart ventricle in health and disease – plasticity and remodeling</i>	14
2. AIMS.....	17
3. MATERIAL AND METHODS.....	19
3.1 <i>Experimental design</i>	19
3.2 <i>Light microscopy</i>	19
3.2.1 AZAN trichrome staining	19
3.2.2 Periodic Acid Schiff (PAS) staining	20
3.2.3 Immunohistochemistry	20
3.2.4 Immunofluorescence	21
3.2.5 Propidium iodide staining	21
3.3 <i>Transmission electron microscopy</i>	21
3.3.1 Toluidine blue staining	22
3.4 <i>Morphometric and stereological analyses</i>	22
3.4.1 Volume densities of cardiomyocytes, blood vessels and connective tissue in the myocardium	22
3.4.2 Cardiomyocytes diameters	23

3.4.3 Cardiomyocytes nuclear profiles sizes	23
3.4.4 Mitochondrial profiles sizes	23
3.5 Western blot	24
3.6 Statistical analysis	24
4. RESULTS.....	26
4.1 Myocardial hypertrophy	26
4.1.1 Volume densities of cardiomyocytes, blood vessels and connective tissue	26
4.1.2 Structural alterations of myocardium	27
4.1.3 Cardiomyocyte diameter	29
4.1.4 Ratio of binucleated cardiomyocytes	32
4.1.5 Microscopic analyses of cardiomyocytes nuclei	34
4.1.6 Proliferating cell nuclear antigen (PCNA)	36
4.1.7 Propidium iodide staining – apoptosis marker	39
4.2 Remodeling of capillary network	42
4.2.1 Expression of vascular and angiogenic markers	42
4.2.1.1 Vascular endothelial growth factor (VEGF)	42
4.2.1.2 Endoglin (CD105)	44
4.2.2 Microscopic analysis of capillary network	45
4.3 Expression of connexin 43 (Cnx43) – cardiac electric coupling marker	47
4.4 NO-synthase system	48
4.4.1 Neuronal nitric oxide synthase (nNOS)	48
4.4.2 Endothelial nitric oxide synthase (eNOS)	51
4.4.3 Inducible nitric oxide synthase (iNOS)	53
4.4.4 Heme oxygenase-1 (HO-1)	55
4.4.5 Heme oxygenase-2 (HO-2)	57
4.5 Mitochondrial remodeling	58
4.5.1 Mitochondrial subpopulations of cardiomyocytes	58

4.5.2 Mitochondrial fusion markers – mitofusin 1 (Mfn1) and 2 (Mfn2)	58
4.5.3 Mitochondrial division marker– mitofilin	62
4.5.4 Uncoupling protein 2 (UCP2)	64
4.6 <i>Sarcoplasmic reticulum remodeling</i>	65
4.7 <i>Ultrastructural alterations of right ventricle myocardium</i>	68
5. DISCUSSION.....	71
5.1 <i>Structural remodeling – cardiomyocyte hypertrophy, tissue proliferation and apoptosis</i>	71
5.2 <i>Cardiomyocyte nuclear changes and binucleation</i>	77
5.3 <i>Capillary recruitment</i>	79
5.4 <i>Molecular basis of structural remodeling of RV myocardium –NOSs</i>	80
6. CONCLUSIONS.....	85
7. REFERENCES.....	88
Biography	104

1. INTRODUCTION

1.1 Myocardial structure and function

1.1.1 Ventricular structure and function

The heart is a contractile organ which contains four muscular chambers, two on the left and two on the right side, associated with systemic and pulmonary blood circuit, respectively. The right atrium receives blood from the systemic circuit and passes it to the right ventricle (RV), which pumps blood into the pulmonary circuit. The left atrium collects blood from the pulmonary circuit and empties it into the left ventricle (LV), which then contracts, ejecting blood into the systemic circuit. One heartbeat consists of atrial contraction and relaxation followed by ventricular contraction and relaxation; these eject equal volumes of blood into the pulmonary and systemic circuits (**Mescher, 2013**).

The heart anatomy reflects its specific function—as a blood pump. The role of both ventricles is to propel blood forward in the circulation. To enable this mechanical role, ventricular function is intimately related to ventricular structure. However, the two ventricles differ (**Sheehan and Redington, 2008**). Morphologically, the RV is distinguished from the left by having coarse trabeculae, a moderator band, and a lack of fibrous continuity between its inlet and outflow valves. In the RV the pulmonary valve sits on a freestanding muscular infundibulum and the crista supraventricularis courses between it and the tricuspid valve to aid free wall contraction toward the interventricular septum. Because it normally operates at a lower pressure than the LV, the RV has a thinner wall. Its septal contour is indented by the dominant LV producing a shape that is difficult to model geometrically (Figure 1).

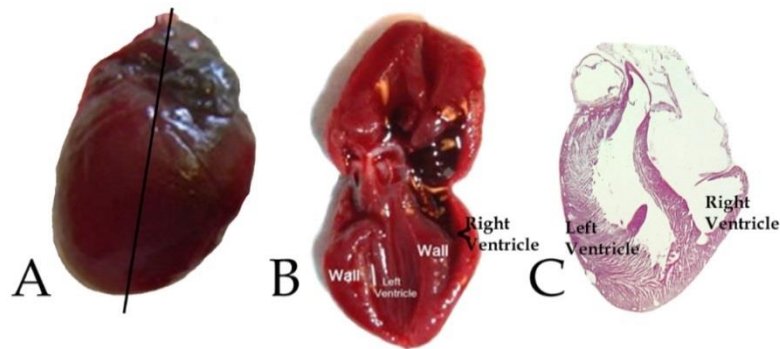


Figure 1. The anatomy of rat heart. A) *Toto* preparation and B) section trough line marked on A. C) Hematoxylin and eosin stained paraffin section of whole heart.

Adopted from: <http://www.anatomyatlases.org/MicroscopicAnatomy/Section08/Plate08148.shtml>

The wall of RV consists of three layers: endocardium, myocardium, and epicardium (Figure 2).

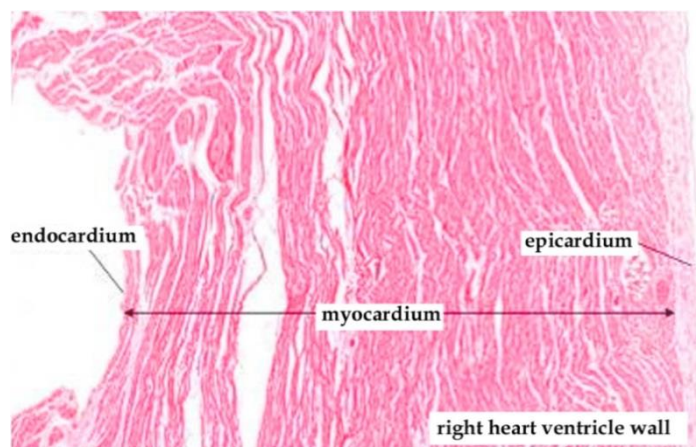


Figure 2. Histological organization of right heart ventricle wall. Paraffin section, hematoxylin and eosin staining. Mag. x5, orig.

The outer epicardium is a relatively thin layer of tissue that consists of a covering mesothelium and a thin underlying layer of loose connective tissue that merges into the connective tissue sheaths of the myocardium. The loose connective tissue supports the blood vessels and nerves that supply the heart.

Myocardium, the main part of RV wall, is the largest of the three layers, it consists of a continuous wrapping of cardiac muscle forming concentric-arranged layers of muscle tissue around the chambers. The ventricular

myocardium originates at the fibrous skeleton and wraps around the ventricular chambers in a spiral towards the apex of the heart. Dispersed in between cardiac muscle fibers are fibroblasts and collagen fibers, which provide structural support and distribute force of contraction throughout the myocardium (Figure 3).

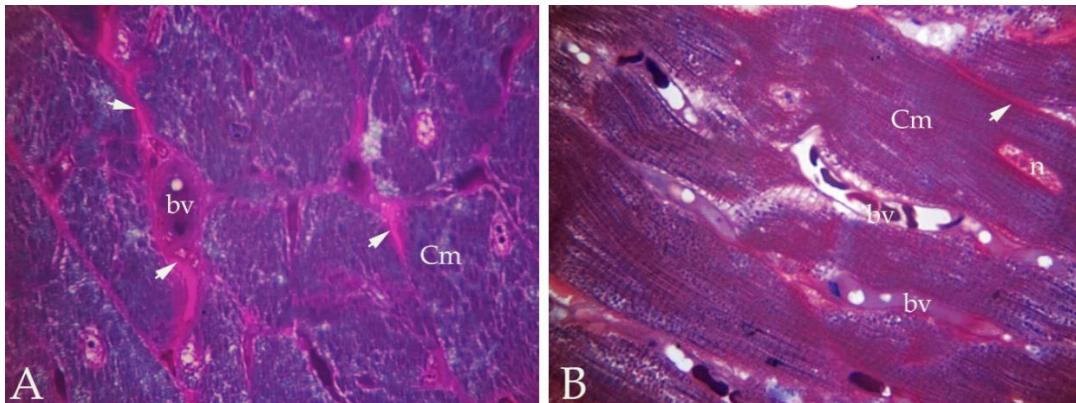


Figure 3. Histological organization of myocardium. Cross- (A) and longitudinal (B) section. Cm-cardiomyocyte; bv-blood vessel; connective tissue (white arrow); n-nucleus. Semi-fine section, basic fuchsin and methylene blue staining. Mag. A-x40 and B-x100, orig.

The inner cardiac wall layer, endocardium, is consisted of an endothelium that lines each chamber. Deep to the endothelium is a layer of subendothelial connective tissue, with some smooth muscle cells, and a deep subendocardial layer of connective tissue that merges with the connective tissue sheaths of the myocardium. The subendocardial layer of the endocardium contains the specialized cardiac muscle cells - Purkinje fibers which belong to heart's impulse-conduction system (Figure 4). Purkinje fibers are specialized to conduct the cardiac action potential that stimulates myocardial contraction.

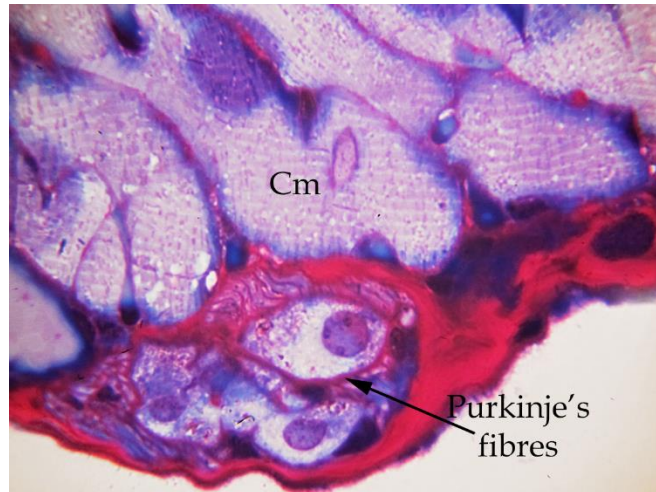


Figure 4. Purkinje's fibers. Semi-fine section, basic fuchsin and methylene blue staining. Cm-cardiomyocyte. Mag. x100, orig.

1.1.2 *Cardiomyocyte structure and function*

The main cell type of myocardium, its morpho-functional unit is contracting cardiac muscle fiber, cardiomyocyte, the most physically energetic cell in the body, which contracts constantly, without tiring. Individual contracting ventricular cardiomyocytes are large, often branched cells, 140 μm in length, and are arranged in the interlacing bundles. These cells are usually mononucleated, or sometimes binucleated, with centrally positioned nucleus/nuclei (Figure 5). Cardiomyocytes are striated with narrow dark and light bands, due to the parallel arrangement of myofibrils that extend from end to end of each cell. The myofibril is the rod-like bundle that forms the contractile elements within cardiomyocytes. Within each contractile element there are contractile, regulatory and structural proteins. Contractile proteins (actin and myosin) constitute 80% of the myofibril, while the rest belongs to regulatory and structural proteins.

Approximately 50% of the cell volume in a contracting cardiomyocyte is occupied by myofibrils, and the remainder contains nucleus, numerous mitochondria, sarcoplasmic reticulum, and the cytoplasm.

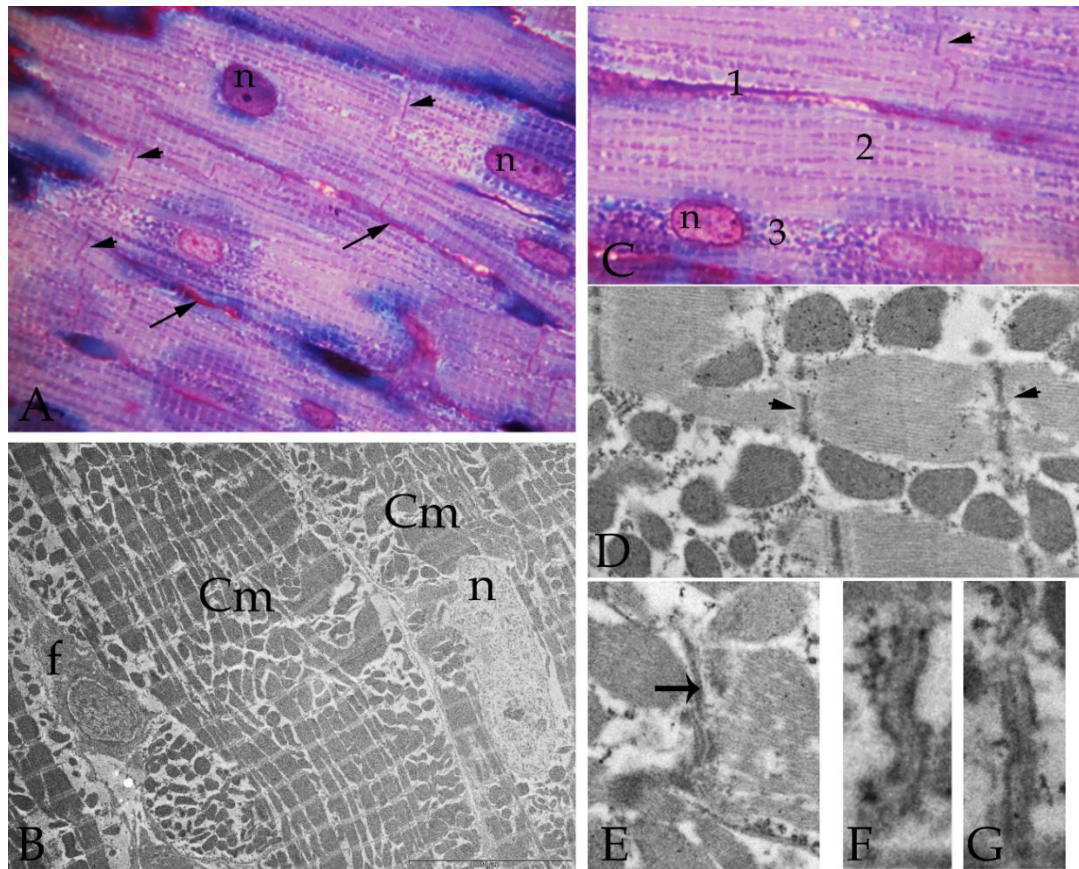


Figure 5. Right ventricle cardiomyocyte's organization. A, C) Semi-fine section, basic fuchsin and methylene blue staining. Cm-cardiomyocyte; blood vessels (arrows); intercalated discs (arrowheads); n-nucleus; Mag. x100, orig. B, D-E-G) Transmission electron micrographs of myocardium: Cm-cardiomyocyte; Z-discs (arrowheads); intercalated discs (→); n-nucleus; f-fibroblast. F) fascia adherens; G) sarcoplasmic reticulum. Mag. B-x8800, D-G-x15000, orig.

A prominent and unique feature of cardiac muscle is the presence of irregularly spaced dark bands between myocytes, intercalated discs that contain three different types of cell-cell junctions - fascia adherens, desmosomes and gap junctions (Figure 5). Force generated by the motor protein myosin in the thick filaments of myofibrils is transmitted along the thin actin filaments to the Z-discs at the ends of the each contractile unit of myofibril - sarcomere, and hence along adjacent myofibrils until the force reaches the intercalated discs membranes at the ends of the cell. Intercalated

discs resemble giant Z-disc, so it seems reasonable to expect that these two structures will contain proteins in common. Besides providing the mechanism for force transmission due to adjacent cardiomyocytes myofibrils anchoring in the region of fascia adherens junctions, intercalated discs also have important function in chemical communication of cells through the 3-nm gap junctions (electrical synapses). Gap junctions of cardiomyocytes provide electrical continuity using ion channels (connexons) that allow an action potential to propagate rapidly to several adjacent cardiomyocytes (**Gutstain et al., 2003**), so that waves of depolarization spread rapidly over the entire heart. Connexons consist of six transmembrane proteins - connexins (Cxs) that allow ions and small molecules to move freely between the adjacent cells.

1.1.3 Cardiac hypertrophy

Cardiac hypertrophy is often defined as an abnormal increase in heart muscle mass and is functionally, mechanistically, and histologically distinguished from normal embryonic and postnatal myocardial growth by characteristic changes in cardiac myocyte shape and volume (Figure 6). Histologically, there are two types of hypertrophy: concentric hypertrophy (increased thickness of ventricular walls with little or no change in chamber volume) and eccentric hypertrophy (increased chamber volume with ventricular wall thickness increased in proportion with chamber dimensions), respectively. Regardless of types, in both forms of hypertrophy, cardiac dry mass is increased (**Dorn and Robbins, 2003**). Experimental and clinical evidences support the view that RV hypertrophy may parallel LV hypertrophy in systemic hypertension but a comprehensive analysis of this issue is lacking.

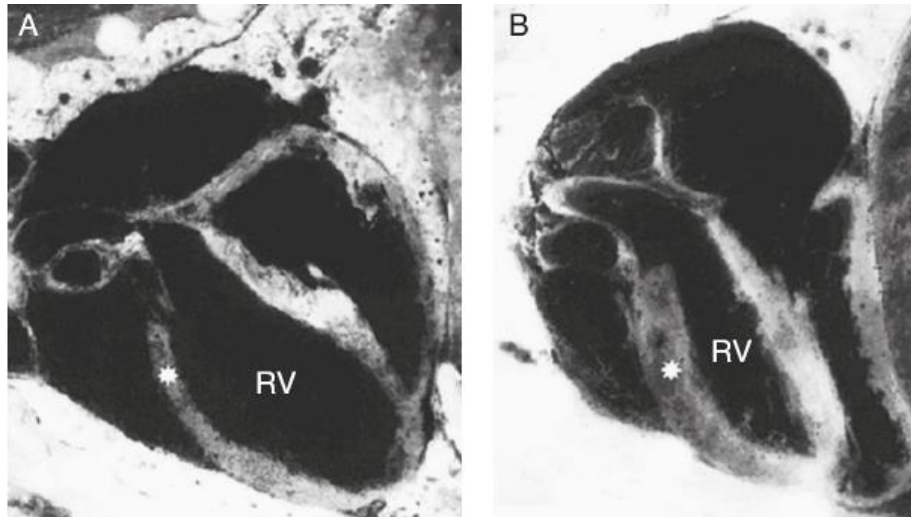


Figure 6. Right heart ventricle hypertrophy (*- B) in rat. Reproduced from Fabris *et al.*, 2001.

1.1.4 Cellular and molecular mechanisms of cardiomyopathy

The heart hypertrophies in response to developmental signals as well as increased workload (Maillet *et al.*, 2013).

Although adult-onset cardiac hypertrophy can ultimately lead to disease, it is not necessarily maladaptive. Progress has been made in our understanding of the structural and molecular characteristics of physiological cardiac hypertrophy, as well as of the endocrine effectors and associated signaling pathways that regulate it. Physiological hypertrophy is initiated by finite signals, which include growth hormones (such as thyroid hormone, insulin, insulin-like growth factor 1 and vascular endothelial growth factor - VEGF) and mechanical forces that converge on a limited number of intracellular signaling pathways (such as phosphoinositide 3-kinase- PI3K, serine/threonine kinase Akt protein kinase B, AMP-activated protein kinase - AMPK and mammalian target of rapamycin - mTOR) to affect gene transcription, protein translation and metabolism. Harnessing adaptive signaling mediators to reinvigorate the diseased heart could have important medical ramifications.

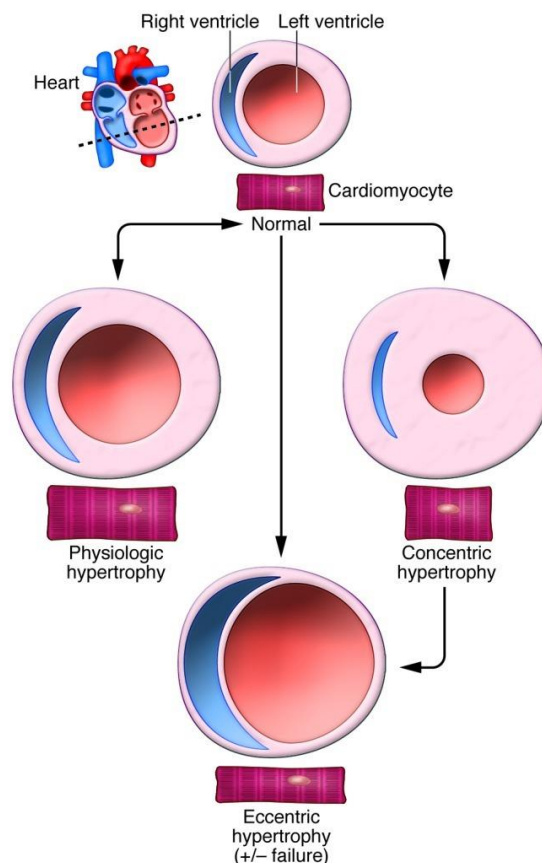


Figure 7.The types of heart ventricles hypertrophy. Reproduced from van Berlo *et al.*, 2013.

When contractile performance is perturbed or reduced in response to diverse (patho-)physiological stimuli, the heart typically remodels and hypertrophies, in association with increases in myocyte cell volume (**Karsner *et al.*, 1925**). Hypertrophy of the myocardium temporarily preserves heart pump function and reduces ventricular wall stress, but prolonged cardiac hypertrophy is a leading predictor for arrhythmias and sudden death as well as dilated cardiomyopathy and heart failure (**Levy *et al.*, 1990; de Simone *et al.*, 2008**). The hypertrophic growth of the myocardium is typically initiated by signal transduction pathways in response to either neuroendocrine factors or an ill-defined mechanical stretch- or wall tension-sensing apparatus (**Grossman *et al.*, 1975; Sharif-Naeini *et al.*, 2010**).

1.2 Nitric oxide (NO)-producing system

1.2.1 Physiological functions of NO in the heart

A role for the free radical signalling molecule nitric oxide (NO) in modulating cardiac function has been recognised for 15 years or more. The precise actions of NO, however, still remain under investigation. This probably stems from the varied (and often opposing) actions of NO in the heart, which are determined by different subcellular compartmentalization and regulation of the NO synthase (NOS) isoforms (**Barouch *et al.*, 2002**).

Family of NOS includes neuronal (nNOS), inducible (iNOS), and endothelial NOS (eNOS). It was initially reported that nNOS and eNOS are constitutively expressed mainly in the nervous system and the vascular endothelium, respectively, synthesizing a small amount of NO in a calcium-dependent manner under basal conditions and upon stimulation, and that iNOS is induced when stimulated by microbial endotoxins or certain proinflammatory cytokines (**Takimoto *et al.*, 2005**). However, recent studies have revealed that nNOS and eNOS are also subject to expressional regulation, and that iNOS may be expressed even under physiological conditions. Thus, it has become evident that all three NOS isoforms are expressed under both physiological and pathological conditions (**Wilcox *et al.*, 1997; Buchwalow *et al.*, 2002; Tsutsui *et al.*, 2015**).

NOSs catalyze the synthesis of NO by the L-arginine oxidation, in the presence of NADPH and tetrahydrobiopterin (BH₄) (**Bendall *et al.*, 2005; Brack *et al.*, 2009**). eNOS and nNOS are both activated by Ca²⁺ and produce NO at different rates (16 nmol of NO min⁻¹ mg⁻¹ for eNOS *vs.* 96 nmol of NO min⁻¹ mg⁻¹ for nNOS) (**Schmidt *et al.*, 1992; Nishida and Ortiz de Montellano, 1998**). A further important difference in the regulation of these two NOS isoforms is that under physiological conditions, eNOS activity is predominantly regulated by phosphorylation (**Dimmeler *et al.*, 1999; Dixit *et al.*, 2005**), whereas nNOS activity and expression are exquisitely regulated by

Ca²⁺ (Sears *et al.*, 2004). It has been shown that in the LV myocardium, the concentration of NO changes cyclically with the heart beat (Pinsky *et al.*, 1997).

Moreover, increasing or decreasing the LV preload appears to be associated with parallel changes in intramyocardial NO levels (Pinsky *et al.*, 1997). Taken together, these findings support the idea that NO is involved in a fast, autoregulatory mechanism that modulates myocardial contraction on a beat-by-beat basis and assists in matching preload with cardiac output (Gregory *et al.*, 2008).

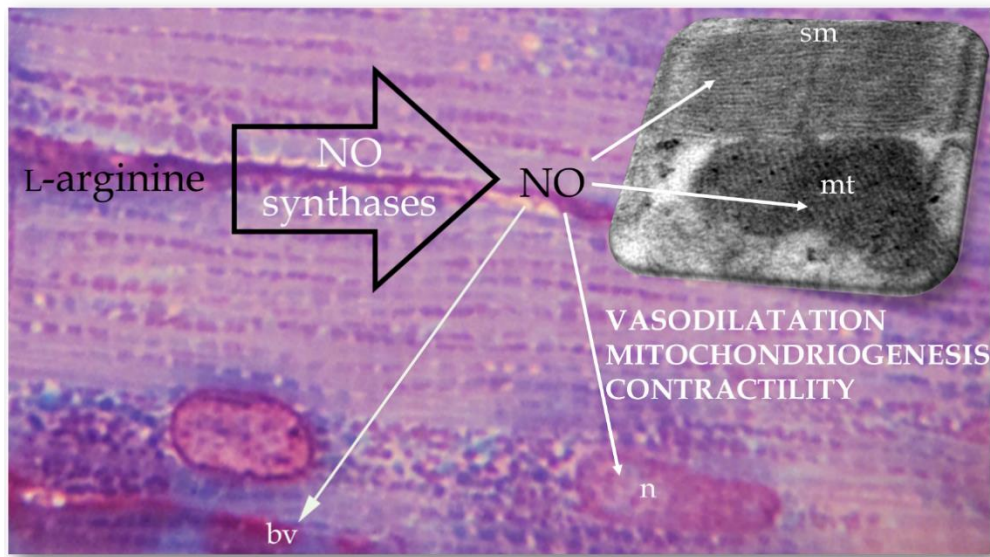


Figure 8. The role of nitric oxide in the heart. Nitric oxide produced from L-arginine by NO synthases promote vasodilatation, mitochondriogenesis, contractility among many other processes in the heart. sm-sarcomere; n-nucleus; bv-blood vessels; NO-nitric oxide.

NO can be produced from virtually all cell types composing the myocardium and thus it regulates cardiac function through both vascular-dependent and -independent effects (Massion *et al.*, 2003). The vascular-dependent effects of NO in the myocardium include: regulation of coronary vessel tone, thrombogenicity, and proliferative and inflammatory properties as well as cellular cross-talk supporting angiogenesis (Massion *et al.*, 2003). NO

also directly affects contractility of cardiomyocytes due to its effects on cardiomyocytes mitochondrial respiration and number.

Generally, NO acts to fine tune and optimise cardiac pump function. Several experimental studies have shown that low (submicromolar) doses of NO exert small positive inotropic effects, which may serve to enhance basal cardiac function (**Cotton *et al.*, 2002**). At slightly higher but still physiological doses, NO enhances myocyte relaxation and diastolic function. Also, physiological levels of NO can modulate and facilitate cardiomyogenesis (**Kanno *et al.*, 2004**). At higher (micromolar) amount, NO might have a negative inotropic effect (**Massion and Balligand, 2007**). Finally, defining what low or high NO amounts really mean *in vivo* is difficult, both in terms of actual quantity of bioactive NO delivered by different exogenous NO donors and the correspondence with amounts of NO synthesized in the heart (**Massion *et al.*, 2004**).

Cardiac remodeling occurs as an adaptive response to chronic increases in hemodynamic load and neurohormonal stimulation, but may become maladaptive over time, leading to harmful structural and functional alterations ultimately manifesting as congestive heart failure. At the cellular level, cardiac myocyte hypertrophy and apoptosis, fibroblast proliferation, and changes in the extracellular matrix are some of the primary alterations underlying the remodeling process. In recent years, NO has been recognized to modulate contractile function, myocardial oxygen metabolism, ventricular hypertrophy, apoptosis and fibrosis (**Jonathan and Kenneth, 2005**). The examination of the expressions/activities of NOSs in the heart might provide new insights into NO biology and its complex role in cardiac remodeling (hypertrophy) and heart failure.

1.2.2 Nitric oxide synthase (NOS) isoforms in the heart

NOS isoforms, nNOS, iNOS and eNOS, have been identified in heart (Paz *et al.*, 2003; Bryan *et al.*, 2009). The eNOS is the predominant NOS isoform expressed in the heart, occurring mainly in vascular endothelium whereas it plays an important roles in regulation of vascular resistance and myocardial perfusion. This isoform may also be expressed in endocardial endothelium, and cardiac myocytes. Whereas eNOS in the cardiomyocytes localizes to sarcolemmal caveolae and to the mitochondria, nNOS is localized to the sarcoplasmic reticulum (SR) (Massion *et al.*, 2003; Schulz *et al.*, 2005; Ziolo *et al.*, 2008). At these specific cells and subcellular compartments NO synthesized by specific NOSs may exert various local-specific intracrine effects.

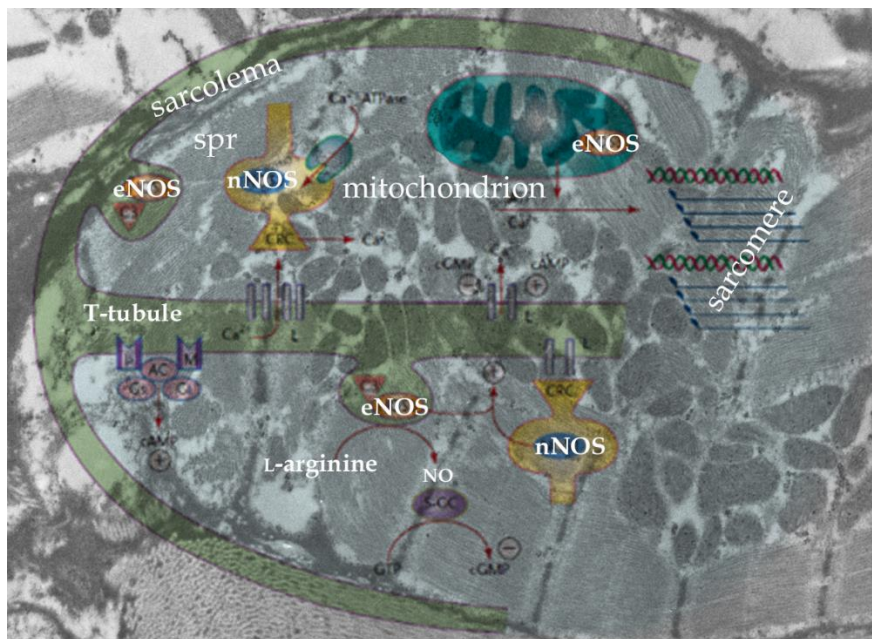


Figure 9. Location and action of nitric oxide synthase isoforms in the cardiomyocyte. spr - sarcoplasmic reticulum; neuronal (nNOS), inducible (iNOS), and endothelial (eNOS) NOS.

Under normal circumstances, receptor-mediated NOS-dependent mechanisms involve eNOS or nNOS while iNOS is mostly stress activated (Paz *et al.*, 2003). Study of Takimoto *et al.* (2002) suggests that nNOS mediates the

vagal stimulation-induced NO release. This may not seem surprising since nNOS is present in ventricular intracardiac nerve fibres (**Sosunov et al., 1995**). Additional to this, nNOS is found in sarcoplasmic reticulum and mitochondria of cardiomyocytes (**Xu et al., 1999; Kanai et al., 2001**) which raises the possibility that NO from cardiomyocytes' nNOS could be responsible for the increase of NO production, seen during vagal stimulation. However, selective inhibition of nNOS did not alter basal NO level, suggesting that the basal NO signal originates from an eNOS-dependent source (such as plasmalemmal and T-tubule caveolae and within coronary endothelium) (**Miethke et al., 2003; Massion et al., 2004**).

1.2.3 NOS system in heart during pathological conditions

The cardiac pathology is frequently associated with the cytokine-induced iNOS, although, iNOS in fact might have a dual role in the heart hypertrophy. On the one hand, it could serve for the cytoprotection, decreased leukocyte adhesion, antiplatelet activity, reduced vascular permeability, and antioxidant activity. On the other hand, the widespread expression of iNOS, especially in noninflammatory cells, may have harmful consequences. Thus, **Heba et al. (2001)** documented relation between expression of tumor necrosis factor alpha (TNF α), iNOS, vascular endothelial growth factor (VEGF) mRNA and development of heart failure after experimental myocardial infarction in rats.

1.3 Effects of cold on heart

Severe cold exposure and pressure overload are both known to prompt oxidative stress and pathological alterations in the heart although the interplay between the two remains elusive (**Lu and Xu, 2013**). Although cold exposure-induced cardiac geometric and functional changes may be associated with cold-induced increase in blood pressure and hemodynamic effects (**Swoap et al., 2004; Cheng and Su, 2010**) it is known that cold stress is associated with a

higher cardiovascular mortality rate (**Sheth et al., 1999; Cheng and Su, 2010; Sun, 2010**).

1.4 Right ventricle in health and disease - plasticity and remodeling

Since RV is restricted in its role to pumping blood through lungs only, and not so frequently (or noticeably) involved in cardiac diseases of epidemic proportions such as myocardial ischemia, cardiomyopathy, or valvulopathy, the it has generally been considered a mere bystander and a victim of cardiovascular pathological processes.

Consequently, knowledge about the role of RV in health in disease has lagged behind that of the LV and little attention has been devoted to how RV dysfunction may be best detected and measured, what specific molecular and cellular mechanisms contribute to maintenance or failure of normal right ventricular function, how right ventricular dysfunction evolves structurally and functionally, or what interventions might best preserve right ventricular function. Nevertheless, even the proportionately limited information related to right ventricular function, its impairment in various disease states, and its impact on the outcome of those diseases suggests that the RV is an important contributor and that further understanding of these issues is of pivotal importance.

Most of the deaths among patients with severe pulmonary arterial hypertension (PAH) are caused by progressive right ventricular pathological remodeling, dysfunction, and failure (**Zuo et al., 2012**). RV failure is the cause of at least 70% of deaths attributable to PAH (**D'Alonzo et al., 1991**). The degree of RV remodeling is an independent prognostic indicator (**van Wolferen et al., 2007**). Many studies have confirmed that RV function is independently associated with prognosis of PAH (**Humbert et al., 2006; van Wolferen et al., 2007; Jing et al., 2007; Vonk Noordegraaf and Naeije, 2008; Voelkel et al., 2011**). Preventing and reversing RV remodeling and failure

together with reducing pulmonary artery pressure (PAP) are therefore viable strategies for the treatment of PAH (**Bogaard *et al.*, 2010; Simon and Pinsky, 2011**).

Unlike that of LV remodeling, the pathophysiology of RV remodeling is not well understood, such that treatments successfully in the case of LV remodeling often have no beneficial effect on RV remodeling. Clinical and experimental evidence suggest that the mechanical stress created by elevated pressure on the pulmonary artery is not the only cause of PAH-induced RV remodeling and failure (**Dore *et al.*, 2005; Bogaard *et al.*, 2009**). Some patients with severe PAH rapidly progress to RV failure but other patients do not (**Voelkel *et al.*, 2011**). RV myocardial function can also be impaired by factors such as sarcoidosis, scleroderma, and amyloidosis. These are potential contributing molecular mechanisms of RV remodeling independent of RV afterload (**Voelkel *et al.*, 2011**). For these reasons, the mechanisms underlying the development of RV hypertrophy and remodeling merit further investigation.

Cardiac remodeling is commonly defined as a physiological or pathological state that may occur after conditions such as myocardial infarction, pressure overload, idiopathic dilated cardiomyopathy or volume overload (**Mihl *et al.*, 2008**).

The mechanisms leading to RV remodeling and dysfunction following acute myocardial infarction involving the LV are not completely clear, but it is frequently assumed that LV failure causes pulmonary hypertension and increased RV afterload leading to RV remodeling and dysfunction (**Toldo *et al.*, 2011**). In addition, infarction or ischemia of the RV and/or the septum are common in patients with acute myocardial infarction and can also contribute to abnormal RV systolic function. Studies concerning RV remodeling are few and the extent, time and causes for RV dilatation and dysfunction remain unclear (**Toldo *et al.*, 2011**).

However, not long ago RV was considered an „unnecessary“ part of the normal circulation (**Sheehan and Redington, 2008**). While factually correct – ablation or replacement of the RV free wall can be well tolerated by experimental animals without reduction in cardiac output, and many surgical algorithms for congenital heart diseases culminate in a circulation devoid of a sub-pulmonary ventricle, a Fontan procedure, for example – it is clear that such circulations are far from normal.

Furthermore, recent studies consistently demonstrate a central role for RV dysfunction in the prognosis and outcomes for a wide variety of acquired and congenital cardiac conditions. Consequently there has been a renewed interest in the singular role of the RV, as well as its influence on global function via biventricular interactions. Namely, right ventricular function is acknowledged as an important prognostic element in cardiovascular pathologies (**Giusca et al., 2010**). Although recent years have seen significant advances in the exploration of cardiac function, assessing right ventricular remodeling still remains a challenge.

2. AIMS

Recent studies suggest that NO might play an important role in the optimization of the adaptive response of the heart, in particular to prolonged (extended) sympathetic stimulation. The origin of NO, especially the impact of sympathetic stimulation on the synthesis of NO in the myocardium remains unsolved. Chronic inhibition of NOS with L-NAME (N^ω-nitro-L-arginine methyl ester) has been long used for the induction of hypertension, which leads to cardiac hypertrophy and the development of heart failure. However, there is no information available regarding does and how L-NAME treatment affect NO-synthetic pathway in the myocardium, and in particular, whether and how possible setting of intracellular levels of NO by inhibition or stimulation of NO-synthetic pathway, may alter the structural remodeling and consequently myocardial function.

Starting from this basis, an experimental study was set up in order to clarify the mechanisms of heart remodeling in the normal physiological response to prolonged stimulation of the sympathetic nervous system, to characterize the expression of enzymes involved in the synthesis of NO, as well as to investigate, the effects of the modulation of NO-synthetic pathway, in order to investigate the basis for the development of new therapeutic approach, especially in the treatment and prevention of the development of heart failure.

Although it is known that reduced NO bioavailability in the vasculature plays an important role in the development of heart failure, the underlying mechanisms are still uncovered. In particular, there are no clear studies that indicate a direct link between heart structural remodeling/functional response and the level of NO in the heart. Therefore, the aim of this doctoral thesis was to characterize the involvement of NO in the structural remodeling of rats' RV myocardium. The modulation of endogenous NO synthesis will broaden our

understanding of NO-dependent regulatory mechanisms and structural remodeling of the myocardium.

3. MATERIAL AND METHODS

3.1 *Experimental design*

The experiments were approved by the Ethical Committee for the Treatment of Experimental Animals of the Institute for Biological Research “Siniša Stanković”, Belgrade. Male Mill Hill hybrid hooded, 2-month-old rats (*Rattus norvegicus*, Berkenhout, 1769) were used. They were divided into three main groups. The first group received L-arginine HCl (2.25%), a substrate for NO synthases, and the second group received N^ω-nitro-L-arginine methyl ester (L-NAME) HCl, (0.01%), an inhibitor of NOSs in drinking water, for 45 days. The third group served as a control. Animals of all three groups were kept either on room temperature (22±1 °C) or in the cold room at 4±1 °C. The animals were kept in individual cages, with food and water *ad libitum*. Each experimental group consisted of six animals. Animals were sacrificed by decapitation, and right heart ventricles were isolated immediately and prepared for light microscopy, electron microscopy and fresh-frozen for Western blot analyses.

3.2 *Light microscopy*

Half of RV of each heart was immediately removed and fixed in 10% buffered solution of formaldehyde. After 72 hours, RVs were rinsed in tap water, dehydrated through serial ethanol solutions of increasing concentrations, cleared in xylene and paraffin-embedded. Paraffin blocks were cut at rotation microtome (Reichert, Austria) at 5 µm-thick sections and used for histochemical staining and immunohistochemistry.

3.2.1 *AZAN trichrome staining*

The 5 µm-thick paraffin sections were brought to water via xylene and ethanol (5-10 minutes each), warmed and placed in 1% azocarmine B water solution at 56°C for 15-30 minutes. The sections were rinsed with distilled

water and placed into aniline alcohol to differentiate nuclei for 30 seconds and then placed into phosphotungstic acid for 1 hour and aniline blue-orange G solution for 1 hour. The sections were rinsed after that with distilled water and dehydrated in 95% and 100% ethanol for 20 seconds each, cleared with xylene 2 times, mount in DPX and examined with a Leica DMLB microscope (Leica Microsystems, Germany).

3.2.2 Periodic Acid Schiff (PAS) staining

Paraffin-embedded sections were brought to water via xylene and ethanol. 10 drops of periodic acid solution were put on the sections and left to act 10 minutes. After washing in distilled water, 10 drops of Schiff reagent were put on the section and left to act 20 minutes, washed in distilled water and incubated with potassium methabisulphite solutions (10 drops, 2 minutes). Sections were drained without rinsing and 10 drops of fixative solution were added and left to act 2 minutes. After rinsing in distilled water, 10 drops of Mayer's hemalum were put and left to act 3 minutes. After rinsing in running tap water for 5 minutes, sections were dehydrated through ascending ethanol solutions, cleared in xylene and mounted in DPX. The sections were examined with a Leica DMLB microscope.

3.2.3 Immunohistochemistry

A series of 5 µm thick sections were deparaffinized and rehydrated, then incubated with 3% H₂O₂ in methanol for 10 minutes at room temperature to block endogenous peroxidase and followed by three washes in phosphate buffered saline (PBS; pH 7.4) of 5 minutes each. The sections were incubated with primary antibody (list and details are provided in Table 1) in PBS (Dako Scientific, Denmark) 90 minutes at 37 °C, followed by three 5 minutes PBS rinses. Immunodetection was assessed by the Dako LSAB Universal Kit (Dako Scientific, Denmark). After three PBS rinses of 5 minutes each, sections were incubated with 0.012% H₂O₂ and 0.05% diaminobenzidine (Sigma-Aldrich

Chemie, Germany) in PBS for 10 minutes in dark. The sections were rinsed in distilled water, counterstained with hematoxylin, mounted and examined with a Leica DMLB microscope.

3.2.4 Immunofluorescence

A series of 5 μm thick sections were deparaffinized and rehydrated. The sections were incubated with iNOS, eNOS or nNOS primary antibody (list and details are provided in Table 1) in PBS overnight at 4°C, followed by PBS washing. Immunodetection was assessed by incubation with FITC-secondary antibody (FITC anti-rabbit, ab6711, dilution 1:200v/v, Abcam, UK). After washing in distilled water, in order to preserve fluorescence signal, the sections were mounted in Mowiol solution (Sigma Aldrich, Germany) and examined with confocal laser scanning microscope Leica TCS SP5 (Leica Microsystems, Germany).

3.2.5 Propidium iodide staining

For the analysis of chromatin condensation and apoptotic changes of nuclei, paraffin sections were deparaffinized, rehydrated and dyed with propidium iodide solution for 10 minutes. After rinsing in distilled water, in order to preserve fluorescence signal, the sections were mounted in Mowiol solution (Sigma Aldrich, Germany) and examined with confocal laser scanning microscope Leica TCS SP5.

3.3 Transmission electron microscopy

Small portion of right heart ventricle excised for light microscopy analysis, of each animals was cut into small pieces, fixed in 2.5% glutaraldehyde in 0.1M phosphate buffer (pH 7.2) postfixed in 1% osmium tetroxide in the same buffer. The specimens were dehydrated through serial ethanol solutions of increasing concentration and were embedded in Araldite (Fluka, Germany). For electron-microscopic examination, the tissue blocks were

trimmed and cut with diamond knives (Diatome, Switzerland) on an UC6 ultramicrotome (Leica Microsystems, Germany) in order to obtain either, 1-2 μm -thick semi-fine sections or thin (70-80 nm thick sections). The semi-fine sections were further used for routine toluidine blue staining or immunohistochemistry.

The thin sections were mounted on copper grids, stained at Leica EM Stain with uranyl acetate/lead citrate (Leica Microsystems, Germany) and examined with a Philips CM12 transmission electron microscope (Philips/FEI, The Netherlands).

3.3.1 Toluidine blue staining

The glass slides with semi-fine section were placed on a hot plate and stained with equal volume of 1% solution of toluidine blue and 1% Na-tetra-borate for 2-3 minutes and rinsed in tap water. The sections were examined with a Leica DMLB microscope.

3.4 Morphometric and stereological analyses

3.4.1 Volume densities of cardiomyocytes, blood vessels and connective tissue in the myocardium

The volume densities of the major myocardial components (cardiomyocytes, blood vessels and stromal connective tissue) were obtained from a standard point-counting technique (**Weibel, 1981**), in the ImageJ image analysis system (NIH, USA). This technique allows determination of the volume fraction of each compartment as a ratio of the number of points falling on the compartment relative to the total number of points falling on the myocardial tissue. An orthogonal grid with 8×10 intersections was superimposed to light micrographs at a final magnification of $\times 1000$ (15 micrographs per animal). Volume densities were expressed as percentage fractions of cardiac muscle tissue.

3.4.2 *Cardiomyocytes diameters*

Morphometric evaluation of the cardiomyocytes diameter was performed using the ImageJ image analysis system. Measurements were performed exclusively on the longitudinal azan trichrome-stained sections of myocardium. 150-260 cardiomyocytes diameters per animal were analyzed in the central region of the cell (nuclear level). Results were presented as mean values \pm SEM. In order to follow the trend of cardiomyocytes diameter change, a histogram of cardiomyocyte size distribution was constructed with class interval of 5 μm .

3.4.3 *Cardiomyocytes nuclear profiles sizes*

Morphometric evaluation of the cardiomyocyte nuclear profiles surface was performed using the ImageJ image analysis system. Measurements were performed exclusively on clearly visible longitudinal toluidine blue stained sections of myocardium in which cardiomyocyte nuclei had a clear outline. 60-75 nuclei per animal were analyzed. Results were presented as mean values \pm SEM. Also, a histogram of nuclear profiles distribution was created with class interval of 10 μm^2 .

3.4.4 *Mitochondrial profiles sizes*

Mitochondria were divided in accordance to their localization to subsarcolemal (SSM), intersarcomeral (ISM) and perinuclear (PNM) subpopulation. Morphometric evaluation of the mitochondrial profiles surface was performed using the ImageJ image analysis system. Measurements were performed exclusively on electron-micrographs of clearly visible sections of myocardium. 200 mitochondria of each population per section were analyzed. Results were presented as mean values \pm SEM.

3.5 Western blot

For analyses by western blotting, proteins were dissolved according to Laemmli (1970) and 10 µg protein samples boiled and electrophoresed in 15% and 7.5% SDS-polyacrylamide gel for further analysis. After that proteins were transferred onto nitrocellulose membranes. After a brief rinse in TBS (Tris buffered saline - 200 mmol l⁻¹ Tris, 1.5 mol l⁻¹ NaCl, pH 7.4), the membranes were incubated in blocking serum (TBS containing 5% bovine serum albumin (BSA)) for 1h at room temperature to block the unbound sites. The membranes were further incubated with primary antibody according to manufactures instruction and recommended dilution (list and details are provided in Table 1). The incubation with primary antibodies was performed in 0.2% Triton X-100 - tris buffered saline (TBS) with 5% BSA, overnight in a cold room. After multiple rinses in TBS-T the membranes were incubated with horseradish peroxidase conjugated IgG secondary antibody (Santa Cruz Biotechnology) at 1:2000 v/v. For detection, the membrane was covered by luminol-based chemiluminescent substrate for 3 min. Immediately after, a piece of X-ray Hyperfilm MP (Amersham API, USA) was placed over the blot and exposed for 1 min. The film than was developed, scanned and quantitative analysis of immunoreactive bands was done by an ImageQuant software (USA). Volume is the sum of all the pixel intensities within a band; 1 pixel=0.007744 mm².

3.6 Statistical Analysis

To test data for normality, the Kolmogorov-Smirnov test was used. Analysis of variance (ANOVA) was used for within-group comparisons of the data. If the F test showed an overall difference, the Student's t-test was used to evaluate the significance of the differences in cases of parametric distribution, or Mann-Whitney test in cases of non-parametric distribution. Statistical significance was set at p<0.05.

Table 1. The list of used primary antibodies for immunohistochemistry, Western blot or immunofluorescence.

Primary antibody	Source/Type	Catalog number/Manufacturer	Analysis
<i>Anti-PCNA</i>	rabbit/polyclonal	sc-7907/Santa Cruz	WB, IHC
<i>Anti-UCP2</i>	mouse/monoclonal	ab67241/Abcam	IHC
<i>Anti-VEGF</i>	mouse/monoclonal	ab68334/Abcam	WB, IHC
<i>Anti-CD105</i>	rabbit/polyclonal	ab107595/Abcam	WB, IHC
<i>Anti-Connexin 43</i>	rabbit/polyclonal	ab11370/Abcam	WB, IHC
<i>Anti-nNOS</i>	rabbit/polyclonal	ab95436/Abcam	WB, IF
<i>Anti-eNOS</i>	rabbit/polyclonal	ab66127/Abcam	WB, IF, IHC
<i>Anti-iNOS</i>	rabbit/polyclonal	ab15323/Abcam	WB, IF
<i>Anti-HO-1</i>	rabbit/polyclonal	ab13243/Abcam, sc-10789/Santa Cruz	WB, IHC
<i>Anti-HO-2</i>	rabbit/polyclonal	ab19241/Abcam	IHC
<i>Anti-Mfn1</i>	mouse/monoclonal	ab57602/Abcam	WB
<i>Anti-Mfn2</i>	mouse/monoclonal	ab56889/Abcam	WB
<i>Anti-mitofilin</i>	rabbit/polyclonal	ab48139/Abcam	WB
<i>Anti-SERCA2</i>	mouse/monoclonal	ab2861/Abcam	WB
<i>Anti-calnexin</i>	rabbit/polyclonal	ab22595/Abcam	WB
<i>Anti-β-actin</i>	rabbit/polyclonal	ab8226/Abcam	WB

*WB-Western blot; IHC-immunohistochemistry; IF-immunofluorescence

4. RESULTS

4.1 Myocardial hypertrophy

The prolonged, 45 days treatment with L-arginine or L-NAME at two different ambient temperature, room or cold, revealed remodeling of three main histological components: cardiomyocytes, blood vessels and connective tissue in right ventricle myocardium of rats (Table 2, Figures 10, 11, 12).

4.1.1 Volume densities of cardiomyocytes, blood vessels and connective tissue

The results of stereological analyses of volume densities of cardiomyocytes, blood vessels and connective tissue are shown in Table 2. Compared with the control group acclimated at room temperature, cold did not significantly change volume density of myocardial tissue components (cardiomyocytes, blood vessels, connective tissue), although a slight decrease in blood vessel volume density was observed.

Chronic treatment with L-arginine at room temperature did not lead to statistically significant changes in volume densities of myocardial tissue components, although blood vessel and connective tissue volume densities have tended to increase. Also no significant changes in volume densities of tissues components were observed in L-arginine-treated cold-acclimated rats when compared with the appropriate control (untreated) cold-acclimated rat. However, when compared with L-arginine treatment at room temperature, cardiomyocyte volume density increased, while volume density of blood vessels decreased.

Chronic treatment with L-NAME, irrespective of ambient temperature acclimation, led to increased connective tissue volume density associated with a decrease in cardiomyocyte volume density (in respect to untreated-cold acclimation nor when compared with L-NAME-treated-room temperature

acclimated rats. L-NAME treatment in cold- acclimated animals also decreased blood vessel volume density, when compared with the identical treatment in room-acclimated animals.

Table 2. Volume densities of cardiomyocytes ($V_{V_{cm}}$), blood vessels ($V_{V_{bv}}$) and connective tissue components ($V_{V_{ct}}$) in myocardium of experimental groups. Results are presented as mean values \pm SEM. Statistical difference - (*) in comparison with referent control group: (*) $p < 0.05$ (**) $p < 0.01$; (#) in comparison with the same treatment at room temperature: (##) $p < 0.01$, (###) $p < 0.001$.

GROUPS	Room temperature-acclimated (22 ± 1 °C)			Cold-acclimated (4 ± 1 °C)		
	Control	L-arginine	L-NAME	Control	L-arginine	L-NAME
(%)						
$V_{V_{cm}}$	82.25 \pm 1.16	79.49 \pm 0.86	77.82 \pm 1.15 (**)	83.81 \pm 1.23	83.06 \pm 1.58 (##)	78.88 \pm 1.27 (**)
$V_{V_{bv}}$	10.03 \pm 0.77	11.24 \pm 0.71	11.13 \pm 0.67	8.97 \pm 0.77	7.53 \pm 0.62 (###)	7.94 \pm 0.68 (##)
$V_{V_{ct}}$	7.73 \pm 0.84	9.10 \pm 0.59	11.06 \pm 1.15 (*)	7.66 \pm 0.79	9.82 \pm 1.69	12.49 \pm 0.99 (**)

4.1.2 Structural alterations of myocardium

The control (untreated room temperature acclimated group) and L-arginine-treated groups acclimated to room temperature and cold, respectively, showed correct arrangement of myofibrils inside cardiomyocytes with maintenance of myocardial striation (Figure 10, 11). A small quantity of connective tissue with scarce collagen fibers was found around the cardiomyocytes.

In contrast, both the room temperature- and cold acclimated L-NAME-treated groups (Figure 10, 11) showed myofibril distortion inside the cardiomyocytes with consequent interruption of the correct myocardial striation pattern. Deposition of collagen fibers around the cardiomyocytes was also increased, leading to connective tissue growth in the myocardium of L-NAME-treated rats.

With regard to the capillary supply in the myocardium, a reduction was evident in all cold- acclimated groups (Figure 10). Ultrastructural changes followed the observed histological changes (Figure 11).

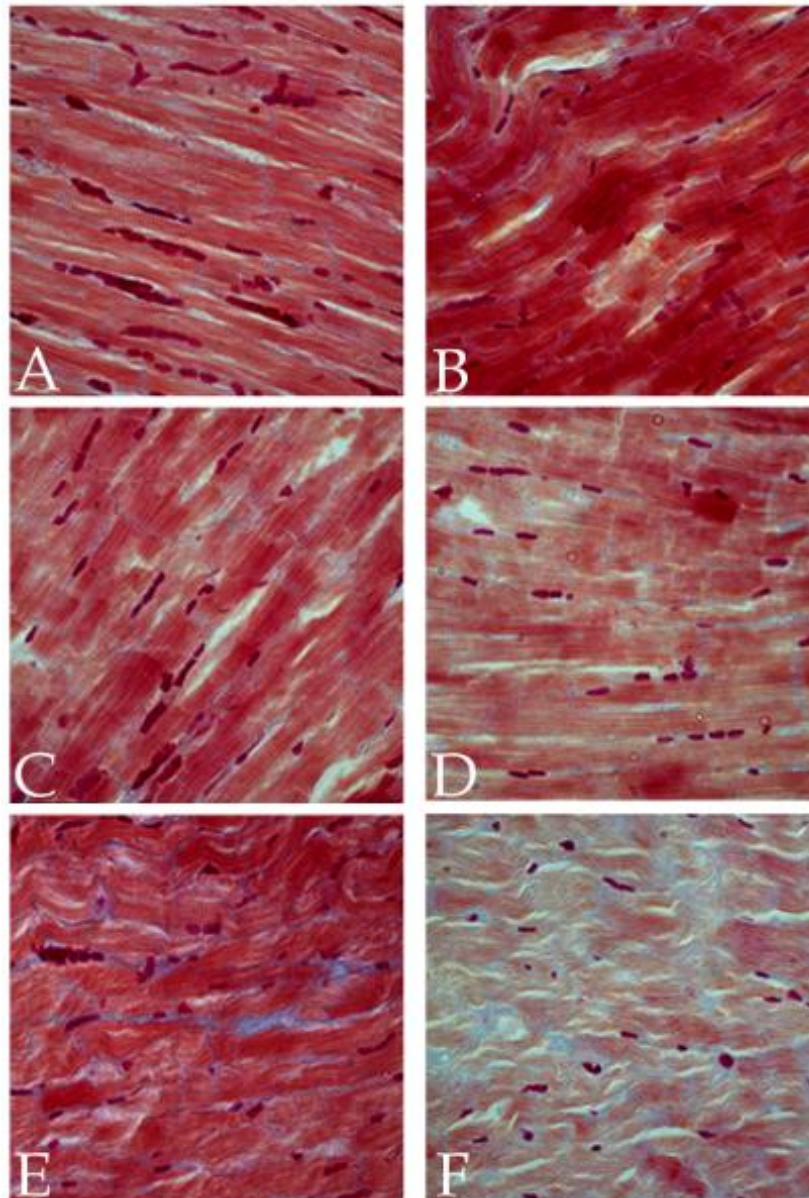


Figure 10. Histological changes in right ventricular myocardium, paraffin sections, Azan trichrome staining. A) Control 22 ± 1 °C; B) Control 4 ± 1 °C; C) L-arginine 22 ± 1 °C; D) L-arginine 4 ± 1 °C; E) L-NAME 22 ± 1 °C; F) L-NAME 4 ± 1 °C. Mag. $\times 100$, orig.

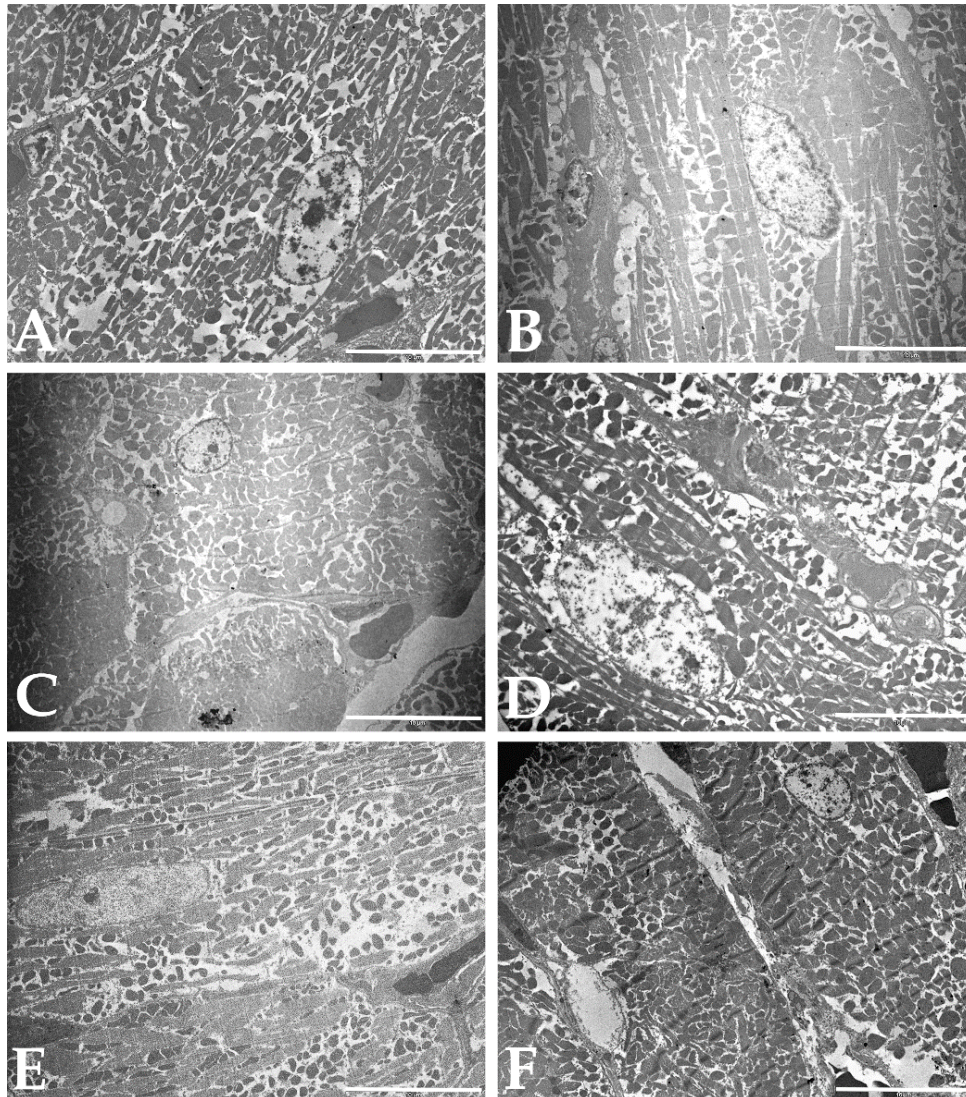


Figure 11. Ultrastructural changes in right ventricular myocardium. A) Control 22±1 °C; B) Control 4±1 °C; C) L-arginine 22±1 °C; D) L-arginine 4±1 °C; E) L-NAME 22±1 °C; F) L-NAME 4±1 °C. Mag. x2650, orig. Bar A-F, 10 μm.

4.1.3 Cardiomyocyte diameter

Compared with the control group (untreated and acclimated) room temperature, increased cardiomyocyte diameter occurred in all experimental groups, however, the diameters were statistically different ($p < 0.01$) only after L-arginine and L-NAME treatment in room temperature-acclimated animals (Table 3).

Table 3. Diameter of cardiomyocytes (μm). Results are presented as mean values \pm SEM. Statistical difference in comparison with referent control group - (**) $p < 0.01$.

GROUPS	Room temperature-acclimated (22 ± 1 °C)			Cold-acclimated (4 ± 1 °C)		
	Control	L-arginine	L-NAME	Control	L-arginine	L-NAME
Cardiomyocyte diameter (μm)	16.08 \pm 0.33	17.25 \pm 0.30 (**)	17.29 \pm 0.28 (**)	16.98 \pm 0.37	17.44 \pm 0.37	17.27 \pm 0.25

The distribution histogram of cardiomyocyte diameters confirmed these results, and showed a shift to greater diameters in all treated and cold-acclimated groups when compared to the room temperature-acclimated control group (Figure 12).

The distribution histogram of nuclear profile size also confirmed these results, and showed a shift to lower values in all treated and cold-acclimated groups when compared with the room temperature-acclimated control group (Figure 13). In the room temperature-acclimated control group, the highest percentage of cardiomyocytes had relatively large nuclei, with cross-sectional area between 40-50 μm^2 , while the percentage of smaller nuclei (with profile surfaces below 30 μm^2) was relatively low. Cold as well as L-arginine and L-NAME treatment, reduced nuclear cross-sectional area with maximum of distribution below 40 μm^2 , and with appearance of nuclei whose area were below 20 μm^2 .

At the other side, nuclear cross-sectional area of binucleated cardiomyocytes was not changed significantly in comparison with the room temperature-acclimated control group (Table 4). The exception is the untreated cold-acclimated group, where the trend of nuclear cross-sectional area decrease was noted. Namely, in this group average nuclear cross-sectional area for the

binucleated cardiomyocytes ($29.2 \mu\text{m}^2$) was similar to the nuclear cross-sectional area of the overall cardiomyocytes' population ($29.5 \mu\text{m}^2$).

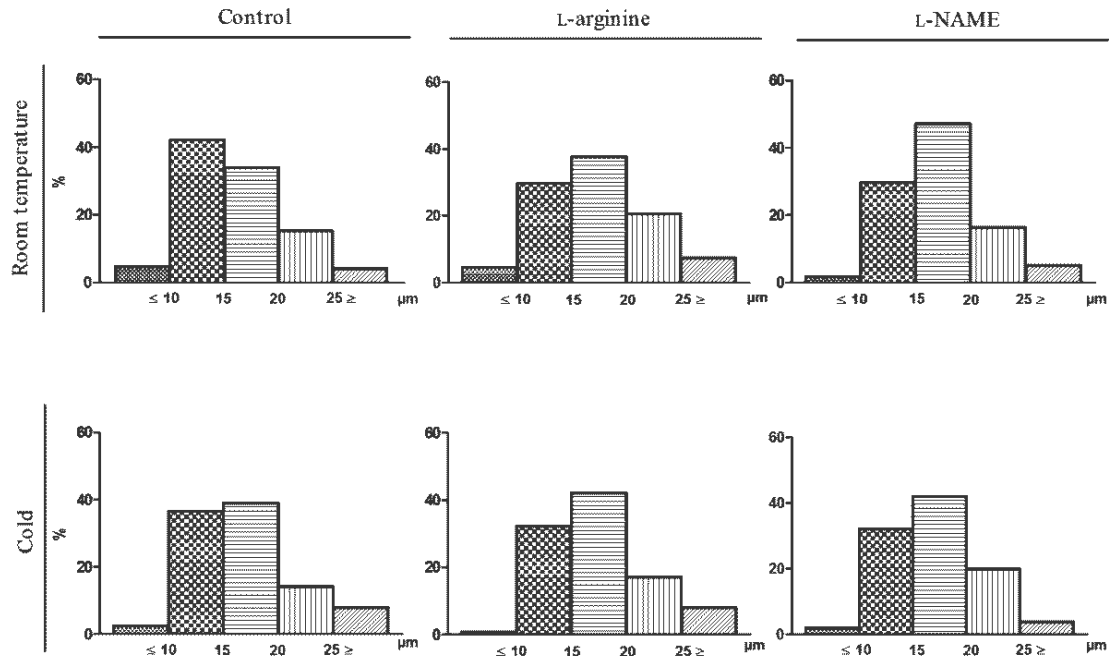


Figure 12. Distribution histogram of cardiomyocytes diameters by their size. In comparison with control group acclimated to room temperature, percentage of cardiomyocytes with diameters over $15 \mu\text{m}$ increases in all other experimental groups.

The very prominent change was observed in size of cardiomyocytes' nuclei (Figure 13, Table 4). Each treatment shifted nuclear profile down size comparing to room temperature-acclimated control. Cold acclimation *per se* induced significant decrease in comparison to room temperature-acclimation. L-arginine treatment showed opposite effects on cardiomyocyte's nuclear profile size (μm^2) different ambient temperature. Namely, L-arginine at room temperature considerably reduced, while in cold detained cardiomyocyte's nuclear profile size. L-NAME treatment regardless of ambient temperature significantly reduces cardiomyocyte's nuclear profile size.

Table 4. Nuclear profile size (μm^2), presented as mean values \pm SEM. Statistical difference comparison: (***) $p < 0.001$, in comparison with appropriate control group; (###) $p < 0.001$, in comparison with room temperature acclimated group treated identically.

GROUPS	Room temperature-acclimated (22 ± 1 °C)			Cold-acclimated (4 ± 1 °C)		
	Control	L-arginine	L-NAME	Control	L-arginine	L-NAME
Nuclear profile size (μm^2)	42.45 \pm 1.67	29.46 \pm 1.29 (***)	34.15 \pm 1.16 (***)	29.53 \pm 1. (###)	31.57 \pm 1.02	27.66 \pm 1.20 (###)

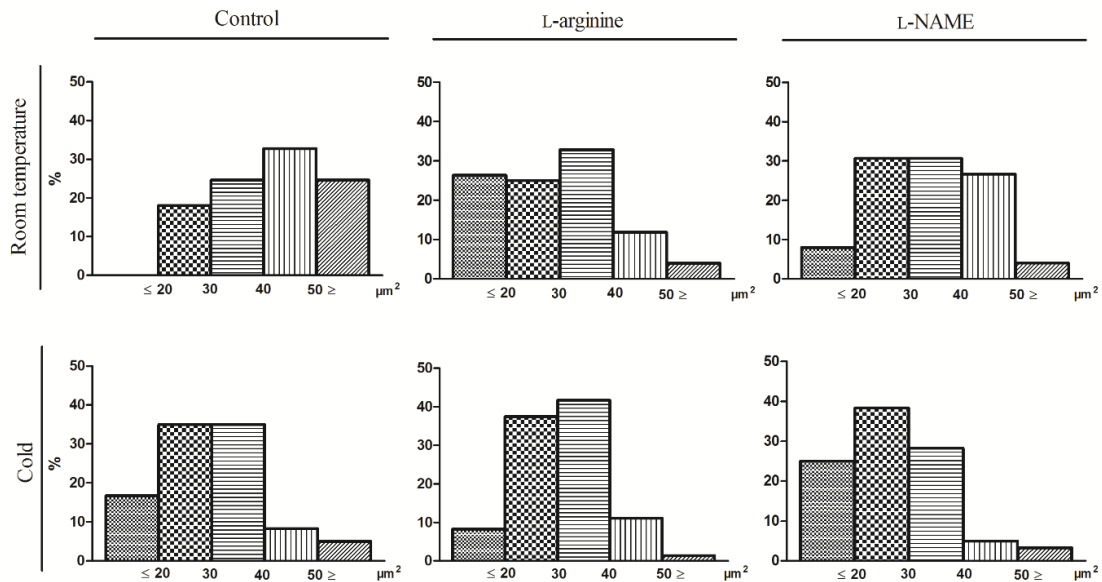


Figure 13. Distribution histogram of cardiomyocytes nuclei based on their profiles sizes (μm^2).

4.1.4 Ratio of binucleated cardiomyocytes

Although ratio of binucleated cardiomyocytes increases in all treated and cold acclimated animals, statistical significance of this increase is evident only in L-NAME-treated groups (Figure 14). Namely, cold acclimation as well as L-arginine treatments showed the trend of increase of binucleation, since

ratio of binucleated cardiomyocytes increased about 1.5 times in comparison with the appropriate controls. In comparison with appropriate controls, L-NAME treatments led to 4.5-fold and 1.9-fold increase of binucleation in right ventricle, respectively ($p < 0.001$ for the room temperature treatments and $p < 0.05$ for the treatments at cold).

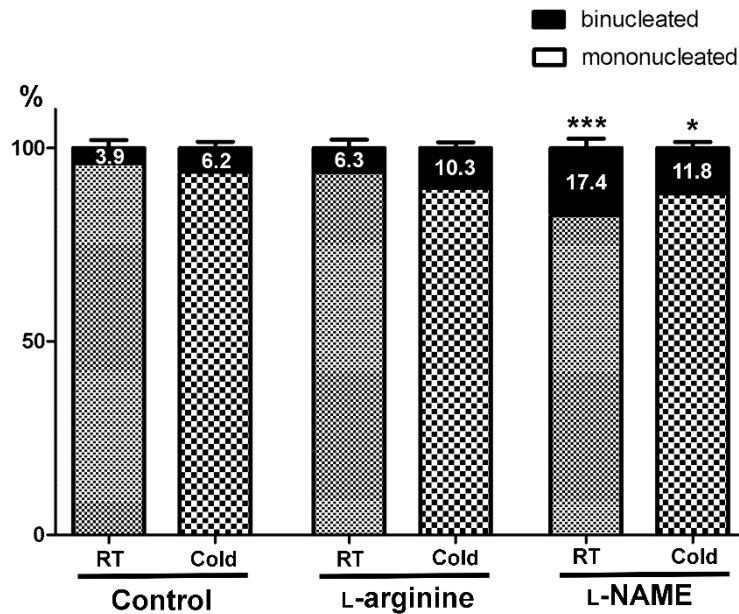


Figure 14. Ratio of mono- and binucleated cardiomyocyte's in room temperature (RT) or cold exposed untreated, L-arginine or L-NAME treated rats. Statistical difference: (*) - in comparison with appropriate control group: (*) $p < 0.05$, (***) $p < 0.001$.

This is in accordance with 2 way ANOVA which indicates the significance of the treatments effect and the effect of interaction between the treatments and acclimation temperature (Table 5).

Table 5. Two way ANOVA for interaction of applied treatment and ambiental temperature in relation with nuclear cross-sectional area and binucleated cardiomyocytes ratio.

	One way ANOVA				Two way ANOVA					
	Room temperature		Cold		Temperature		Treatment		Interaction	
	F	P	F	P	F	P	F	P	F	P
Nuclear cross-sectional area	22.21	<0.001*	2.80	>0.05	29.89	<0.001***	11.18	<0.001***	17.04	<0.001***
Binucleated cardiomyocytes ratio	11.22	<0.001***	3.26	<0.05*	0.02	>0.05	13.65	<0.001***	3.82	<0.05*

4.1.5 Microscopic analyses of cardiomyocytes' nuclei

Histological and ultrastructural analysis confirmed the results of morphometric study on cardiomyocytes' nuclear cross-sectional area, demonstrating the appearance of reduced nuclear size in all treated and cold-acclimated groups, in comparison with the control room-temperature acclimated group (Figure 15). Cardiomyocytes nuclei of control room-temperature acclimated animals showed elongated, oval-shaped, mostly euchromatic appearance at the longitudinal sections through the tissue (Figure 15A).

On the other side, L-arginine and L-NAME-treatments, as well as the cold acclimation led to the decrease of nuclear cross-sectional area followed by their rounding (Figure 15B-F). Also, appearance of heterochromatic cardiomyocytes nuclei was increased in the L-arginine-treated animals (Figure 15C and D).

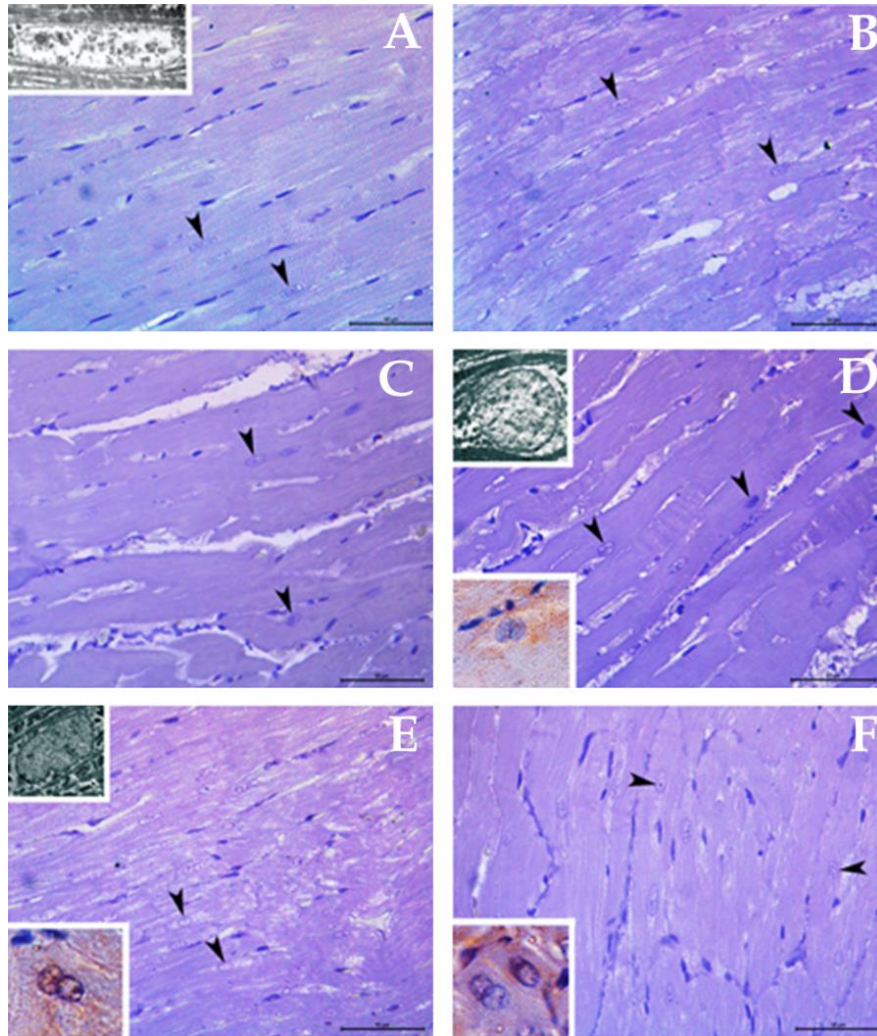


Figure 15. Nuclear morphology and presence of binuclear cardiomyocytes. A) Control 22 ± 1 °C; B) Control 4 ± 1 °C; C) L-arginine 22 ± 1 °C; D) L-arginine 4 ± 1 °C; E) L-NAME 22 ± 1 °C; F) L-NAME 4 ± 1 °C. Mag. $\times 100$, orig.

Immunohistochemical study demonstrated proliferating cell nuclear antigen (PCNA) expression in the binucleated cardiomyocytes of all groups (Figure 15, lower insets on D, E and F). PCNA positivity was detected in the cytoplasm, especially in the perinuclear regions, as well in the nuclei.

Ultrastructural analysis, taking into consideration very thin section (40 nm) revealed increased presence of symmetric invaginations of nuclear envelope suggesting closed nuclear division (Figure 16).

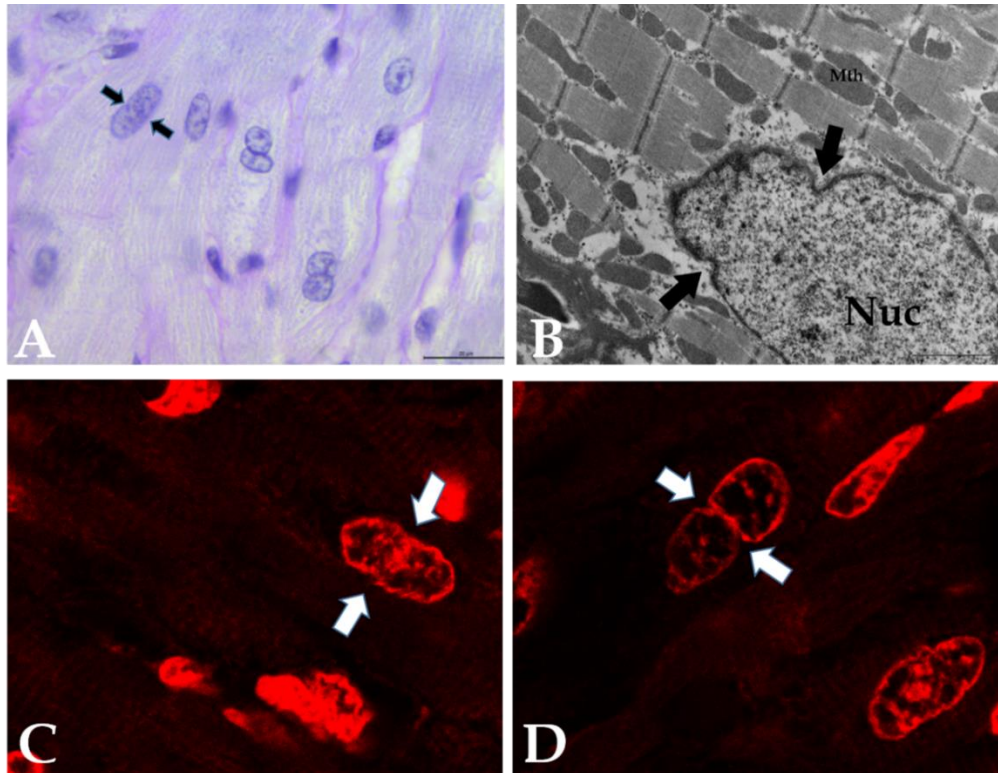


Figure 16. Cardiomyocytes' nuclear division in closed form. (A-D) L-NAME 22±1 °C. A) PAS staining; B) transmission electron microscopy; C, D) propidium iodide staining. Mag.: A-x100, orig; B-x8800; C,D-x63, orig.

4.1.6 Proliferating cell nuclear antigen (PCNA)

Results of PCNA protein expression are shown in Figure 17. In comparison with room temperature-acclimated control animals, cold acclimation as well as L-NAME treatment during room temperature acclimation, decreased PCNA protein expression in RV myocardium of rats. At the other side, L-arginine treatments maintained PCNA expression at room temperature control level, even during the cold acclimation. Similar effect was also noticed in the group treated with L-NAME on cold.

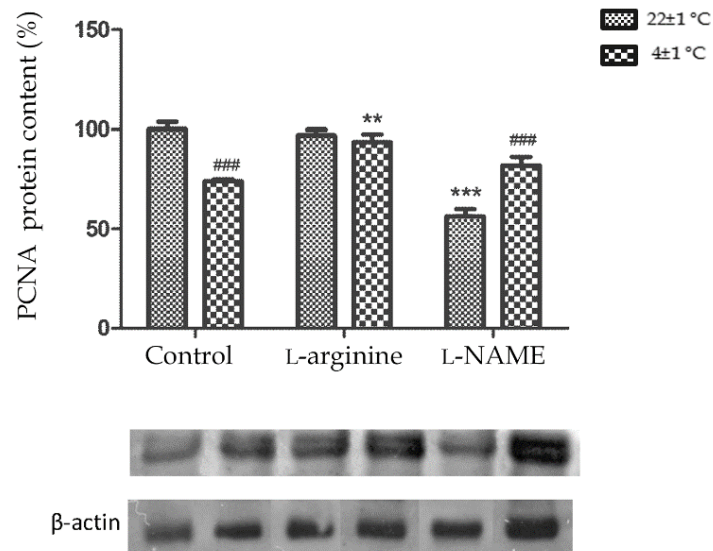


Figure 17. PCNA protein expressions in the right heart ventricle rats kept at 22±1 °C or 4±1 °C, untreated, L-arginine or L-NAME-treated. Statistical difference - (*) in comparison with referent control group: (**) p<0.01, (***) p<0.001: (#) in comparison with the same treatment at room temperature: (###) p<0.001.

Immunohistochemical detection of PCNA in the myocardium (Figure 18) revealed granular reaction distributed in the cardiomyocytes of all groups, especially in the cytoplasm and in some nuclei. Tissue immunoreactivity was visible decreased after cold exposure, and PCNA-immunopositivity of cardiomyocytes was rare and hardly visible, mostly cytoplasmic, in cold exposed control group. Slightly stronger PCNA positivity was detected in the endothelial cells and in the fibrous sheet at the surface of myocardial tissue. In the tissue samples from L-arginine-treated animals acclimated to room temperature, strong immunopositivity was detected in cardiomyocytes, as cytoplasmic and mostly nuclear reaction.

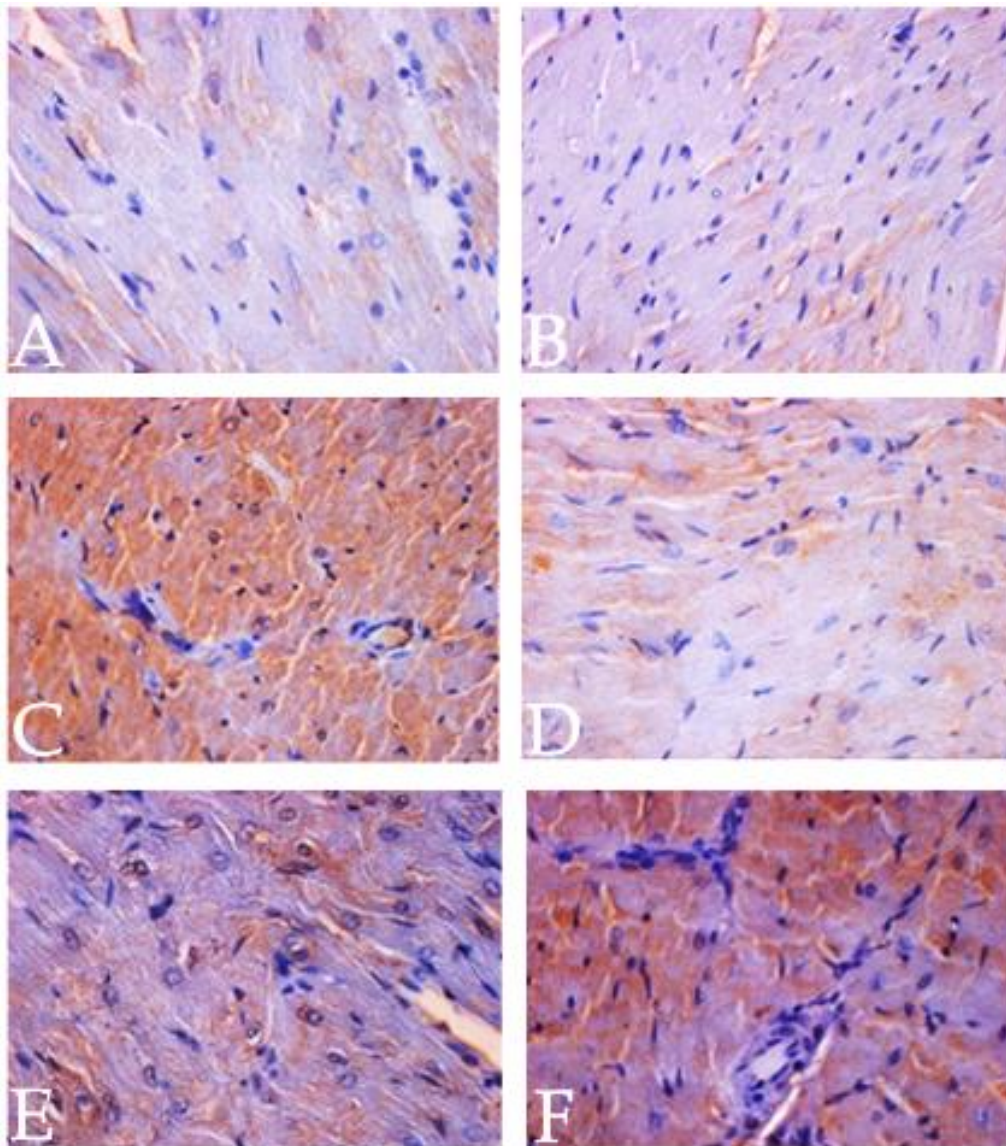


Figure 18. Immunohistochemical detection of PCNA. A) Control 22±1 °C; B) Control 4±1 °C; C) L-arginine 22±1 °C; D) L-arginine 4±1 °C; E) L-NAME 22±1 °C; F) L-NAME 4±1 °C. Mag. x100, orig.

Comparable weaker immunoreaction was detected in the cardiomyocytes of L-arginine-treated animals, acclimated to cold, with rare positivity of nuclei. In the tissue of L-NAME treated animals, without regard to acclimation temperature immunoreactivity of cardiomyocytes was strong, cytoplasmic and sometimes nuclear, especially in the regions of irregular cardiomyocyte distribution (Figure 18).

Also, strong immunoreactivity of connective tissue was detected in all groups, with cytoplasmic and nuclear immunopositivity of fibroblasts. Some endothelial cells were also PCNA-positive. In all groups, especially in the L-arginine and L-NAME-treated groups, nuclear and cytoplasmic PCNA immunopositivity of binuclear cardiomyocytes was detected (Figure 15).

4.1.7 Propidium iodide staining – apoptosis marker

Propidium iodide staining of paraffin sections revealed a small number of apoptotic nuclei in all L-arginine and L-NAME-treated groups without regard to ambient temperature. In L-NAME-treated, room temperature-acclimated group slight increase of apoptotic nuclei number was observed. Regarding cell type in this experimental groups, apoptotic nuclei mainly belong to interstitial cells, fibroblast. Only in room temperature-acclimated, L-arginine or L-NAME-treated groups a few cardiomyocytes showed signs of apoptosis (Figure 19C, D; Figure 19B-F). In case of binuclear cardiomyocytes, nuclei did not show any signs of chromatin condensation and fragmentation (Figure 19E).

Ultrastructural analysis of dying cardiomyocytes (Figures 20, 21), especially in L-arginine treated, room-temperature-acclimated group (Figure 20B-F), revealed condensed cells with remnants of sarcomeres, and sporadic small lipid droplets while mitochondria were absent. It is interesting that apoptotic cardiomyocytes retained in very close apposition to capillaries and the surrounding cardiomyocytes.

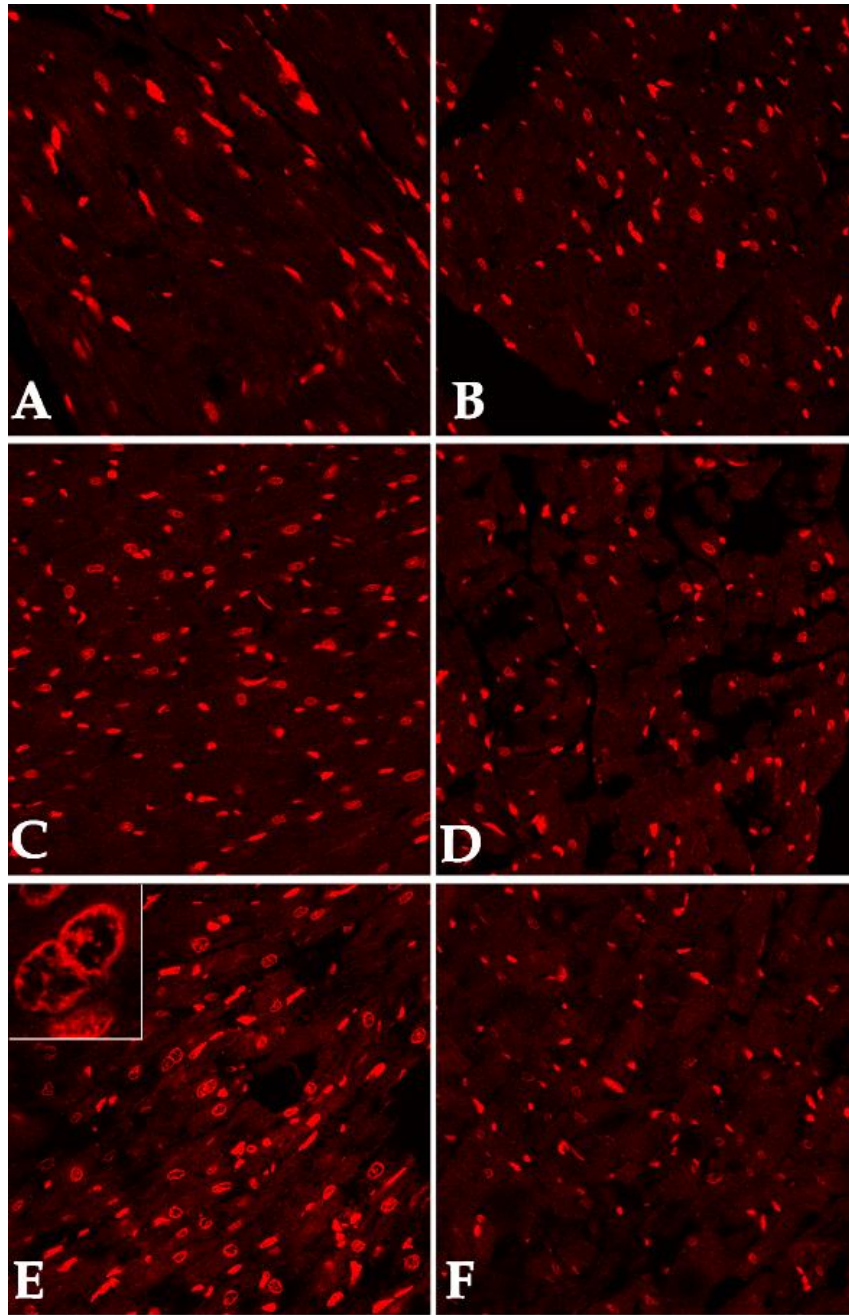


Figure 19. Propidium iodide staining of apoptotic nuclei. A) Control 22 ± 1 °C; B) Control 4 ± 1 °C; C) L-arginine 22 ± 1 °C; D) L-arginine 4 ± 1 °C; E) L-NAME 22 ± 1 °C; F) L-NAME 4 ± 1 °C. Mag. x63, orig.

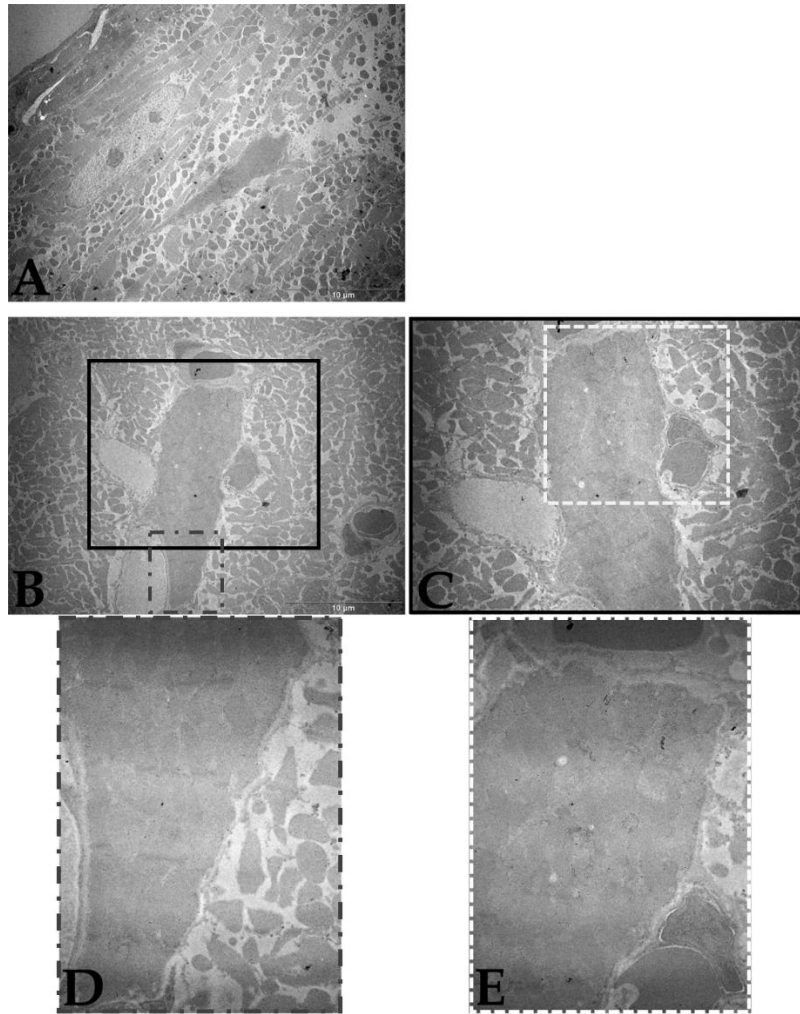


Figure 20. Apoptotic cardiomyocytes in room temperature-acclimated animals treated with L-NAME (A) or L-arginine (B-E). Different frames designate corresponding enlarged area. Mag.: A, B-x2650; C-x4400; D,E-x8800.

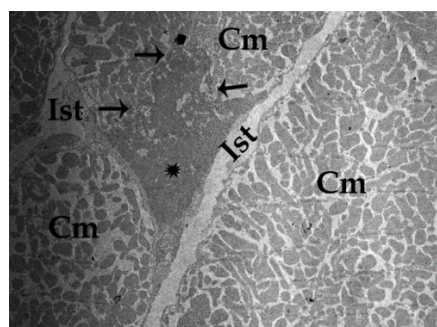


Figure 21. The first sign of apoptosis in cardiomyocyte (Cm), partial myofibril (*). Interstitium (Ist). L-arginine 22 ± 1 °C. Mag. x2650, orig.

4.2 Remodeling of capillary network

4.2.1 Expression of vascular and angiogenic markers

4.2.1.1 Vascular endothelial growth factor (VEGF)

Both L-NAME and L-arginine-treated groups acclimated to room temperature showed a significant increase of VEGF protein expression in comparison with appropriate control (Figure 22). Also, cold-acclimated control showed a significant increase of VEGF expression in comparison with room-temperature-acclimated control animals ($p < 0.001$). Cold-acclimated L-arginine-treated group showed a similar expression level of VEGF in comparison with L-arginine-treated animals acclimated to room temperature. At the other side, cold-acclimated L-NAME-treated group was characterized by slightly decreased VEGF expression in comparison with the identical treatment of room temperature -acclimated animals ($p < 0.05$).

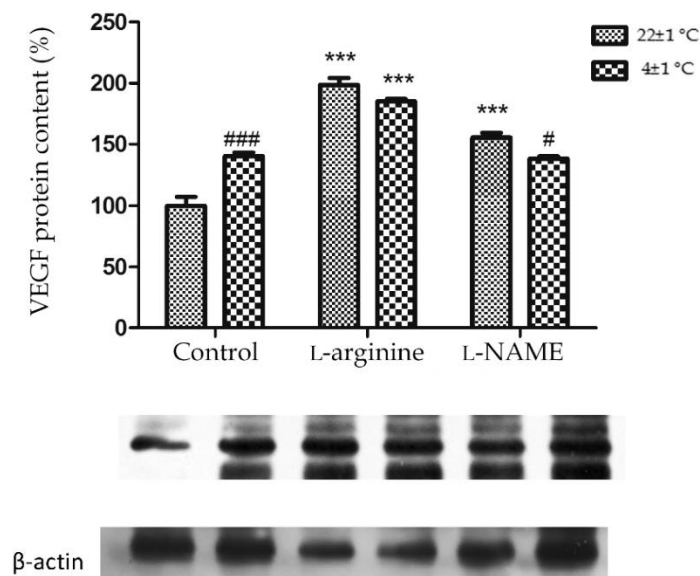


Figure 22. VEGF protein expression in the right ventricle myocardium of rats kept at 22±1 °C or 4±1 °C, untreated, L-arginine or L-NAME-treated. Statistical significance - (*) in comparison with referent control group: (***) $p < 0.001$; (#) in comparison with the same treatment at room temperature; (#) $p < 0.05$, (###) $p < 0.001$.

Immunohistochemically, VEGF was localized primarily in cardiomyocytes and endothelial cells of all groups. Immunopositivity was weak, homogenously distributed among cells. Subcellular localization of VEGF was cytoplasmic, mostly perinuclear and sometimes nuclear. The strongest immunopositivity was detected in the cardiac tissue of L-NAME-treated groups, where moderate cytoplasmic and occasionally nuclear reactivity was detected in the cardiomyocytes, including binuclear cells (Figure 23).

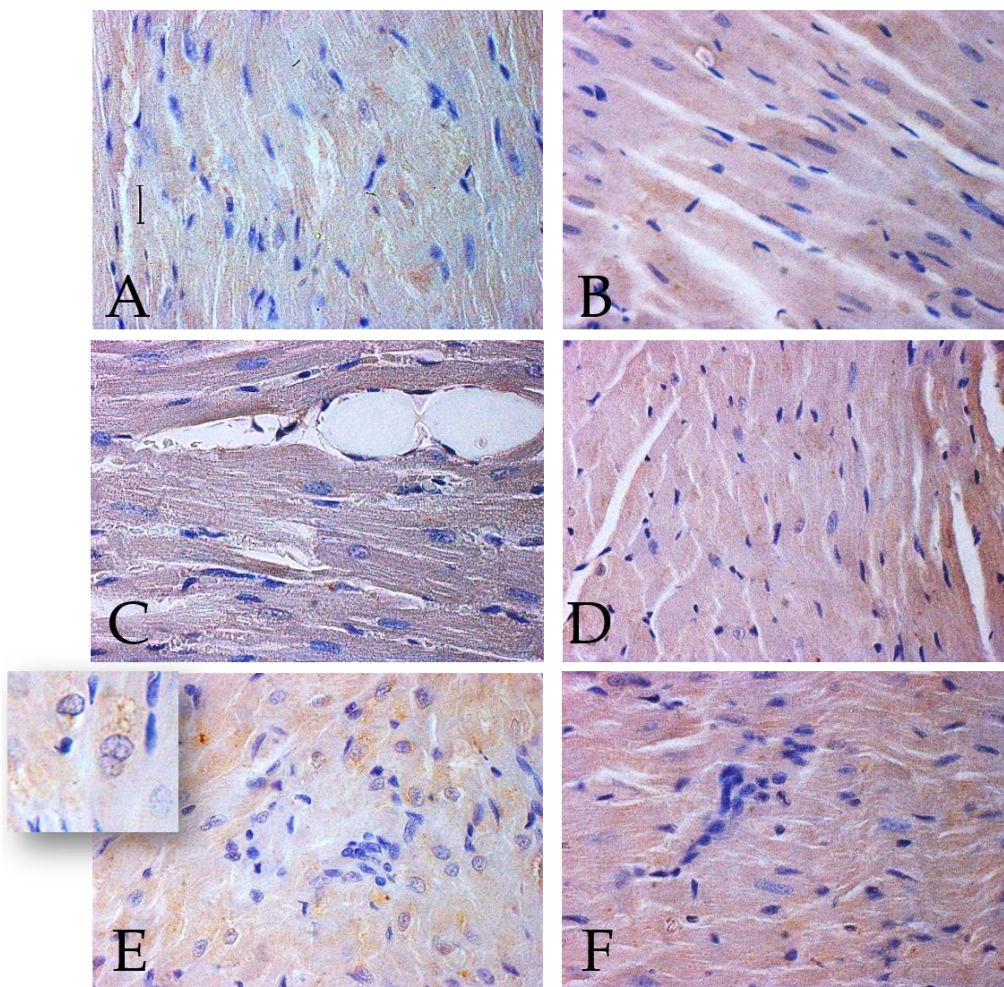


Figure 23. Immunohistochemical detection of VEGF. A) Control 22±1 °C; B) Control 4±1 °C; C) L-arginine 22±1 °C; D) L-arginine 4±1 °C; E) L-NAME 22±1 °C; F) L-NAME 4±1 °C. Mag. x100, orig.

4.2.1.2 Endoglin (CD105)

The only group with altered CD105 protein expression was cold-acclimated L-arginine-treated group where significant increase of CD105 in comparison with both the appropriate control and room-temperature-acclimated L-arginine-treated animals was detected (Figure 24).

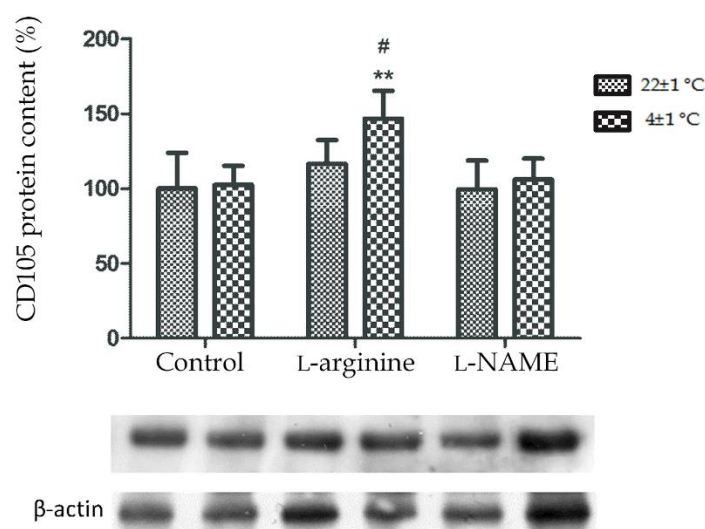


Figure 24. CD105 protein expression in the right ventricle myocardium of rats kept at 22±1 °C or 4±1 °C, untreated, L-arginine or L-NAME-treated. Statistical significance: (**) p<0.01 - in comparison with referent control group; (#) p<0.05 - in comparison with the same treatment at room temperature.

Immunohistochemical demonstration of CD105 in the myocardium revealed strong immunopositivity in the capillaries of all groups. Immunoreactivity of cardiomyocytes was moderate in the myocardia of control and L-arginine groups, and strong in the tissue of L-NAME-treated groups. Cardiomyocytes of L-NAME-treated animals showed heterogeneous pattern among cells, with granular cytoplasmic reaction. Also, nuclear reactivity was detected in cardiomyocytes of L-NAME-treated groups, especially in the room temperature-acclimated group (Figure 25).

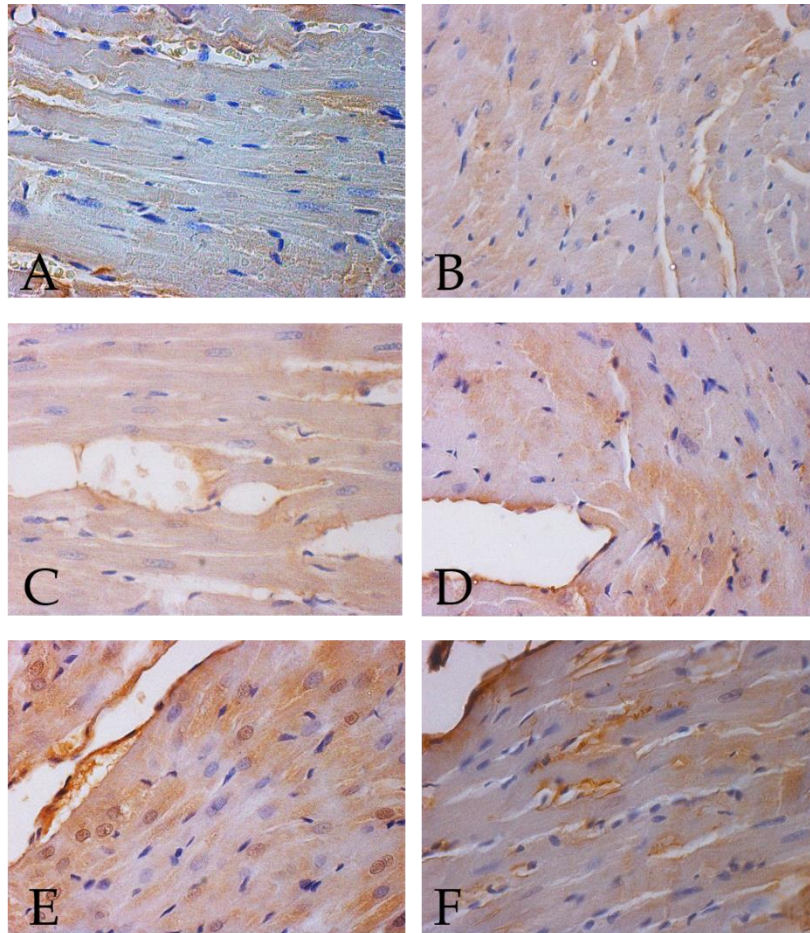


Figure 25. Immunohistochemical detection of CD105. A) Control 22±1 °C; B) Control 4±1 °C; C) L-arginine 22±1 °C; D) L-arginine 4±1 °C; E) L-NAME 22±1 °C; F) L-NAME 4±1 °C. Mag. x100, orig.

4.2.2 Microscopic analysis of capillary network

The hypertrophy of right heart ventricular cardiomyocytes induced by cold acclimation and L-arginine/L-NAME treatments is accompanied by changes in blood flow in surrounding blood vessels. After 45 days of cold exposure as well as L-arginine and L-NAME treatments the number of erythrocytes' profiles in myocardial blood vessels slightly decrease in comparison to room temperature-acclimated control (Figure 26). In addition, in all aforementioned experimental groups capillaries dilatation was noticeable, but only in L-arginine-treated, room temperature-acclimated rats the distance between cardiomyocytes and capillaries was reduced.

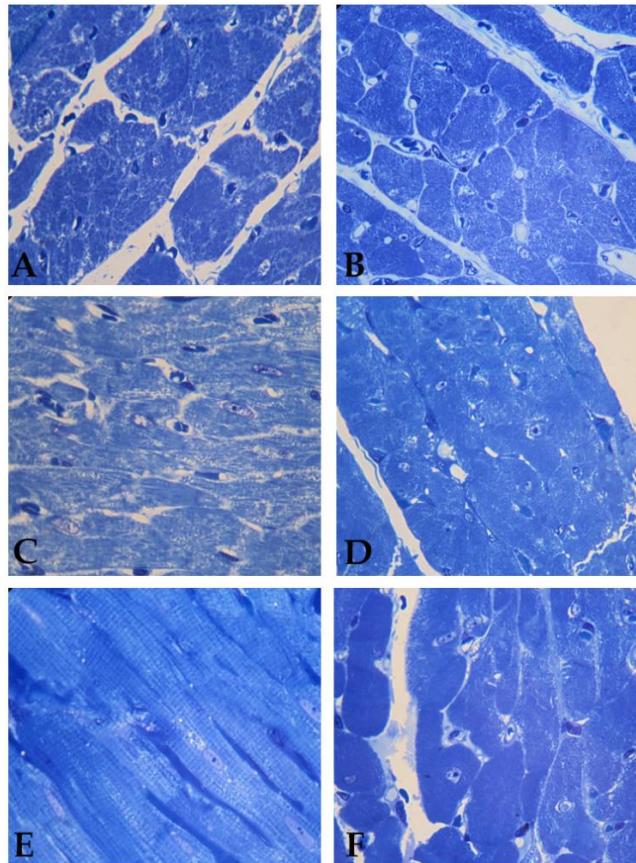


Figure 26. Right ventricular myocardium, semi-fine sections, toluidine blue staining. A) Control 22 ± 1 °C; B) Control 4 ± 1 °C; C) L-arginine 22 ± 1 °C; D) L-arginine 4 ± 1 °C; E) L-NAME 22 ± 1 °C; F) L-NAME 4 ± 1 °C. Mag. x100, orig.

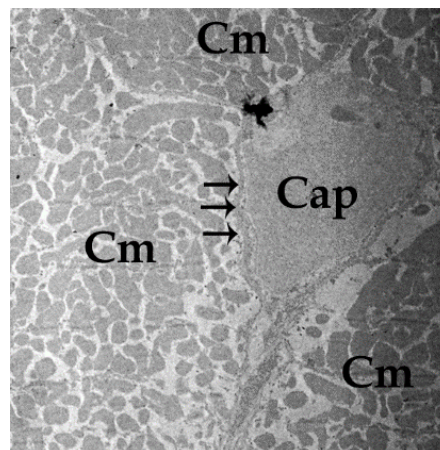


Figure 27. The distance (\rightarrow) between cardiomyocyte (Cm) and capillaries (Cap). L-arginine 22 ± 1 °C. Mag. x2650, orig.

4.3 Expression of connexin 43 (Cnx43) - cardiac electric coupling marker

In comparison with appropriate control, protein level of Cnx43 declined after L-arginine treatment on room temperature ($p < 0.001$) and to a lesser extent, after L-NAME treatment at room temperature ($p < 0.001$). Cold acclimation and L-NAME treatment during cold acclimation did not affect Cnx43 expression level in the myocardial tissue of RV, while L-arginine treatment on cold restored it to control level (Figure 28).

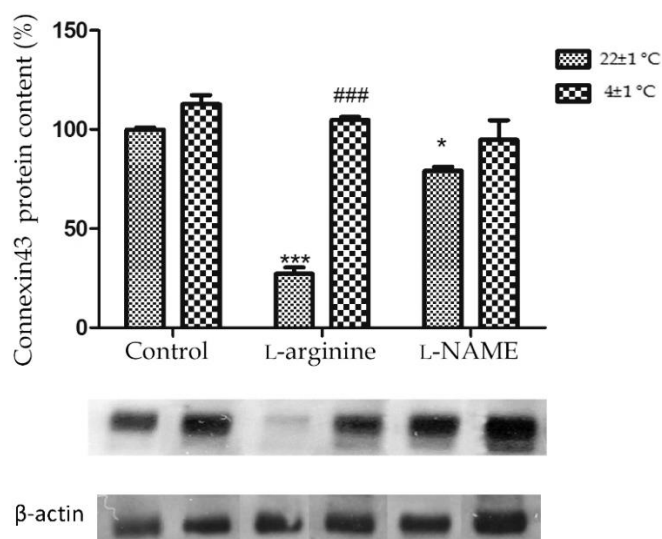


Figure 28. Connexin 43 protein expression in the right ventricle myocardium of rats kept at 22±1 °C or 4±1 °C, untreated, L-arginine or L-NAME-treated. Statistical significance - (*) in comparison with referent control group; (*) $p < 0.05$, (***) $p < 0.001$; (#) in comparison with the same treatment at room temperature: (#) $p < 0.001$.

Immunohistochemical staining for Cnx43 clearly showed positivity in the region of intercalated disks gap junctions between cardiomyocytes (Figure 29).

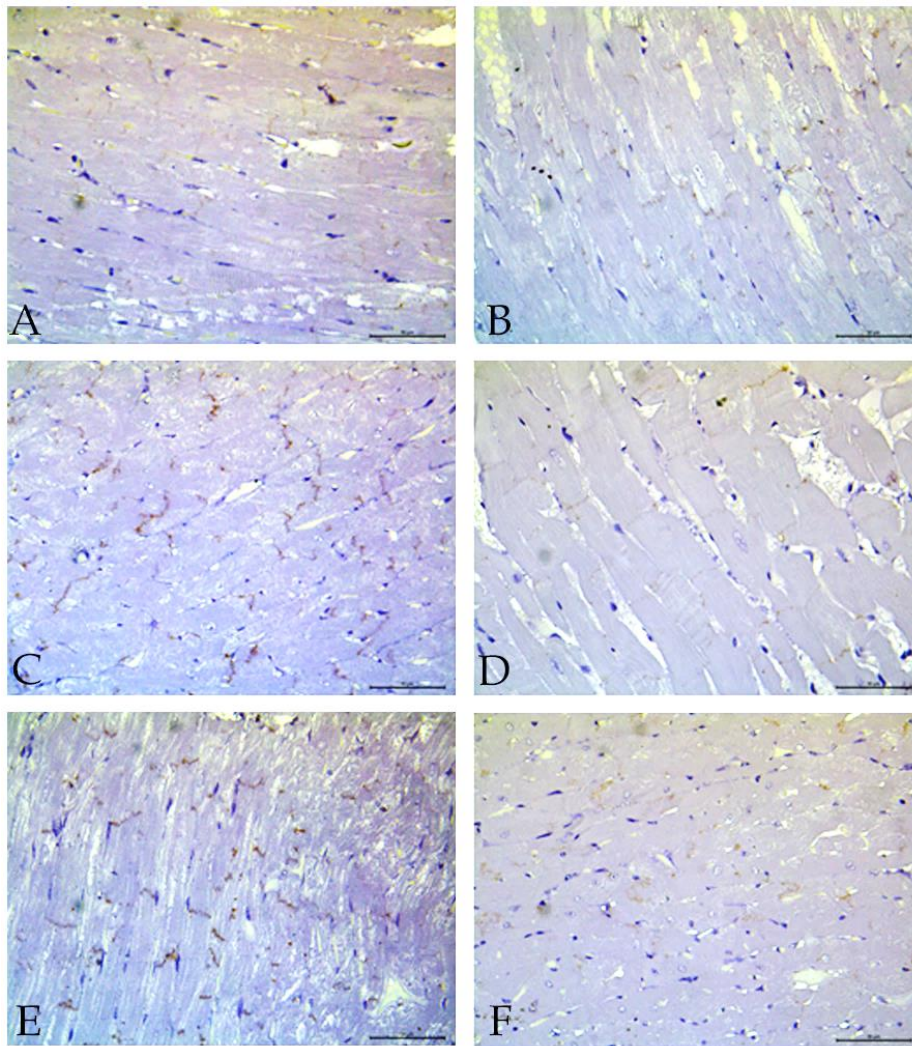


Figure 29. Immunohistochemical detection of Cnx43. A) Control 22±1 °C; B) Control 4±1 °C; C) L-arginine 22±1 °C; D) L-arginine 4±1 °C; E) L-NAME 22±1 °C; F) L-NAME 4±1 °C. Mag. x100, orig.

4.4 NO-synthase system

4.4.1 Neuronal nitric oxide synthase (nNOS)

The results of protein expression of nNOS in RV myocardium are presented in Figure 30. L-NAME treatment ($p < 0.01$) as well as cold acclimation ($p < 0.001$) led to the decrease of nNOS expression in RV myocardium of rats, when compared with untreated room-temperature-acclimated group. On the

other hand, L-arginine treatment did not influence expression of nNOS significantly in RV of room-temperature-acclimated rats, in comparison with untreated control.

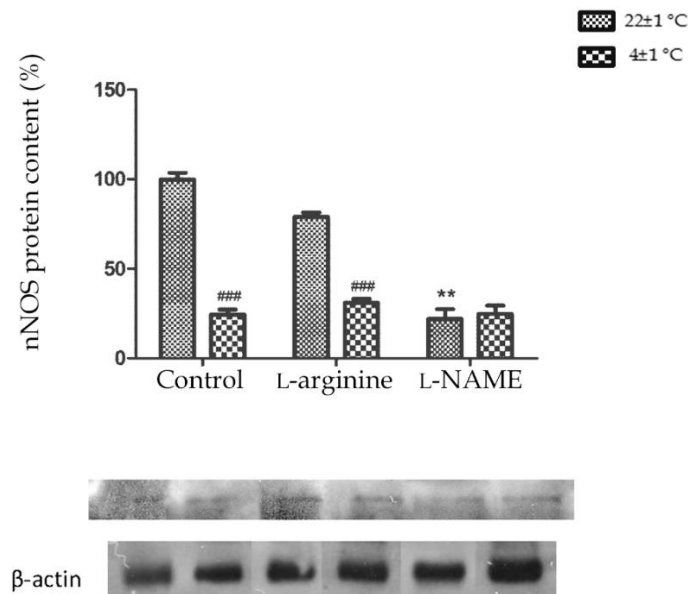


Figure 30. nNOS protein expression in the right ventricle myocardium of rats kept at 22±1 °C or 4±1 °C, untreated, L-arginine or L-NAME-treated. Statistical significance - (**) p<0.01, in comparison with referent control group; (###) p<0.001, in comparison with the same treatment at room temperature.

Immunofluorescence analysis (Figure 31) revealed nNOS localization primarily in cardiomyocytes of RV, with different level of immunoexpression among adjacent cells. Subcellular localization of nNOS was at Z-discs and intercalar discs level, while in L-NAME-treated animals acclimated to room temperature, sarcoplasmic perinuclear granular reaction was also observed.

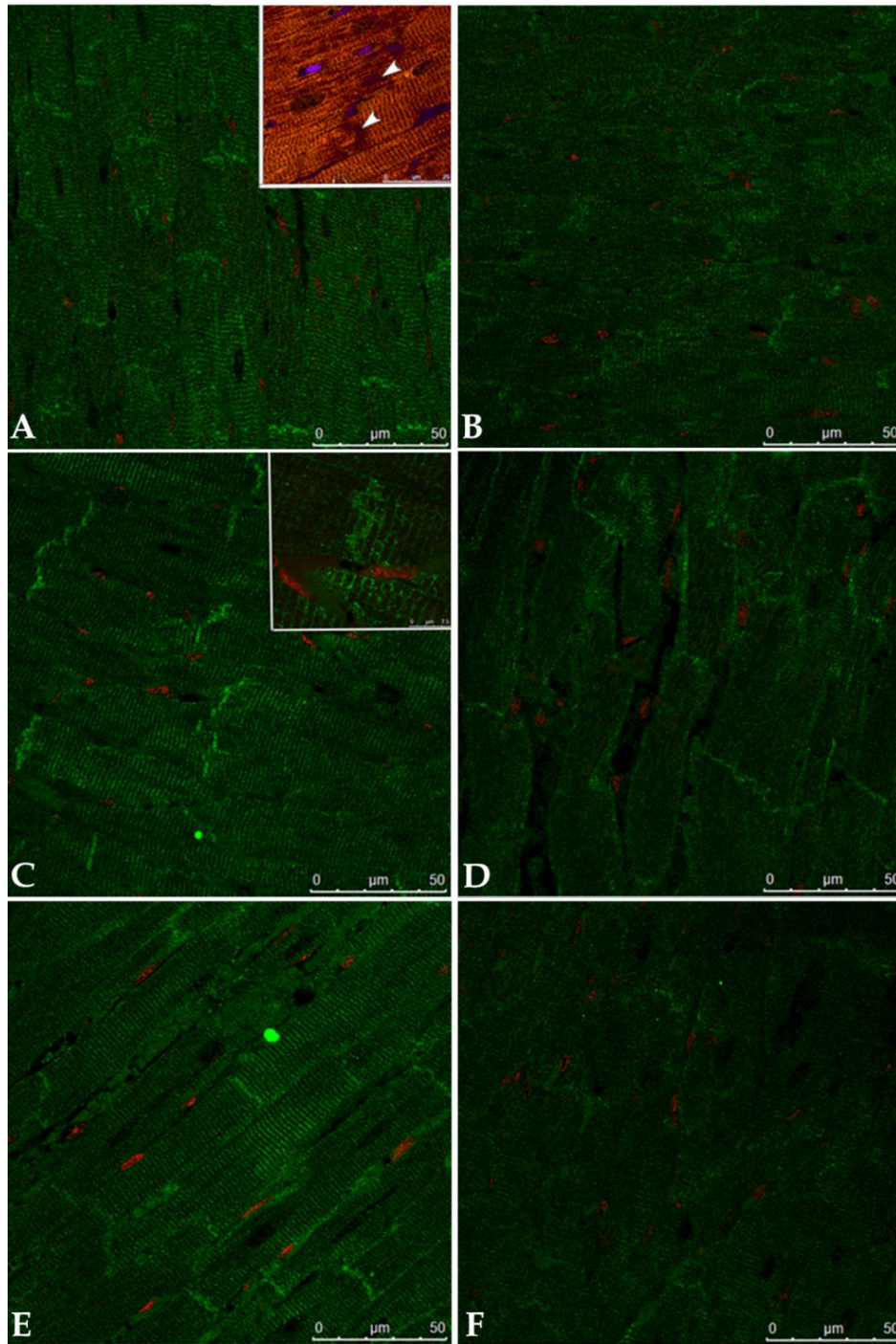


Figure 31. Immunofluorescence detection of nNOS in right ventricle myocardium of rats. A) Control 22±1 °C; B) Control 4±1 °C; C) L-arginine 22±1 °C; D) L-arginine 4±1 °C; E) L-NAME 22±1 °C; F) L-NAME 4±1 °C. Mag. x63, orig. Inset A: intercalar discs-white arrowheads.

4.4.2 Endothelial nitric synthase (eNOS)

The results of protein expression of eNOS in right ventricular myocardium are presented in Figure 32. Cold acclimation, as well as L-arginine treatment increased eNOS expression. No additional effect of L-arginine on cold-induced increase of eNOS expression was noted. L-NAME treatment of room temperature-acclimated animals did not alter expression of eNOS in comparison with untreated control. Also, in L-NAME-treated-cold-acclimated group, eNOS expression was maintained at the level of L-NAME-treated room temperature-acclimated group.

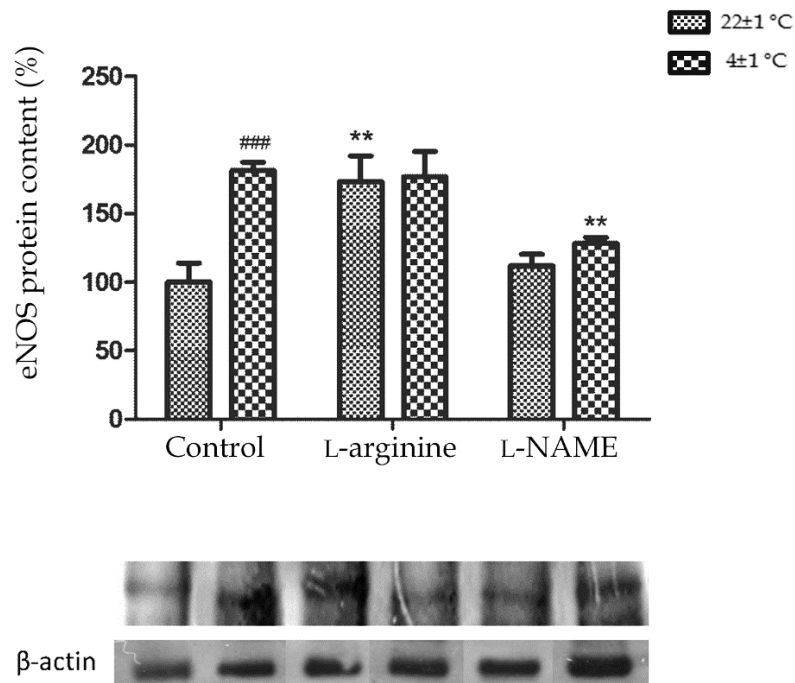


Figure 32. eNOS protein expression in the right ventricle myocardium of rats kept at 22±1 °C or 4±1 °C, untreated, L-arginine or L-NAME-treated. Statistical significance: (**) p<0.01 - in comparison with referent control group; (###) p<0.001 - in comparison with the same treatment at room temperature.

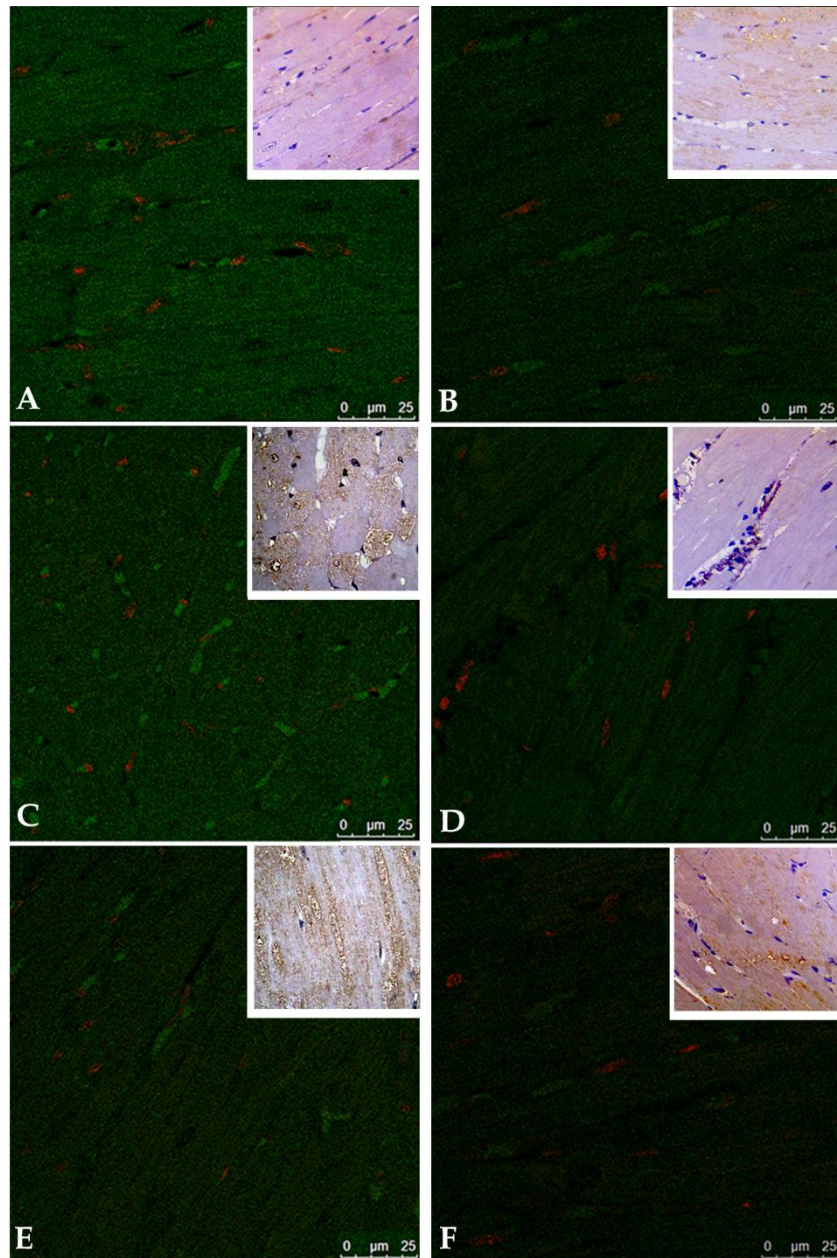


Figure 33. Immunofluorescence and immunohistochemical detection of eNOS in right ventricle myocardium of rats. A) Control 22 ± 1 °C; B) Control 4 ± 1 °C; C) L-arginine 22 ± 1 °C; D) L-arginine 4 ± 1 °C; E) L-NAME 22 ± 1 °C; F) L-NAME 4 ± 1 °C. Mag. x63, orig.

Immunofluorescence (Figure 33) and immunohistochemical (Figure 33 insets) labeling revealed heterogeneous distribution of this enzyme among cardiomyocytes. Granular pattern of immunopositivity was visible in the sarcoplasm, especially in perinuclear region, and in close vicinity to sarcolemma. Also, some cardiomyocytes showed nuclear positivity for eNOS (Figure 33C inset). In the tissue samples from L-arginine and L-NAME-treated animals, immunoreactivity in the interstitium was also visible.

4.4.3 Inducible nitric oxide synthase (iNOS)

iNOS expression was not detected by Western blotting. Similarly, immunofluorescence and immunohistochemical technique did not reveal immunopositivity of cardiomyocytes in either experimental group irrespective of primary antibody used. The only exception is immunofluorescent iNOS positivity of some interstitial and/or perivascular cells in RV myocardia of all experimental groups (Figure 34).

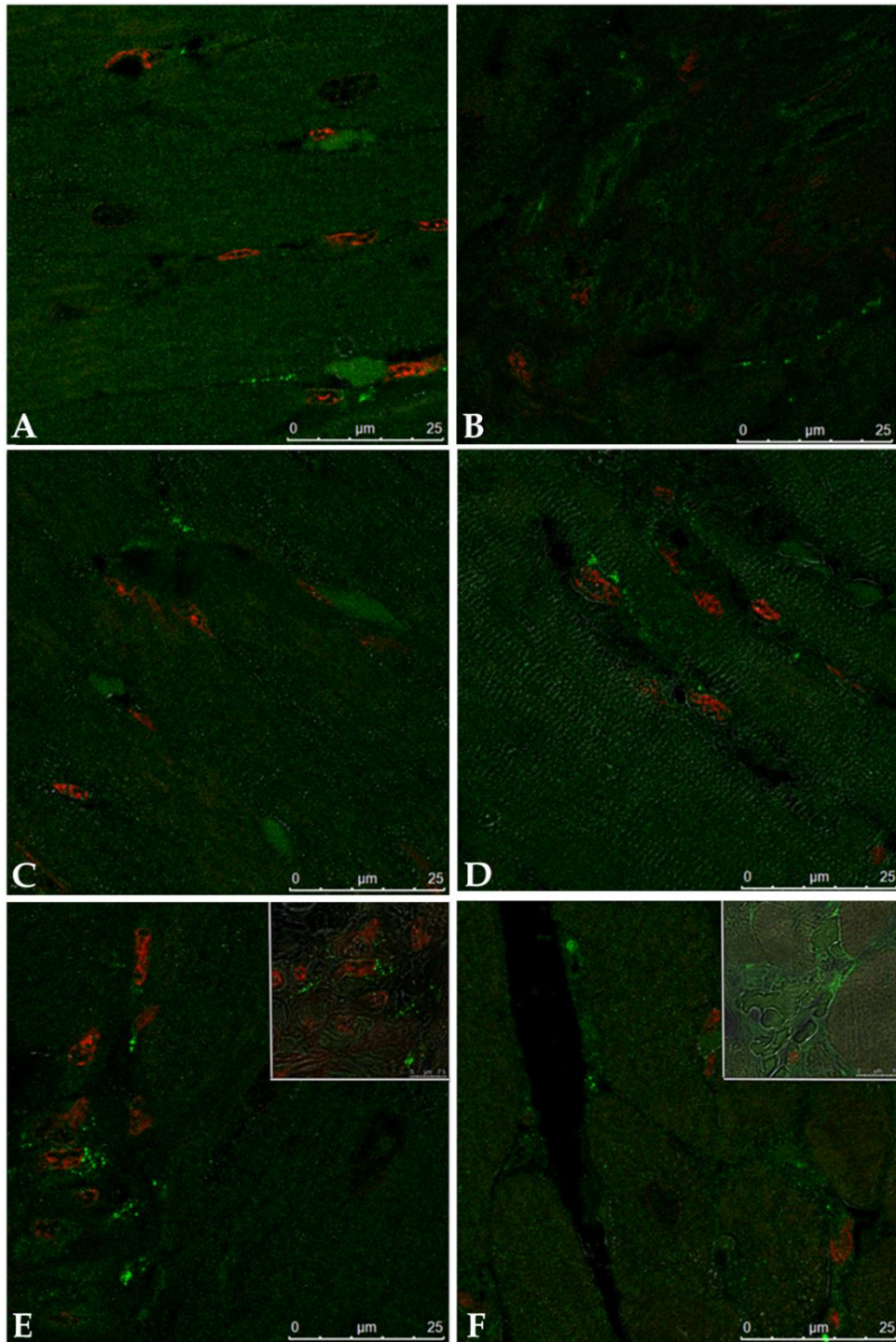


Figure 34. Immunofluorescence detection of iNOS in right ventricle myocardium of rats. A) Control 22±1 °C; B) Control 4±1 °C; C) L-arginine 22±1 °C; D) L-arginine 4±1 °C; E) L-NAME 22±1 °C; F) L-NAME 4±1 °C. Mag. x63, orig.

4.4.4 Heme oxygenase-1 (HO-1)

In comparison with the corresponding controls, both L-arginine and L-NAME treatments decreased HO-1 expression level in the RV myocardium. Also, cold acclimation led to the additional decline of HO-1 expression, without regard of treatment applied (Figure 35).

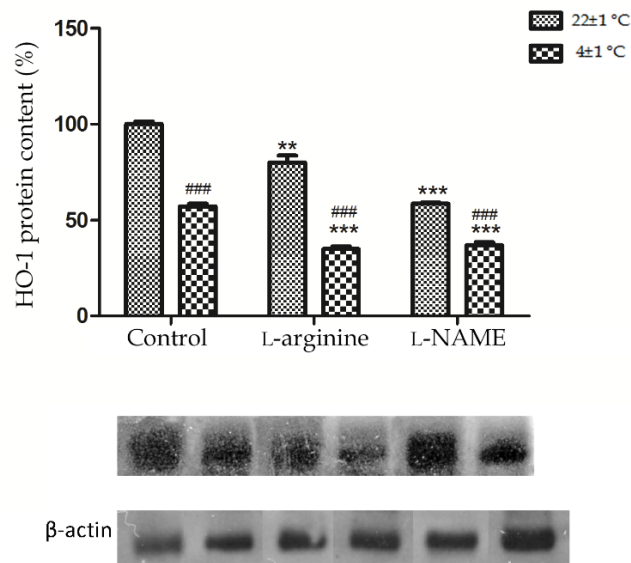


Figure 35. HO-1 protein expression in the right ventricle myocardium of rats kept at 22±1 °C or 4±1 °C, untreated, L-arginine or L-NAME-treated. Statistical significance - (*) in comparison with referent control group: (**) p<0.01, (***) p<0.001; (#) in comparison with the same treatment at room temperature: (###) p<0.001.

Immunohistochemical analysis revealed that HO-1 positivity of the myocardia of control group acclimated to room temperature was weak or moderate, while in control group acclimated to cold heterogeneous distribution of HO-1 among cells was noted (Figure 36). Also, in the control group acclimated to cold, granular cytoplasmic immunopositivity inside of cardiomyocytes was detected.

In the myocardia of L-arginine-treated animals weak immunopositivity was detected without regard to ambient temperature acclimation. In L-NAME-treated group acclimated to room temperature, strong granular immunopositivity in the cytoplasm of cardiomyocytes, especially around nuclei, was noted. The pattern of distribution among cells was heterogeneous. L-NAME-treated group acclimated to cold have weak to moderate cytoplasmic immunopositivity inside of cardiomyocytes and stronger immunopositivity in the interstitium.

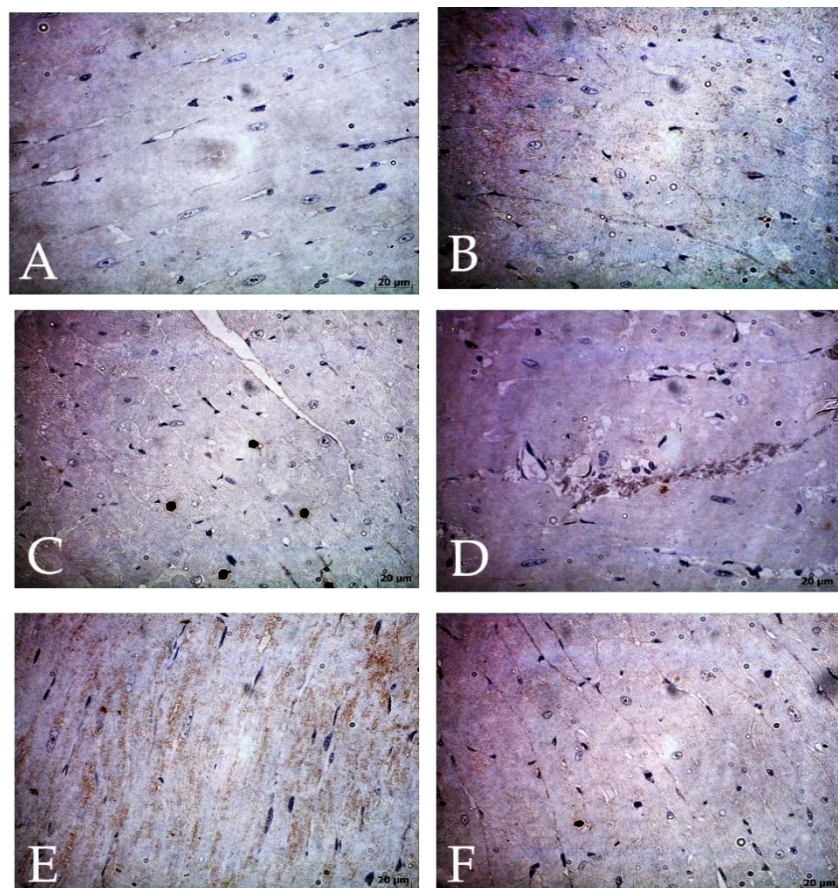


Figure 36. Immunohistochemical detection of HO-1 in right ventricle myocardium of rats. A) Control 22±1 °C; B) Control 4±1 °C; C) L-arginine 22±1 °C; D) L-arginine 4±1 °C; E) L-NAME 22±1 °C; F) L-NAME 4±1 °C. Mag. x100, orig.

4.4.5 Heme oxygenase-2 (HO-2)

Immunohistochemical analysis revealed weak to moderate HO-2 immunopositivity in the tissue of control groups acclimated to room temperature, while in control group acclimated to cold granular cytoplasmic immunopositivity inside of cardiomyocytes was detected. Also, in the control group acclimated to cold, heterogeneous distribution of HO-1 among cells was noted (Figure 37). L-arginine treatments induced increased immunopositivity of cardiomyocytes, while L-NAME treatment induced strong HO-2 immunoexpression on both, room temperature and cold.

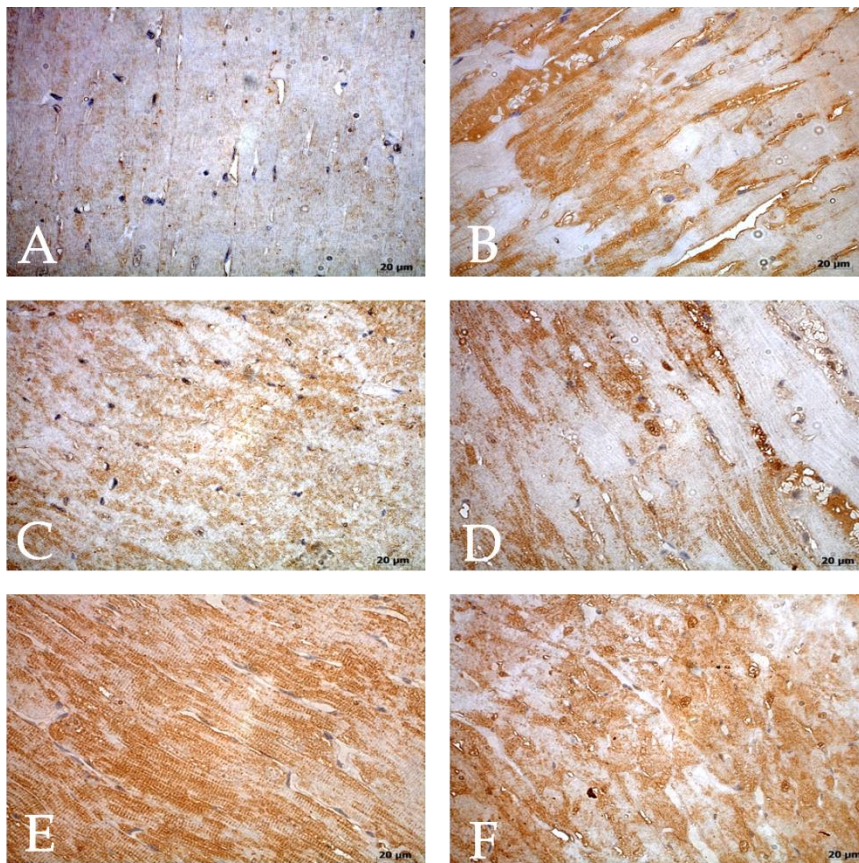


Figure 37. Immunohistochemical detection of HO-2 in right ventricle myocardium of rats. A) Control 22±1 °C; B) Control 4±1 °C; C) L-arginine 22±1 °C; D) L-arginine 4±1 °C; E) L-NAME 22±1 °C; F) L-NAME 4±1 °C. Mag. x100, orig.

4.5 Mitochondrial remodeling

4.5.1 Mitochondrial subpopulations of cardiomyocytes

Morphometric analysis at the ultrastructural level (Figure 41) revealed that cold acclimation decreased profile size of cardiomyocytes mitochondria especially of perinuclear and intersarcomeral subpopulations, in comparison with the room temperature-acclimated group.

L-arginine treatment at room temperature also decreased profile surface of all mitochondrial subpopulations of cardiomyocytes in comparison with the appropriate control (Table 6). Cold-acclimated L-arginine treated animals had statistically significant increased mitochondrial profile size of all subpopulations, in comparison with both cold acclimated control and L-arginine-treated animals acclimated to room temperature.

L-NAME treatment during room temperature acclimation did not affect mitochondrial size. At the other side, when compared to both cold acclimated control and L-NAME-treated group acclimated to room temperature, profile surface of perinuclear and subsarcolemal mitochondria increased in cardiomyocytes of cold acclimated L-NAME-treated animals, while in intersarcomeral region mitochondrial profiles decreased (Figures 38-41).

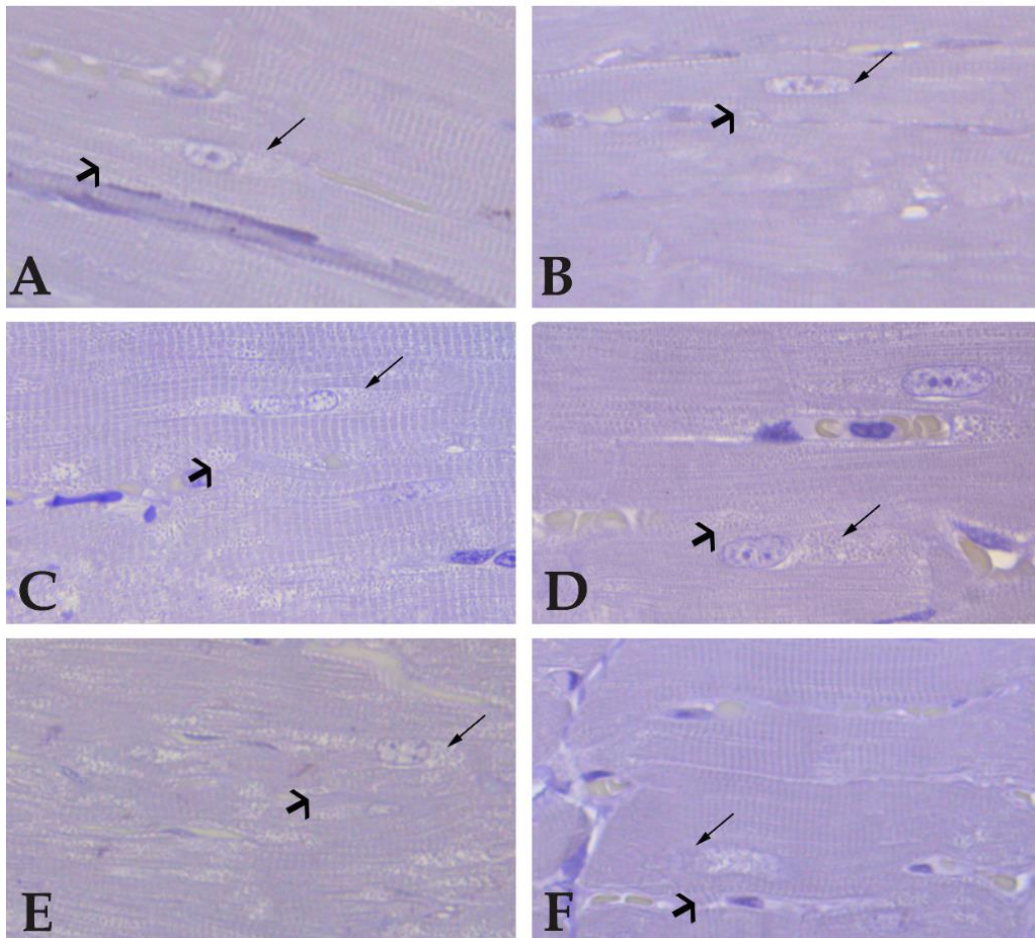


Figure 38. Mitochondrial subpopulation in cardiomyocyte: perinuclear (thin arrow), subsarcolemal (thick arrow) and intersarcomeral's. Hematoxylin staining, mag. x100, orig. A) Control 22 ± 1 °C; B) Control 4 ± 1 °C; C) L-arginine 22 ± 1 °C; D) L-arginine 4 ± 1 °C; E) L-NAME 22 ± 1 °C; F) L-NAME 4 ± 1 °C. Mag. x100, orig.

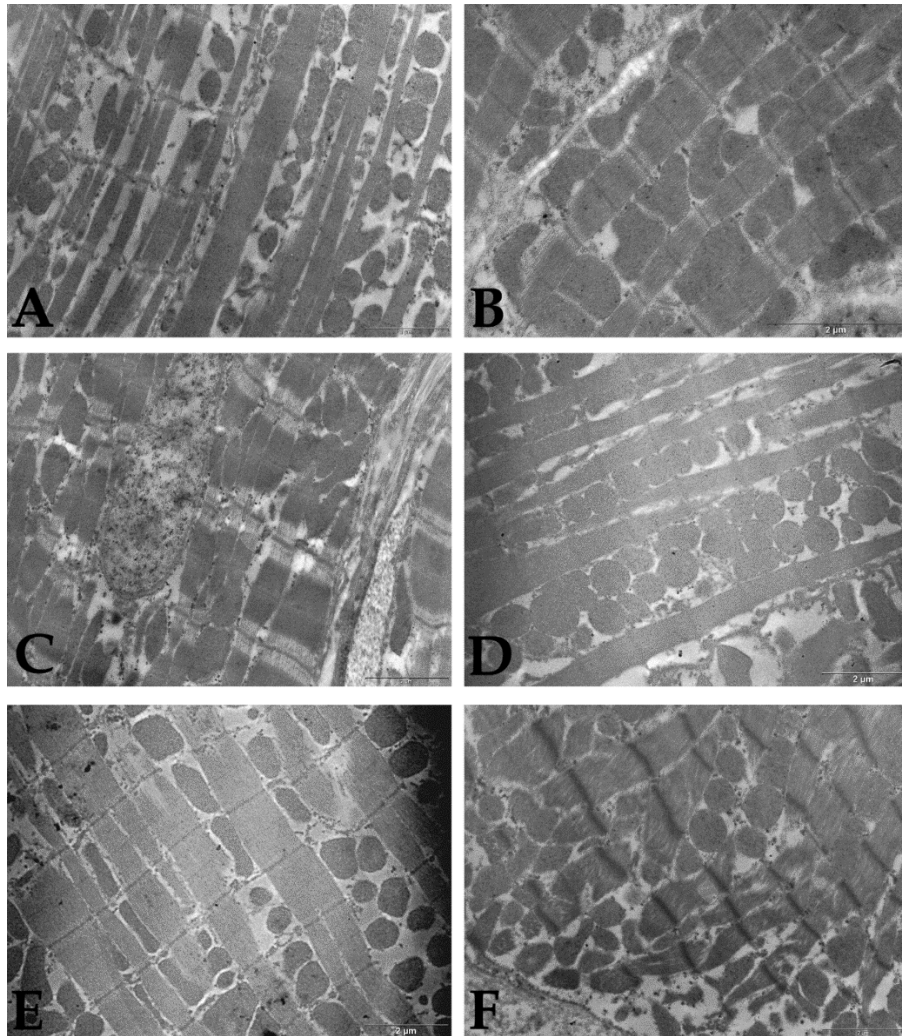


Figure 39. Ultrastructure of mitochondrial subpopulations. A) Control 22 ± 1 °C; B) Control 4 ± 1 °C; C) L-arginine 22 ± 1 °C; D) L-arginine 4 ± 1 °C; E) L-NAME 22 ± 1 °C; F) L-NAME 4 ± 1 °C. Mag. x15000, orig.

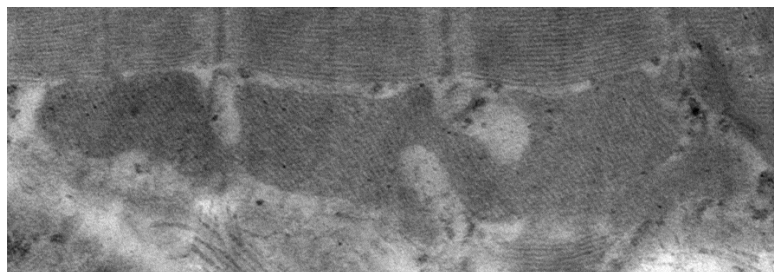


Figure 40. Mitochondrial reticulum in cardiomyocyte of cold-acclimated animals. Mag. x15000, orig.

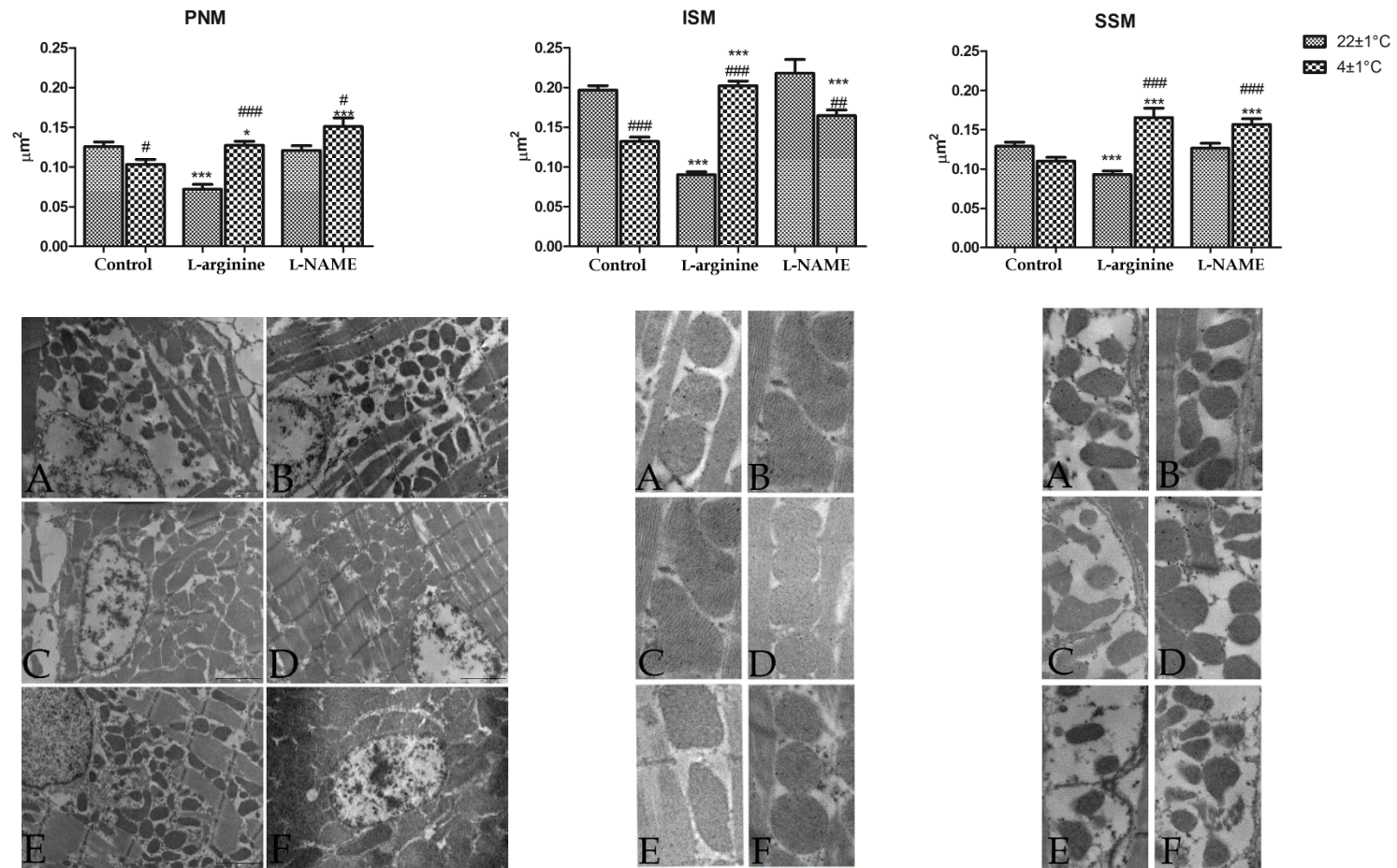


Figure 41. Profile surface size of three mitochondrial populations in cardiomyocytes. PNM-perinuclear; ISM-intersarcomeral; SSM-subsarcolemal and their ultrastructural appearance. A) Control 22±1 °C; B) Control 4±1 °C; C) L-arginine 22±1 °C; D) L-arginine 4±1 °C; E) L-NAME 22±1°C; F) L-NAME 4±1 °C. Statistical significance - (*) comparison between experimental groups and appropriate controls: (*) p<0.05, (***) p<0.001; (#) comparison between experimental groups on different temperature: (#) p<0.05, (##) p<0.01, (###) p<0.001.

4.5.2 Mitochondrial fusion markers – mitofusin 1 (Mfn1) and 2 (Mfn2)

Mfn1 protein expression statistically did not alter after cold exposure nor after drug treatments, although cold exposure slightly increased expression of this protein in the tissue (Figure 42) as compared to room temperature kept controls.

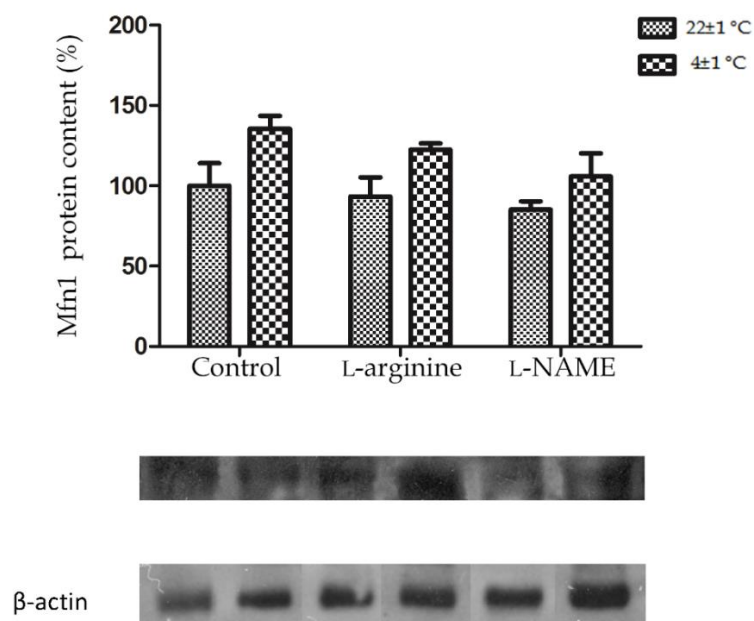


Figure 42. Mfn1 protein expression in the right ventricle myocardium of rats kept at 22±1 °C or 4±1 °C, untreated, L-arginine or L-NAME-treated. No statistical significance was noted.

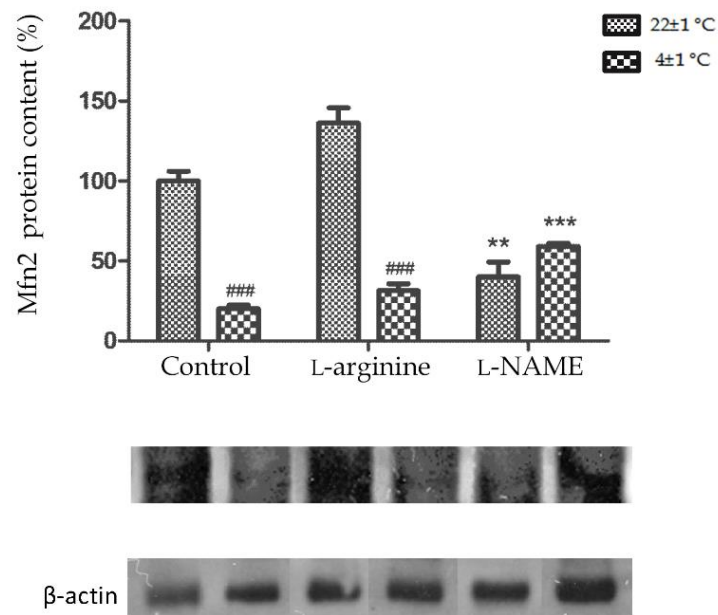


Figure 43. Mfn2 protein expression in the right ventricle myocardium of rats kept at 22±1 °C or 4±1 °C, untreated, L-arginine or L-NAME-treated. Statistical significance - (*) in comparison with appropriate controls: (**) p<0.01, (***) p<0.001; (#) in comparison with the same treatment at the room temperature: (###) p<0.001.

Mfn2 expression decreased in myocardium after cold acclimation independent of treatment applied, similarly as L-NAME-treatment. On the other hand, L-arginine treatment on room temperature did not alter Mfn2 expression significantly in the RV myocardium (Figure 43).

L-arginine treatment on room temperature decreased mitochondrial size despite the fact that the level of Mfn2 was not changed, while L-NAME treatment reversed the size of mitochondria although the level of Mfn2 declines. Another factor that affects the reduction of mitochondrial size is mitofilin.

4.5.3 Mitochondrial division marker – mitofilin

RV myocardial level of mitofilin protein expression decreased after cold exposure as after L-arginine and L-NAME treatments (Figure 44) in comparison to the room-temperature acclimated controls.

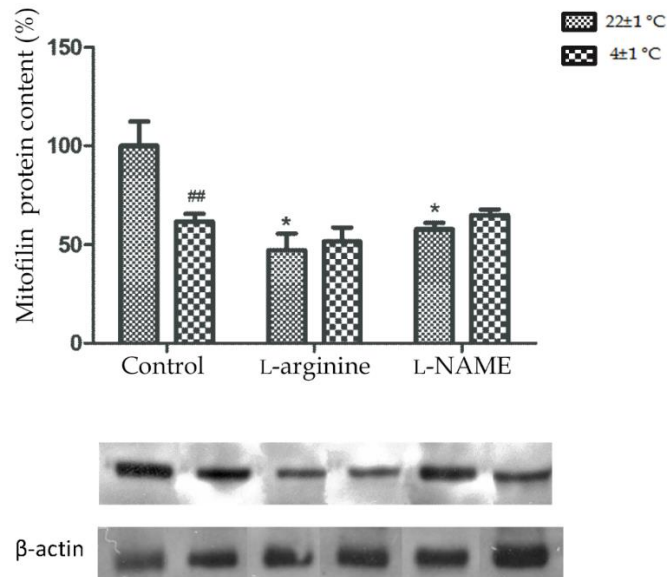


Figure 44. Mitofilin protein expression in the right ventricle myocardium of rats kept at 22±1 °C or 4±1 °C, untreated, L-arginine or L-NAME-treated. Statistical significance: (*) p<0.05 - in comparison with appropriate controls; (##) p<0.01 - in comparison with the same treatment at the room temperature.

4.5.4 Uncoupling protein 2 (UCP2)

Weak to moderate granular UCP2 cytoplasmic immunopositivity in cardiomyocytes of control and L-NAME-treated animals was detected. Also, slight nuclear positivity was also demonstrated in these cells. In comparison with control group, immunopositivity of cardiomyocytes of L-arginine-treated room temperature-acclimated animals was slightly increased, visible also as a granular cytoplasmic and nuclear reaction, homogenously distributed among the cells. In the cardiomyocytes of L-arginine-treated cold-acclimated group,

the level of immunopositivity was similar to the level noted in the L-arginine-treated group acclimated to room temperature, with the strongest reaction in the subsarcolemal region.

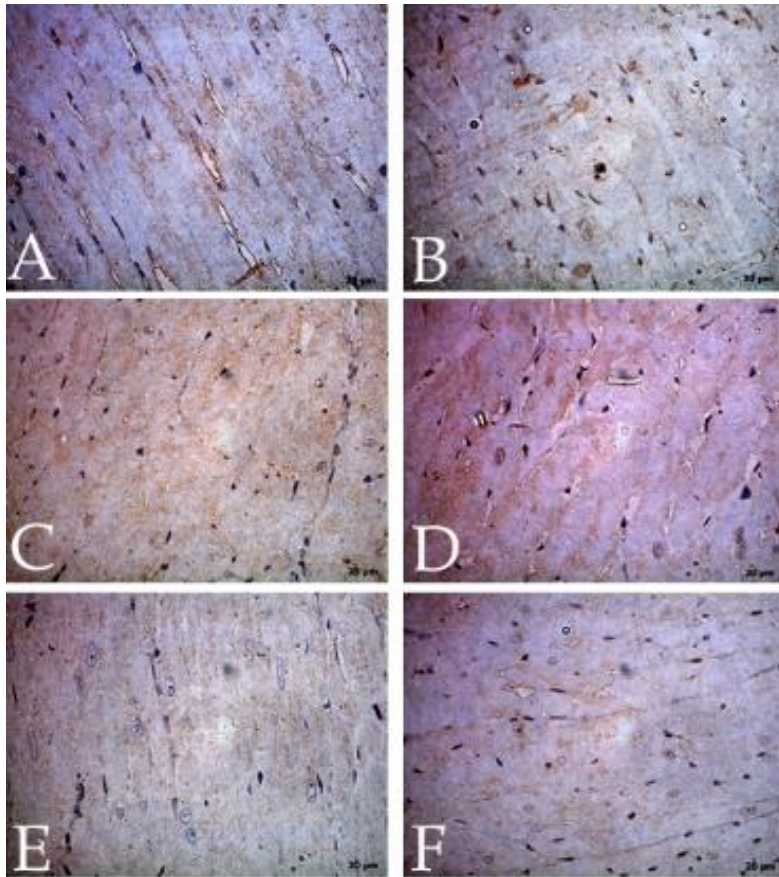


Figure 45. Immunohistochemical detection of UCP2. A) Control 22±1 °C; B) Control 4±1 °C; C) L-arginine 22±1 °C; D) L-arginine 4±1 °C; E) L-NAME 22±1 °C; F) L-NAME 4±1 °C. Mag. x100, orig.

4.6 Sarcoplasmic reticulum remodeling

In order to analyze potential sarcoplasmic reticulum remodeling, protein expression of calnexin and sarcoplasmic reticulum Ca²⁺ ATPase (SERCA2) was detected.

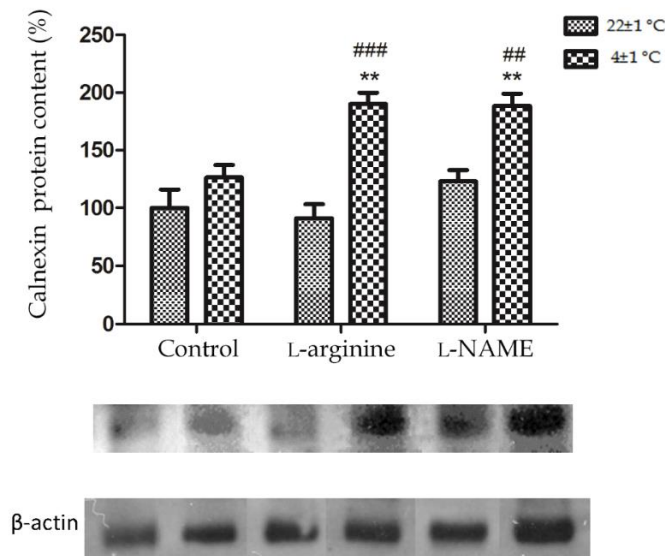


Figure 46. Calnexin protein expression in the right ventricle myocardium of rats kept at 22±1 °C or 4±1 °C, untreated, L-arginine or L-NAME-treated. Statistical significance - (*) in comparison with appropriate controls: (**) p<0.01; (#) in comparison with the same treatment at the room temperature: (##) p<0.01; (###) p<0.001.

Protein expression of calnexin was increased in all cold acclimated groups, especially after drug treatments, where statistically significant difference was noted in comparison with both cold-acclimated control and room temperature-acclimated groups treated same way.

Immunohistochemical detection of calnexin (Figure 47) in the RV myocardium revealed mostly homogenous distribution of this protein among cardiomyocytes in all experimental groups. A granular immunopositivity was visible in the sarcoplasm, in particular in perinuclear region, and in close vicinity to sarcolemma. This was especially evident in the tissue of cold-acclimated L-arginine treated group, where strong granular reactivity around nuclei and in subsarcolemmal region was visible.

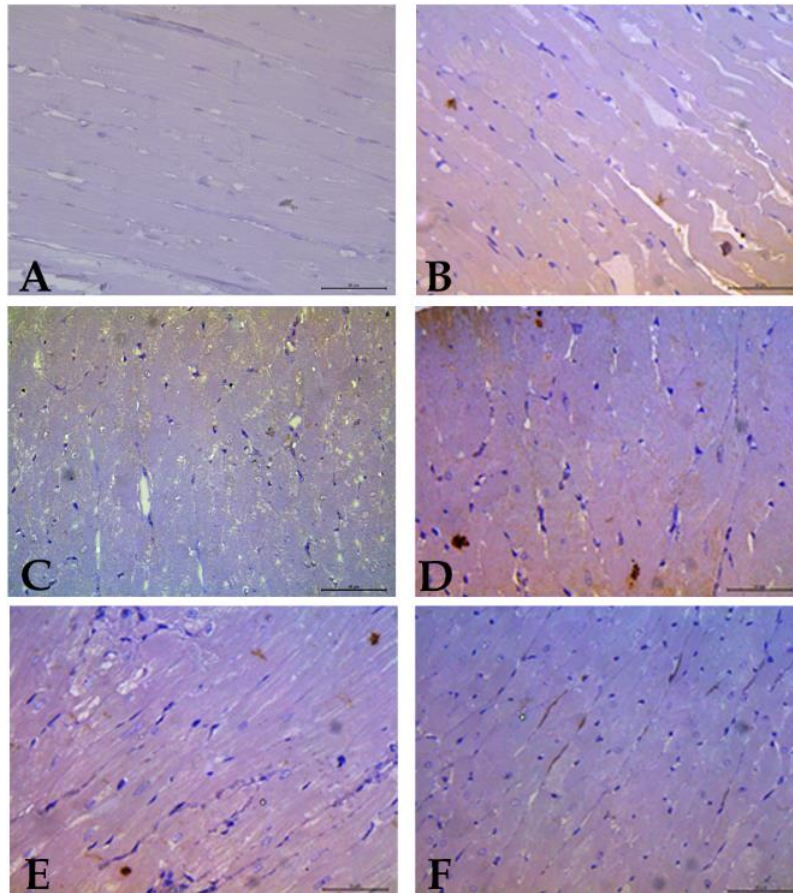


Figure 47. Immunohistochemical detection of calnexin. A) Control 22 ± 1 °C; B) Control 4 ± 1 °C; C) L-arginine 22 ± 1 °C; D) L-arginine 4 ± 1 °C; E) L-NAME 22 ± 1 °C; F) L-NAME 4 ± 1 °C. Mag. $\times 100$, orig.

Cold acclimation *per se* significantly decreased protein expression of SERCA2 in RV myocardium (Figure 48).

L-arginine and L-NAME treatments at room temperature did not change the level of SERCA2 in the tissue, but they increased it during cold acclimation, in comparison with the same treatment during room temperature-acclimation (L-arginine) and in comparison with cold acclimated control (L-arginine and L-NAME)

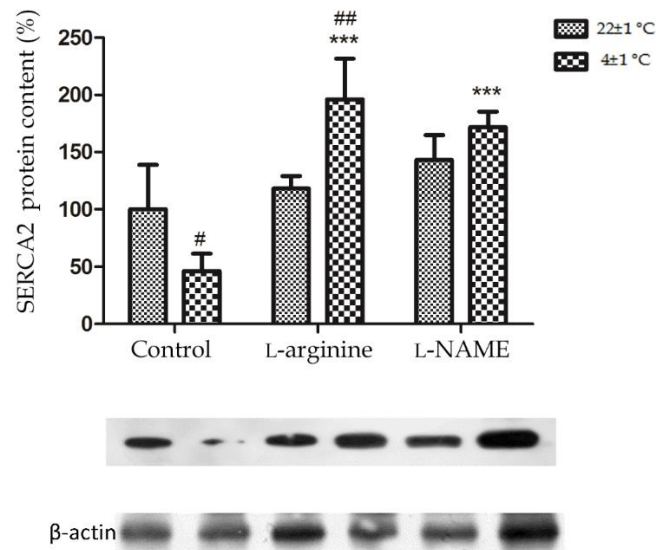


Figure 48. SERCA2 protein expression in the right ventricle myocardium of rats kept at 22±1 °C or 4±1 °C, untreated, L-arginine or L-NAME-treated. Statistical significance - (*) in comparison with appropriate controls: (***) p<0.001; (#) in comparison with the same treatment at the room temperature: (#) p<0.05; (##) p<0.01.

4.7 Ultrastructural alterations of right ventricle myocardium

Besides gross ultrastructural changes characteristic for every experimental group additional electron-microscopic analysis revealed alteration in cardiomyocytes' and interstitial space. One of the most profound histological changes of myocardium induced by L-NAME treatment was fibrosis, caused by deposition of large amount of collagen fibers (Figure 49). In addition to quantitative difference in fibers amount in L-arginine treatment comparing to control (Figure 49C), the collagen fibers also appeared thicker.

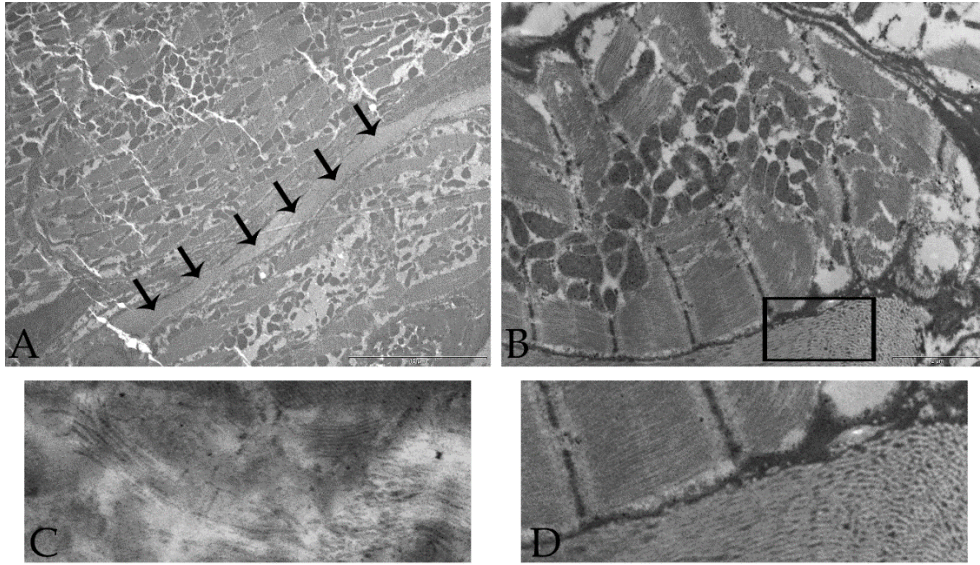


Figure 49. Fibrosis (→) is the hallmark of L-NAME treatment. A, B, D) L-NAME 22±1 °C; C) Control 4±1 °C. D) - enlarged area marked on B. Mag. A - x2650; B-x8800; C, D-x15000, orig.

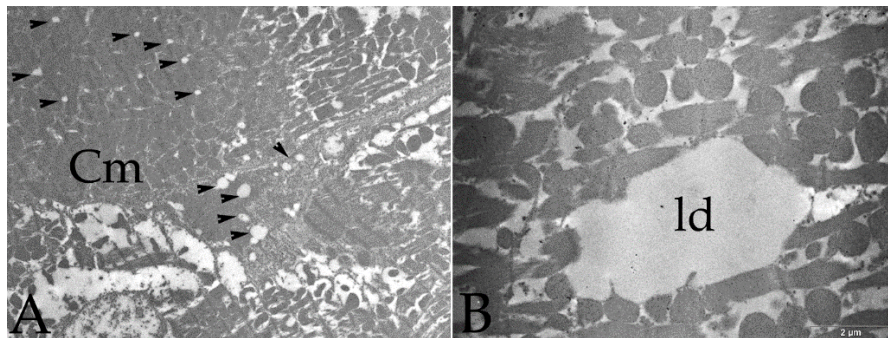


Figure 50. Lipid depositions (▶, ld) in cardiomyocytes (Cm) cytoplasm and interstitial cells. A, B) L-arginine 4±1 °C. Mag. A - x2650; B -x8800, orig.

In L-arginine-treated, cold-acclimated animal, large depositions of lipid bodies were observed. Lipid bodies were localized in cardiomyocyte as well as in interstitial cell, presumably fibroblasts (Figure 50).

In cardiomyocyte of L-arginine and L-NAME treated animals independent of ambient temperature a small number of lipofuscin granules were found in perinuclear mitochondrial area (Figure 51).

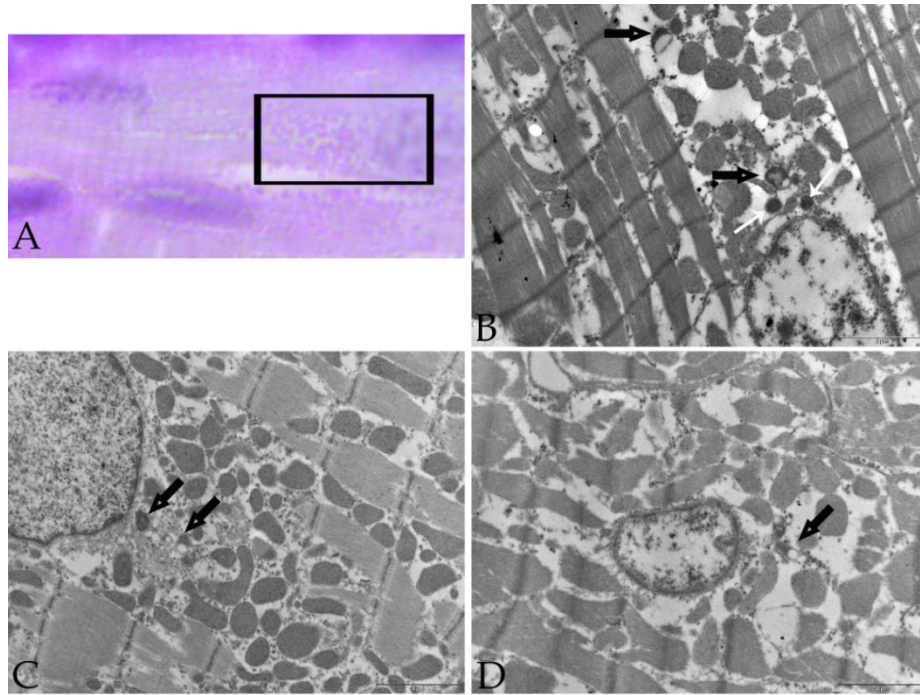


Figure 51. Lipofuscinogenesis in cardiomyocytes. A, B) L-arginine 4 ± 1 °C; C) L-NAME 22 ± 1 °C; D) L-NAME 4 ± 1 °C. Mag. A- $\times 100$; B-D- $\times 8800$.

5. DISCUSSION

This thesis deals with structural remodeling of rats' RV myocardium induced by chronic modulation of NO-producing system and cold acclimation. In order to examine possible effects of NO on myocardial structure and molecular basis of its remodeling, adult male rats were treated with L-arginine and L-NAME for 45 days on room temperature or cold, respectively.

5.1. Structural remodeling - cardiomyocyte hypertrophy, tissue proliferation and apoptosis

Our results demonstrated that cold acclimation *per se* does not significantly alter the volume densities of myocardial tissue components, but leads to a trend in cardiomyocyte hypertrophy followed by a downward trend in capillarity (Hmaid *et al.*, 2016). Also, cold-acclimated control animals showed a significant decrease of PCNA expression in comparison with room temperature-acclimated control animals. Tissue PCNA immunoreactivity was visible decreased after cold exposure, since in cold exposed control group immunopositivity of cardiomyocytes was rare and hardly visible, mostly cytoplasmic. Slightly stronger PCNA positivity was detected in the endothelial cells and in the fibrous sheet at the surface of myocardial tissue. Taken together, these results do not indicate the cold-induced RV hypertrophy nor the proliferation of cardiomyocytes, at least at the histological level.

The only significant effect of L-arginine treatment demonstrated in this study is an increase of cardiomyocyte diameter, i.e. their hypertrophy. Since we were unable to identify any pathological changes in the myocardial structure (no signs of increased collagen deposition or of myofibril distortion), these results demonstrated that the structural alterations observed after the L-arginine treatment corresponded to physiologic cardiac hypertrophy. Namely, L-arginine treatment in room temperature-acclimated rats led to cardiomyocyte hypertrophy which was followed by a simultaneous increase in capillarity and

interstitial connective tissue in the myocardium, maintaining the relative ratio of tissue components unaltered. Regardless of the increase in cardiomyocyte size, no statistically significant changes of their volume density or in blood vessels and stromal connective tissue occurred in the myocardium. L-arginine treatment following cold acclimation acts synergistically with cold by increasing cardiomyocyte size and decreasing myocardial capillarity. Compared to the room temperature-acclimated group treated with L-arginine, the volume density was increased and was followed by a decrease in blood vessel volume density. This imbalance between cardiomyocyte enlargement and capillary supply could be considered to be the effect of cold, since a decreased trend in myocardial capillarity was observed in all cold-acclimated groups.

In comparison with room temperature acclimated control group, the expression level of PCNA, a marker of cell proliferation, was unchanged in the myocardia of L-arginine treated rats, without regard to ambient temperature acclimation. Still, PCNA was mostly localized in the cardiomyocytes nuclei in L-arginine-treated room temperature-acclimated group, while in cold acclimated L-arginine treated animals, was localized mostly in the cytoplasmic compartment of cardiomyocytes.

Cardiomyocyte hypertrophy (enlargement) occurs *via* intracellular signaling pathways within these cells (**Heineke and Molkentin, 2006**) and is commonly connected with cardiac hypertrophy, which refers to cardiac thickening and remodeling. This process may be due to cardiac pathology, to long-term exercise training (**Pelliccia et al., 2002; Maron et al., 2003**) or chronic cold exposure (**Cheng and Hauton, 2008**). Hypertrophic effect of chronic L-arginine supplementation on cardiomyocyte observed in our study is inconsistent with previous findings demonstrating the anti-proliferative effects of NO in the heart (**Kolpakov et al., 1995**). It should be noted that the anti-proliferative effect of NO and therefore of L-arginine, was observed during L-arginine treatment of existing pathological myocardial hypertrophy, a

condition that is known to be associated with reduced NO biosynthesis (Pechanova *et al.*, 1999). Our previous studies demonstrated L-arginine-stimulated thermogenic activation in brown adipose tissue and acceleration of cold-induced antioxidative defense in the skeletal muscle of these animals (Petrovic *et al.*, 2005; Petrovic *et al.*, 2008), suggesting that the observed cardiomyocyte hypertrophy in L-arginine-treated animals is an indirect consequence of increased peripheral circulatory demands. It remains to be elucidated whether L-arginine-induced hypertrophy of cardiomyocytes also includes direct NO-dependent or NO-independent mechanisms. In line with the NO-independent effects of applied treatments are the results showing that NOSs inhibitor, L-NAME, displayed similar PCNA expression level, as L-arginine during cold acclimation. Notably however, immunohistochemical examination revealed various PCNA-positive cells that undergo proliferation by these treatments. Precisely, cold-acclimated L-NAME treated animals showed a significant increase of PCNA immunoexpression in RV myocardium in comparison with room temperature acclimated L-NAME treated animals. Also, in the tissue of L-NAME treated animals, without regard to acclimation temperature, immunoreactivity of cardiomyocytes was strong, cytoplasmic and sometimes nuclear, especially in the regions of irregular cardiomyocytic distribution. Besides, strong reactivity of connective tissue was detected, with cytoplasmic and nuclear immunopositivity of fibrocytes and fibroblasts clearly indicating pro-fibrotic changes.

Essentially, the most prominent effect of the NOS inhibitor, L-NAME, on rat myocardia observed in this study was fibrosis which was demonstrated as an increase in interstitial connective tissue volume density accompanied by increased collagen abundance in the interstitium. This effect was followed by cardiomyocyte hypertrophy despite a decrease in their volume density. These alterations were observed in both the room temperature- and cold-acclimated L-NAME-treated groups, compared with the appropriate controls. When compared to the room temperature-acclimated group treated with L-NAME,

identical treatment in cold-acclimated animals additionally enhanced interstitial fibrosis (**Hmaid *et al.*, 2016**).

Pathological cardiac hypertrophy is characterized not only by the growth of myocardial fibers, but also by changes in cardiac architecture and cellular metabolism and, finally, by myocardial dysfunction with increased morbidity and mortality. Specific genetic expression profiles, different from the adaptive profiles involved in physiological hypertrophy, are activated (**McMullen *et al.*, 2003**). Pressure or volume overload causes initial hypertrophy, which represents a compensatory mechanism for maintaining cardiac function. If these stimuli persist, structural and functional cardiac anomalies develop. Thus, cardiac sarcomeres become bigger with abnormal proteins, resulting in a bioenergetics deficit that affects their function. The cardiac muscle fibers are disorganized, and separated by an excessive interstitial connective tissue since collagen metabolism is changed, resulting in decreased degradation and increased deposition of collagen in the extracellular matrix (**Diez *et al.*, 1995; Rossi, 2001**). In these initial phases, collagen composition is normal with an enlarged ventricle (**Creemers and Pinto, 2011**). However, with long-term myocardial remodeling, there is a buildup of fibroblasts and extracellular matrix proteins, causing abnormal structure and function in the heart, resulting in the condition known as myocardial fibrosis (**Brown *et al.*, 2005; Krenning *et al.*, 2010**), which is closely related to the amount of ventricular hypertrophy (**Creemers and Pinto, 2011**). Consequently, myocardial fibrosis causes regional myocardial dysfunction (**Rajiv *et al.*, 2004**).

The mechanisms responsible for myocardial fibrosis in hypertrophy are still not fully understood. However, growth factors such as fibroblast growth factor-2 (FGF-2), transforming growth factor β (TGF β), platelet-derived growth factor, and plasma hormones such as angiotensin II, endothelin-1 and catecholamines, have been found to contribute to the regulation of this process (**Creemers and Pinto, 2011**). With regard to the effects of chronic L-NAME administration, inhibited NOS activity in the myocardium, brain and kidney,

and induced hypertension, hypertrophy and fibrotic remodeling of the left ventricle have been demonstrated, suggesting that chronic L-NAME treatment could be used in a model of pathological cardiac hypertrophy. Myocardial structural alterations such as fibrosis and an increase in collagenous proteins were described after 4 weeks of L-NAME administration (**Pechanova et al., 1997; Pechanova et al., 1999**), while extensive areas of fibrosis and myocardial necrosis were observed after 8 weeks of L-NAME administration (**Moreno et al., 1995**). It should be mentioned that the dose of L-NAME used in our study (approximately 10 mg/kg/day) was four times lower than that in the above-mentioned experiments (40 mg/kg/day), and is considered a low dose which was demonstrated to have no toxic effects (**Saha et al., 1996**).

In summary, chronic L-arginine supplementation induces low level right ventricular hypertrophy in room temperature-acclimated rats and significantly augments ventricular hypertrophy in cold-acclimated animals. This L-arginine-induced ventricular hypertrophy could be considered physiological, since no signs of myocardial fibrosis were observed. In contrast, chronic treatment with L-NAME, an inhibitor of NOSs, caused pathological right ventricular hypertrophy with signs of myocardial fibrosis, demonstrating the role of NOS producing pathway impairment, most likely associated also with NO depletion, in the development of cardiovascular disease.

Small number of apoptotic nuclei is not unexpected after long-term 45 day treatment, but appearance of apoptotic cardiomyocytes after L-arginine treatment at room temperature suggests higher cell turnover and possible link with cardiomyocyte growth. Namely, as **Fernandez-Sola et al. (2006)** showed, myocyte growth and hypertrophy have been found not to be adaptive processes only but also key points in apoptotic activation (**van Empel and De Windt, 2004**). Although there are strong evidence that myocardium rarely go through apoptosis in normal state, this mode of cell death has been implicated in a variety of cardiac diseases (**Saraste et al., 1999**) and (**Neuss et al., 2001**) may be responsible for the progressive intrinsic contractile dysfunction and

myocyte loss in dilated cardiomyopathies of either ischemic or idiopathic origin (**Sabahh and Sharov, 1998**) and (**Regula and Kirshenbaum, 2005**). Also, **Jänkälä *et al.* (2002)** described the induction of myocardial apoptosis in rats through combined calcium carbimide and ethanol treatment. It is interesting that the degree of cardiac apoptosis in long-term high-dose alcohol consumers was similar to that found in hypertensive patients with comparable structural heart damage. Further studies are needed to determine specific mechanisms and factors influencing the triggering and development of cardiomyocyte apoptosis (**Feuerstein, 2001; Gustafsson and Gottlieb, 2003; Webster and Bishopric, 2003**).

Improvement in the methodological approach to the analysis of the myocardium has provided clear evidence of cardiac myocyte proliferation, questioning the general belief that the growth of the adult heart under physiological and pathological conditions can occur only by cellular hypertrophy. Myocyte regeneration contributes via myocyte death to the physiological turnover of myocytes and via myocyte hypertrophy to cardiac remodeling. Several questions, however, remain to be answered. Among them, it is still unknown whether myocyte multiplication exerts a positive and/or negative effect on ventricular anatomy and cardiac function. The addition of newly generated myocytes leads to cavity dilation with relative thinning of the wall. Conversely, myocyte proliferation, characterized by the parallel addition of cells, can be expected to increase wall thickness, decrease chamber size, and ameliorate cardiac performance (**Leri *et al.*, 2002**).

Cardiac hypertrophy and ensuing heart failure are among the most common causes of mortality worldwide, yet the triggering mechanisms for progression of hypertrophy to failure are not fully understood. Tissue homeostasis depends on proper relationships between cell proliferation, differentiation, and death and any imbalance between them results in compromised cardiac function (**Sarkar *et al.*, 2004**). Taken together, our data are in line with findings that the stress of extensive myocardial damage from

longstanding hypertrophy may cause myocytes to reenter the cell cycle (**Sarkar et al., 2004**). Namely, **Sarkar et al. (2004)** demonstrated, for the first time in an animal model, that cell death and regeneration occur simultaneously in myocytes during end-stage heart failure, a phenomenon not observed at the onset of the disease process.

5.2. Cardiomyocyte nuclear changes and binucleation

With regard to cardiomyocyte nuclear size changes, our results demonstrated a reduction in all L-arginine- and L-NAME-treated groups, as well as in the cold-acclimated control group. The greatest reduction in nuclear size was noted in the L-NAME-treated animals acclimated to cold. It was shown that cardiomyocyte nuclear size decreased in rats acutely exposed to extreme cold (**Meneghini et al., 2008**). To our knowledge, the present study showed for the first time chronic cold acclimation-induced nuclear size reduction. Considering cardiomyocyte nuclear size reduction in the chronic L-arginine and L-NAME-treated groups, this phenomenon may be a feedback to hypertrophic cells involved in preventing further growth of cardiomyocytes.

Our study indicates that cardiomyocytes nuclear alterations, involving increased binucleation and decreased nuclear size (expressed as decreased cross-sectional area of nuclei), play important role in the myocardial and cardiomyocytes hypertrophy. Namely, the present work demonstrated increase in binucleation of RV cardiomyocytes in L-NAME-treated group which was followed by the decrease of nuclear size, primarily in mono nucleated cardiomyocytes.

Cellular binucleation indicates acytokinetic mitosis which in cardiomyocytes occurs during the early postnatal transition from hyperplastic to hypertrophic growth (**Katzberg et al., 1977; Anversa et al., 1980; Clubb and Bishop, 1984; Ferrans and Rodriguez, 1987; Li et al., 1996**). Besides in physiological growth, induction of DNA synthesis and karyokinesis without cytoplasmic division in cardiomyocytes has also been linked to increased

metabolic demands and hypertrophic stress in general (**Ferrans and Rodriguez, 1987; Capasso et al., 1992; Barbera et al., 2000**) resulting in binucleation or polyploidy (**Erokhina et al., 1997; Soonpaa and Field, 1998; MacLellan and Schneider, 2000; Pasumarthi et al., 2005**). In adult humans, increased percentage of binucleated cardiomyocytes has been reported in cardiomyopathic hearts and in postmyocardial infarction (**Ahuja et al., 2007**). Previous findings (**Simko et al., 2005**), including our ongoing study, suggest that chronic L-NAME treatment could be used as a model of pathological cardiac hypertrophy, involving both myocardial fibrosis and cardiomyocyte hypertrophy. Considering that binucleation may result in hypertrophic growth (**Katzberg et al., 1977; Ferrans and Rodriguez, 1987; Li et al., 1996**), here obtained results showing significantly increased percentage of binucleated cardiomyocytes in the L-NAME group may have preceding role in the cardiomyocyte hypertrophy. The possible cause for the increased binucleation in RV during cardiac hypertrophy could be found in the tissue microenvironment since it has been recently shown that cardiac fibroblasts have important role in the promotion of cardiomyocyte proliferation during embryonic development through paracrine signaling (**Ieda et al., 2009**). Also, studies from **Kuhn et al. (2007)**, indicates that fibroblast-synthesized matrix protein periostin could induce differentiated cardiomyocytes to reenter the cell cycle and undergo cell division *in vivo*. Myocardial fibrosis demonstrated previously, as well in our ongoing study, during the L-NAME-induced RV hypertrophy may thus induce the increase of cardiomyocytes binucleation as an abortive cell cycle mode in which DNA replication is uncoupled from cell division in the absence of the cell division machinery. PCNA positivity of binucleated cardiomyocytes, demonstrated in this study, confirms their cell cycle activity since this protein is used frequently as a marker of cell hyperplasia and DNA replication, as well as of DNA repair (**Beltrami et al., 1997; Wood and Shivji, 1997**). At present, it stays unclear whether binucleation represents an advantage or disadvantage for cardiomyocytes, or is just a sign of

mitotic stimulus. There are data showing that increased binucleation in heart is linked to the increase of cell viability and protection from apoptosis in cardiomyocytes (**Anatskaya and Vinogradov, 2007**). At the other side, species whose adult hearts have higher percentage of binucleated cardiomyocytes have lower proliferative potential of cardiomyocytes in response to stress or injury (**Anversa et al., 2002; Rubart and Field, 2006**). Still, it should be mentioned that level of binucleation in RV of rats used in this study was significantly lower than in previous reports of the other laboratories since the ratio of binuclear cardiomyocytes in our study goes from 3.6 % in control, room temperature-acclimated group to 17.4 % as it was noted in L-NAME treated group acclimated to room temperature.

Hence, chronic treatment with the non-selective inhibitor of NOSs, L-NAME increases the proportion of binuclear cardiomyocytes and decreases the nuclear size of mononuclear cardiomyocytes in RV of rats, indicating the involvement of described nuclear alterations in L-NAME-induced cardiac hypertrophy. According to our information, this is the first demonstration of nuclear alteration in cardiomyocytes after chronic L-NAME treatment which highlight their important role in the cardiomyocyte hypertrophy. As such, this study has potential pharmacological significance in preventing negative outcomes resulting from cardiac hypertrophy. However, additional examination of underlying mechanisms involved in partially correlated effects of L-arginine and L-NAME are needed.

5.3 Capillary recruitment

As it was shown stereologically, capillarity of RV myocardium remains unaltered in both L-arginine and L-NAME treatment on room temperature, and decreases during cold acclimation without regard to treatment type. To analyze potential involvement of angiogenesis in RV myocardial hypertrophy, protein expression of the common angiogenic markers, VEGF and endoglin (CD105) was examined. The VEGF expression was increased in both cold acclimated

and all L-NAME and L-arginine treated groups, especially in groups treated with L-arginine. Immunohistochemically, VEGF was localized primarily in cardiomyocytes and endothelial cells. Immunopositivity was weak, homogenously distributed among cells. Subcellular localization of VEGF was cytoplasmic, mostly perinuclear and occasionally nuclear. The strongest immunopositivity was detected in the tissue of L-NAME-treated groups, where moderate cytoplasmic and occasionally nuclear reactivity was detected in the cardiomyocytes, including binuclear cells.

The only group with altered CD105 expression level was the cold-acclimated L-arginine treated group where significant increase of CD105 in comparison with both appropriate control and RT-acclimated L-arginine treated animals was detected. Immunohistochemical demonstration of CD105 in the myocardium revealed strong immunopositivity in the capillaries of all groups. Immunoreactivity of cardiomyocytes was moderate in the myocardia of control and L-arginine groups, and strong in the tissue of L-NAME-treated groups. Cardiomyocytes of L-NAME-treated animals showed heterogeneous pattern among cells, with granular cytoplasmic reaction. Also, nuclear reactivity was detected in cardiomyocytes of L-NAME-treated groups, especially in the room temperature-acclimated group.

Taken together, these results suggest potential involvement of capillary recruitment during RV remodeling demonstrated in this study, especially in L-arginine treated animals where the highest level of angiogenic markers was noticed. However, capillary recruitment does not fully compensate for RV hypertrophy, at least in cold-acclimated groups, since capillarity decreases, without regard to strong CD105 and VEGF immunopositivity of endothelial cells and cardiomyocytes.

5.4. Molecular basis of structural remodeling RV myocardium - NOSs

In order to examine if the chronic changes in NO level in RV induced by treatment with a general NOS inhibitor, L-NAME, or with the NO precursor, L-

arginine are connected with the alterations of NO synthesis in the RV itself, we examined the tissue expression and the localization of different NOS isoforms. Also, to reveal whether the cold acclimation leads to NO-dependent structural alterations in RV, the expression levels of NOSs were examined in the RV of rats.

As discussed previously, NO depletion plays a significant role in the development of right ventricular hypertrophy (**Giesbrecht, 1995; Beltrami et al., 1997; Cheng and Hauton, 2008**). In accordance, the most prominent effect of the chronic NOS inhibition induced by L-NAME supplementation on rat RV myocardium observed in this study was fibrosis, which was demonstrated as an increase in interstitial connective tissue volume density accompanied by increased collagen abundance. This effect was followed by cardiomyocyte hypertrophy. These alterations were observed in both, the room temperature- and cold-acclimated L-NAME-treated groups, compared with the appropriate controls. When compared to the room temperature-acclimated group treated with L-NAME, identical treatment during cold acclimation additionally enhanced interstitial fibrosis.

Analysis of NOSs expression indicates that mentioned structural alterations observed during chronic L-NAME treatment are followed by a selective inhibition of nNOS isoform expression. eNOS expression is affected in the group acclimated to cold only, whereas L-NAME treatment decreases it to control level. It was shown that eNOS and nNOS mediate independent, and in some cases opposite effects on cardiac structure and function, determined by their different spatial localization in cardiomyocytes. The pool of eNOS is claimed to be distributed between sarcolemmal and T-tubular caveolae (**Anversa et al., 2002; Rubart and Field, 2006; Stephen et al., 2009**), where it is associated with myocyte-specific caveolin-3 (**Cavalier-Smith, 2005**). nNOS is demonstrated to be expressed in the sarcolemma (**Damy et al., 2003; Xu et al., 2003; Damy et al., 2004**) and in the sarcoplasmic reticulum (SR) (**Xu et al., 1999; Barouch et al., 2002**), whereas nNOS-alpha (also known as mitochondrial NOS)

is expressed in mitochondria (Elfering *et al.*, 2002). Immunohistochemically, in our study nNOS is shown to be localized at sarcolemmal and Z-discs level. Since SR is localized around Z-discs, this indicates specific spatial localization of nNOS. On the other hand, subcellular distribution of eNOS was not so apparently organized as for nNOS, demonstrating different level of sarcolemmal and cytoplasmic reactivity among cardiomyocytes. As shown previously, the functional net effect of NO in cardiomyocytes depends on specific stimulus acting on a specific isoform at a particular subcellular location in a specific microenvironment. Sarcolemma-bound eNOS inhibited the L-type Ca^{2+} channel and attenuated the β -adrenergic receptor-stimulated increase in myocardial contractility, suggesting a net negative inotropic effect of eNOS (Gyurko *et al.*, 2000; Brunner *et al.*, 2001; Barouch *et al.*, 2002), while SR-bound nNOS stimulates SR Ca^{2+} release and reuptake and potentiating the cardiac force-frequency response (Khan *et al.*, 2003; Dawson *et al.*, 2005). Accordingly, in *nNOS*^{-/-} mice β -adrenergic receptor stimulation elicits a decreased inotropic response compared to wild-type mice (Barouch *et al.*, 2002; Dawson *et al.*, 2005). These results suggest that nNOS has an opposite, facilitative effect on contractility. Decrease of nNOS expression and maintenance of eNOS expression demonstrated in our study indicate decrease of inotropic response in RV of L-NAME-treated rats. Also, unique changes in NO compartmentalization secondary to nNOS and eNOS sub cellular localization might be involved in the development of cardiac hypertrophy (Loyer *et al.*, 2008). According to the previous studies, expression of eNOS in cardiomyocytes isolated from pressure-overload hearts reduces (Bayraktutan *et al.*, 1998), while nNOS undergoes up regulation (Massion *et al.*, 2003). These results are in discrepancy with our results demonstrating chronic L-NAME treatment down regulating the nNOS expression. The possible explanation could be in the treatment duration, since chronic hypertrophy of RV was shown to significantly decrease cardiomyocyte contraction amplitude and speed of shortening (Spann *et al.*, 1967; Vescovo *et al.*, 1989) which is effects

attributable to nNOS inhibition in cardiomyocytes. Cold acclimation of rats, as shown in our study, does not induce RV fibrosis or statistical alterations of cardiomyocyte diameter. The only significant modification was in the blood vessels volume density which decreases in RV myocardium after cold acclimation. Taken all together, these results do not indicate the cold-induced RV hypertrophy, at least at histological level. Concerning the effect of cold on the expression of NOSs in the tissue, chronic cold acclimation affects both constitutive isoforms, having opposite effects on them - it downregulates nNOS expression and up regulates eNOS expression. From the aforementioned it follows that the cold acclimation effects in RV myocardium does not include same mechanisms as during the L-NAME-induced chronic inhibition of NO production, although cold-induced stimulation of sympathetic nervous system could induce nNOS inhibition, as it was shown for the L-NAME treatment **(Giaid and Saleh, 1995)**. Detailed elucidation of cold effects in RV requires further examinations.

On the other hand, chronic treatment with an NO precursor, L-arginine, does not lead to significant structural alterations in RV myocardium of rats. Concerning its effect on NOSs expression, up regulation of eNOS was demonstrated. This result is in accordance with previous studies in which eNOS was shown to mediate the beneficial effects of cardiovascular drugs commonly used in patients with heart failure, strategies to increase its expression and/or coupled catalytic activity in the myocardium offer new therapeutic avenues for the treatment of this disease **(Massion and Balligand, 2007)**. Beside its effects on excitation-contraction coupling in response to stretch, eNOS acts as an „endogenous beta-blocker“ by restoring the sympathovagal balance, opposing excessive hypertrophy as well as promoting vasodilatation and neoangiogenesis, thereby contributing to tissue repair.

Concerning the expression of iNOS isoform in the RV of rats, we were not been able to detect it by both western blotting and immunohistochemical technique in any of the experimental groups. Bearing in mind previous reports

demonstrating iNOS expression during heart damage only (**Jung *et al.*, 2000; Kleinert *et al.*, 2003; Zhang *et al.*, 2007; Umar and van der Laarse, 2010**), our results could point to the absence of detrimental effects of applied drug treatments and cold acclimation in RV myocardium. This is especially important for chronic L-NAME treatment-induced fibrosis and cardiomyocyte hypertrophy, indicating the absence of cardiac dysfunction despite the observed structural alterations.

In conclusion, the data demonstrate the involvement of chronic NOS system inhibition in the development of cardiac fibrosis, at least in RV of rats. L-NAME, as a potent non-selective inhibitor of NOSs acts at the level of translation on constitutive NOS isoforms in RV, by decreasing the expression of nNOS and by maintaining the expression of eNOS at control level. At the other side, NO precursor, L-arginine upregulates eNOS expression, thus indicating the primary effects of eNOS in the NO production, at least in the RV of rats. Since cold acclimation, which in our experiment is not shown to induce structural signs of RV hypertrophy upregulates eNOS expression and down regulates nNOS expression, this could be a confirmation of protective role of eNOS during increased cardiac afterload.

6. CONCLUSIONS

Our results demonstrated that cold acclimation *per se* does not significantly alter the volume densities of myocardial tissue components, but leads to a trend in cardiomyocyte hypertrophy followed by a downward trend in capillarity.

L-arginine treatment in room temperature-acclimated rats led to cardiomyocyte hypertrophy which was followed by a simultaneous increase in capillarity and interstitial connective tissue in the myocardium. L-arginine treatment following cold acclimation acts synergistically with cold by increasing cardiomyocyte size and decreasing myocardial capillarity. Compared to the room temperature-acclimated group treated with L-arginine, the volume density was additionally increased and was followed by a decrease in blood vessel volume density. Cardiomyocyte hypertrophy in L-arginine-treated animals was observed and it might be an indirect consequence of increased peripheral circulatory demands.

The most prominent effect of the NOS inhibitor, L-NAME, on rat myocardia observed in this study was fibrosis which was demonstrated as an increase in interstitial connective tissue volume density accompanied by increased collagen abundance in the interstitium. This effect was followed by cardiomyocyte hypertrophy despite a decrease in their volume density. These alterations were observed in both the room temperature- and cold-acclimated L-NAME-treated groups, compared with the appropriate controls. When compared to the room temperature-acclimated group treated with L-NAME, identical treatment in cold-acclimated animals additionally enhanced interstitial fibrosis.

Regarding nitric oxide synthases, all cold-acclimated groups had decreased nNOS expression in comparison with adequate room temperature-acclimated groups. The exception were L-NAME treated groups, since decrease

of nNOS expression was seen already after the treatment at room temperature, similarly to cold-acclimated animals. L-NAME treatment and cold acclimation decreased nNOS expression. Cold acclimation, as well as L-arginine treatment increased eNOS expression. No additional effect of L-arginine on cold-induced increase of eNOS expression was noted. L-NAME treatment of room temperature-acclimated animals did not alter expression of eNOS in comparison with untreated control. However, L-NAME-treated-cold-acclimated group, eNOS expression was returned to control level, as it was noted in L-NAME-treated room temperature-acclimated group. iNOS expression was not detected in either experimental group, confirming non-pathological mode of right ventricle structural remodeling.

The mitochondrial populations in cardiomyocytes were also remodeled, L-arginine treatment at room temperature decreased profile surface of all mitochondrial subpopulations. On the other hand, L-NAME *per se* did not affect mitochondrial size. Cold acclimation decreased profile size of cardiomyocytic mitochondria, although statistically significant in perinuclear and intersarcomeral subpopulations only. Cold-acclimated L-arginine treated animals had statistically significant increased mitochondrial profile size. Also, L-NAME treated animals acclimated to cold have increased profile surface of mitochondria in perinuclear and subsarcolemal region, while in intersarcolemal region mitochondrial profiles decreased.

These findings suggest that rat right ventricular hypertrophy associated with modulation of NO production and/or cold, unlike hypertrophy due to pressure overload, is associated with a number of structural adaptations which may aid the heart in functioning in the specific environment.

Hence, the data demonstrate the involvement of chronic NOS system inhibition in the development of cardiac fibrosis, at least in RV of rats. L-NAME, as a potent non-selective inhibitor of NOSs acts at the level of translation on constitutive NOS isoforms in RV, by decreasing the expression of nNOS and by maintaining the expression of eNOS at control level. At the

other side, NO precursor, L-arginine upregulates eNOS expression, thus indicating the primary effects of eNOS in the NO production, at least in the RV of rats. Since cold acclimation, which in our experiment is not shown to induce structural signs of RV hypertrophy upregulates eNOS expression and down regulates nNOS expression, this could be a confirmation of protective role of eNOS during increased cardiac afterload.

7. REFERENCES

- Ahuja, P., Sdek, P., MacLellan, W.R.** (2007). Cardiac myocyte cell cycle control in development, disease, and regeneration. *Physiol Rev.* 87: 521-544.
- Anatskaya, O.V., Vinogradov, A.E.** (2007). Genome multiplication as adaptation to tissue survival: evidence from gene expression in mammalian heart and liver. *Genomics.* 89: 70-80.
- Anversa, P., Leri, A., Kajstura, J., Nadal-Ginard, B.** (2002). Myocyte growth and cardiac repair. *J Mol Cell Cardiol.* 34: 91-105.
- Anversa, P., Olivetti, G., Loud, A.V.** (1980). Morphometric study of early postnatal development in the left and right ventricular myocardium of the rat. I. Hypertrophy, hyperplasia, and binucleation of myocytes. *Circ Res.* 46: 495-502.
- Barbera, A., Giraud, G.D., Reller, M.D., Maylie, J., Morton, M.J., Thornburg, K.L.** (2000). Right ventricular systolic pressure load alters myocyte maturation in fetal sheep. *Am J Physiol Regul Integr Comp Physiol.* 279: R1157-1164.
- Barouch, L.A., Harrison, R.W., Skaf, M.W., Rosas, G.O., Cappola, T.P., Kobeissi, Z.A., Hobai, I.A., Lemmon, C.A., Burnett, A.L., O'Rourke, B., Rodriguez, E.R., Huang, P.L., Lima, J.A., Berkowitz, D.E., Hare, J.M.** (2002). Nitric oxide regulates the heart by spatial confinement of nitric oxide synthase isoforms. *Nature.* 416: 337-339.
- Bayraktutan, U., Yang, Z.K., Shah, A.M.** (1998). Selective dysregulation of nitric oxide synthase type 3 in cardiac myocytes but not coronary microvascular endothelial cells of spontaneously hypertensive rat. *Cardiovasc Res.* 38: 719-726.
- Beltrami, C.A., Di Loreto, C., Finato, N., Rocco, M., Artico, D., Cigola, E., Gambert, S.R., Olivetti, G., Kajstura, J., Anversa, P.** (1997). Proliferating cell nuclear antigen (PCNA), DNA synthesis and mitosis in myocytes

following cardiac transplantation in man. *J Mol Cell Cardiol.* 29: 2789-2802.

Bendall, J.K., Alp, N.J., Warrick, N., Cai, S., Adlam, D., Rockett, K., Yokoyama, M., Kawashima, S., Channon, K.M. (2005). Stoichiometric relationships between endothelial tetrahydrobiopterin, endothelial NO synthase (eNOS) activity, and eNOS coupling in vivo: insights from transgenic mice with endothelial-targeted GTP cyclohydrolase 1 and eNOS overexpression. *Circ Res.* 97: 864-871.

Bogaard, H.J., Natarajan, R., Henderson, S.C., Long, C.S., Kraskauskas, D., Smithson, L., Ockaili, R., McCord, J.M., Voelkel, N.F. (2009). Chronic Pulmonary Artery Pressure Elevation Is Insufficient to Explain Right Heart Failure. *Circulation.* 120: 1951-1960.

Bogaard, H.J., Natarajan, R., Mizuno, S., Abbate, A., Chang, P.J., Chau, V.Q., Hoke, N.N., Kraskauskas, D., Kasper, M., Salloum, F.N., Voelkel, N.F. (2010). Adrenergic receptor blockade reverses right heart remodeling and dysfunction in pulmonary hypertensive rats. *Am J Respir Crit Care Med.* 182: 652-660.

Brack, K.E., Patel, V.H., Mantravardi, R., Coote, J.H., Ng, G.A. (2009). Direct evidence of nitric oxide release from neuronal nitric oxide synthase activation in the left ventricle as a result of cervical vagus nerve stimulation. *The Journal of Physiology.* 587: 3045-3054.

Brown, R.D., Ambler, S.K., Mitchell, M.D., Long, C.S. (2005). The cardiac fibroblast: therapeutic target in myocardial remodeling and failure. *Annu Rev Pharmacol Toxicol.* 45: 657-687.

Brunner, F., Andrew, P., Wölkart, G., Zechner, R., Mayer, B. (2001). Myocardial contractile function and heart rate in mice with myocyte-specific overexpression of endothelial nitric oxide synthase. *Circulation.* 104: 3097-3102.

Brunner, F., Andrew, P., Wölkart, G., Zechner, R., Mayer, B. (2001). Over expression of endothelial nitric oxide synthase. *Circulation.* 104: 3097-3102.

Bryan, N.S., Bian, K., Murad, F. (2009). Discovery of the nitric oxide signaling pathway and targets for drug development. *Front Biosci.* 14: 1-18.

Buchwalow, I.B. Podzuweit, T. Bocker, W. Samoilova, V.E. Thomas, S. Wellner, M. Baba, H.A., Robenek, H., Schnekenburger, J., Lerch, M.M. (2002). Vascular smooth muscle and nitric oxide synthase. *FASEB J.* 16: 500-508.

Capasso, J.M., Bruno, S., Cheng, W., Li, P., Rodgers, R., Darzynkiewicz, Z., Anversa, P. (1992). Ventricular loading is coupled with DNA synthesis in adult cardiac myocytes after acute and chronic myocardial infarction in rats. *Circ Res.* 71: 1379-1389.

Cavalier-Smith, T. (2005). Economy, speed and size matter: evolutionary forces driving nuclear genome miniaturization and expansion. *Ann Bot.* 95: 147-175.

Cheng, X., Su, H. (2010). Effects of climatic temperature stress on cardiovascular diseases. *Eur J Intern Med.* 21: 164-167.

Cheng, Y., Hauton, D. (2008). Cold acclimation induces physiological cardiac hypertrophy and increases assimilation of triacylglycerol metabolism through lipoprotein lipase. *Biochim Biophys Acta.* 1781: 618-626.

Clubb, F.J.Jr., Bishop, S.P. (1984). Formation of binucleated myocardial cells in the neonatal rat. An index for growth hypertrophy. *Lab Invest.* 50: 571-577.

Cotton, J.M., Kearney, M.T., Shah, A.M. (2002). Nitric oxide and myocardial function in heart failure: friend or foe? *Heart.* 88:564-566.

Creemers, E.E., Pinto, Y.M. (2011). Molecular mechanisms that control interstitial fibrosis in the pressure-overloaded heart. *Cardiovasc Res.* 89: 265-272.

D'Alonzo, G.E., Barst, R.J., Ayres, S.M., Bergofsky, E.H., Brundage, B.H., Detre, K.M., Fishman, A.P., Goldring, R.M., Groves, B.M., Kernis, J.T.

(1991). Survival in patients with primary pulmonary hypertension. Results from a national prospective registry. *Ann Intern Med.* 115: 343-349.

Damy, T., Ratajczak, P., Robidel, E., Bendall, J.K., Oliviéro, P., Boczkowski, J., Ebrahimian, T., Marotte, F., Samuel, J.L., Heymes, C. (2003). Up-regulation of cardiac nitric oxide synthase 1-derived nitric oxide after myocardial infarction in senescent rats. *FASEB J.* 17: 1934-1936.

Damy, T., Ratajczak, P., Shah, A.M., Camors, E., Marty, I., Hasenfuss, G., Marotte, F., Samuel, J.L., Heymes, C. (2004). Increased neuronal nitric oxide synthase-derived NO production in the failing human heart. *Lancet.* 363: 1365-1367.

Dawson, D., Lygate, C.A., Zhang, M.H., Hulbert, K., Neubauer, S., Casadei, B. (2005). nNOS gene deletion exacerbates pathological left ventricular remodeling and functional deterioration after myocardial infarction. *Circulation.* 112: 3729-3737.

de Simone, G, Gottdiener, J.S., Chinali, M., Maurer, M.S. (2008). Left ventricular mass predicts heart failure not related to previous myocardial infarction: the Cardiovascular Health Study. *Eur Heart J.* 29: 741-747.

Diez, J., Laviades, C., Mayor, G., Gil, M.J., Monreal, I. (1995). Increased serum concentrations of procollagen peptides in essential hypertension. Relation to cardiac alterations. *Circulation.* 91: 1450-1456.

Dimmeler, S., Fleming, I., Fisslthaler, B., Hermann, C., Busse, R., Zeiher, A.M. (1999). Activation of nitric oxide synthase in endothelial cells by Akt-dependent phosphorylation. *Nature.* 399: 601-605.

Dixit, M., Loot, A.E., Mohamed, A., Fisslthaler, B., Boulanger, C.M., Ceacareanu, B., Hassid, A., Busse, R., Fleming, I. (2005). Gab1, SHP2, and protein kinase A are crucial for the activation of the endothelial NO synthase by fluid shear stress. *Circ Res.* 97: 1236-1244.

Dore, A., Houde, C., Chan, K.L., Ducharme, A., Khairy, P., Juneau, M., Marcotte, F., Mercier, L.A. (2005). Angiotensin receptor blockade and

exercise capacity in adults with systemic right ventricles: a multicenter, randomized, placebo-controlled clinical trial. *Circulation*. 112: 2411-2416.

Dorn, G.W.2nd., Robbins, J. (2003). Phenotyping hypertrophy: eschew obfuscation. *Circ Res*. 92: 1171-1175.

Elfering, S.L., Sarkela, T.M., Giulivi, C. (2002). Biochemistry of mitochondrial nitric-oxide synthase. *J BiolChem*. 277: 38079-38086.

Erokhina, I.L., Selivanova, G.V., Vlasova, T.D., Emel'ianova, O.I. (1997). Correlation between the level of polyploidy and hypertrophy and degree of human atrial cardiomyocyte damage in certain congenital and acquired heart pathologies. *Tsitologiya*. 39: 889-899.

Fabris, V.E., Pato, M.D., Belik, J. (2001). Progressive lung and cardiac changes associated with pulmonary hypertension in the fetal rat. *Pediatr Pulmonol*. 31: 344-353.

Fernández-Solà, J., Fatjó, F., Sacanella, E., Estruch, R., Bosch X., Urbano-Márquez, A., Nicolás J.M. (2006). Evidence of apoptosis in alcoholic cardiomyopathy. *Hum Pathol*. 37: 1100-1110.

Ferrans, V.J., Rodriguez, E.R. (1987). Evidence of myocyte hyperplasia in hypertrophic cardiomyopathy and other disorders with myocardial hypertrophy? *Z Kardiol*. 76: 20-25.

Feuerstein, G.Z. (2001). Apoptosis: new opportunities for novel therapeutics for heart diseases. *Cardiovasc Drugs Ther*. 15: 547-551.

Forstermann, U. Sessa, W.C. (2012). Nitric oxide synthases: regulation and function. *Eur Heart J*. 33: 829-37, 837a-837d.

Giaid, A., Saleh, D. (1995). Reduced expression of endothelial nitric oxide synthase in the lungs of patients with pulmonary hypertension. *N Engl J Med*. 333: 214-221.

Giesbrecht, G.G. (1995). The respiratory system in a cold environment. *Aviat Space Environ Med*. 66: 890-902.

- Giusca, S., Jurcut, R., Gingham, C., Voigt, J.U.** (2010). The right ventricle: anatomy, physiology and functional assessment. *Acta Cardiol.* 65: 67-77.
- Gregory, L., Luigi, V., David, A.E., Barbara, C.** (2008). Does nitric oxide modulate cardiac ryanodine receptor function? Implications for excitation-contraction coupling. *Cardiovascular Research.* 77: 256-264.
- Grossman, W., Jones, D., McLaurin, L.P.** (1975). Wall stress and patterns of hypertrophy in the human left ventricle. *J Clin Invest.* 56: 56-64.
- Gustafsson, A.B., Gottlieb, R.A.** (2003). Mechanisms of apoptosis in the heart. *J Clin Immunol.* 23: 447-459.
- Gutstein, D.E., Liu, F.Y., Meyers, M.B., Choo, A., Fishman, G.I.** (2003). The organization of adherens junctions and desmosomes at the cardiac intercalated disc is independent of gap junctions. *J Cell Sci.* 116: 875-885.
- Gyurko, R., Kuhlencordt, P., Fishman, M.C., Huang, P.L.** (2000). Modulation of mouse cardiac function in vivo by eNOS and ANP. *Am J Physiol Heart Circ Physiol.* 278: H971-H981.
- Heba, G., Krzemiński, T., Porc, M., Grzyb, J., Dembińska-Kieć, A.** (2001). Relation between expression of TNF alpha, iNOS, VEGF mRNA and development of heart failure after experimental myocardial infarction in rats. *J Physiol Pharmacol.* 52: 39-52.
- Heineke, J., Molkentin, J.D.** (2006). Regulation of cardiac hypertrophy by intracellular signalling pathways. *Nat Rev Mol Cell Biol.* 7: 589-600.
- Hmaid, A.A.A., Markelic, M., Otasevic, V., Masovic, S., Jankovic, A., Korać, B., Korac, A.** (2016). Structural alterations in rat myocardium induced by chronic L-arginine and L- NAME supplementation. *Saudi J Biol Sci.* doi: <http://dx.doi.org/10.1016/j.sjbs.2016.01.022>.
- Humbert, M., Sitbon, O., Chaouat, A., Bertocchi, M., Habib, G., Gressin, V., Yaici, A., Weitzenblum, E., Cordier, J.F., Chabot, F., Dromer, C., Pison, C., Reynaud-Gaubert, M., Haloun, A., Laurent, M., Hachulla, E., Simonneau, G.** (2006). Pulmonary arterial hypertension in France: results

from a national registry. *Am J Respir Crit Care Med.* 173: 1023-1030.

Ieda, M., Tsuchihashi, T., Ivey, K.N., Ross, R.S., Hong, T.T., Shaw, R.M., Srivastava, D. (2009). Cardiac fibroblasts regulate myocardial proliferation through beta1 integrin signaling. *Dev Cell.* 16: 233-244.

Jänkälä, H., Eriksson, C.J., Eklund, K.K., Härkönen, M., Mäki, T. (2002). Combined calcium carbimide and ethanol treatment induces high blood acetaldehyde levels, myocardial apoptosis and altered expression of apoptosis-regulating genes in rat. *Alcohol Alcohol.* 37: 222-228.

Jing, Z.C., Xu, X.Q., Han, Z.Y., Wu, Y., Deng, K.W., Deng, K.W., Wang, H., Wang, Z.W., Cheng, X.S., Xu, B., Hu, S.S., Hui, R.T., Yang, Y.J. (2007). Registry and survival study in chinese patients with idiopathic and familial pulmonary arterial hypertension. *Chest.* 132: 373-379.

Jonathan, P., Kenneth, D.B. (2005). Nitric Oxide and cardiac remodeling. *Heart Failure Clinics.* 1: 275-286.

Jung, F., Palmer, L.A., Zhou, N., Johns, R.A. (2000). Hypoxic regulation of inducible nitric oxide synthase via hypoxia inducible factor-1 in cardiac myocytes. *Circ Res.* 86: 319-325.

Kanai, A.J., Pearce, L.L., Clemens, P.R., Birder, L.A., VanBibber, M.M., Choi, S.Y., de Groat, W.C., Pererson, J. (2001). Identification of a neuronal nitric oxide synthase in isolated cardiac mitochondria using electrochemical detection. *Proc Natl Acad Sci U S A.* 98: 14126-14131.

Kanno, S., Kim, P.K., Sallam, K., Lei, J., Billiar, T.R., Shears, L.L. 2nd. (2004). Nitric oxide facilitates cardiomyogenesis in mouse embryonic stem cells. *Proc Natl Acad Sci U S A.* 101: 12277-12281.

Karsner, H.T., Saphir, O., Todd, T.W. (1925). The state of the cardiac muscle in hypertrophy and atrophy. *Am J Pathol.* 1: 351-372.

Katzberg, A.A., Farmer, B.B., Harris, R.A. (1977). The predominance of binucleation in isolated rat heart myocytes. *Am J Anat.* 149: 489-499.

Khan, S.A., Skaf, M.W., Harrison, R.W., Lee, K., Minhas, K.M., Kumar, A.,

Fradley, M., Shoukas, A.A., Berkowitz, D.E., Hare, J.M. (2003). Nitric oxide regulation of myocardial contractility and calcium cycling: independent impact of neuronal and endothelial nitric oxide synthases. *Circ Res.* 92: 1322-1329.

Kleinert, H., Schwarz, P.M., Forstermann, U. (2003). Regulation of the expression of inducible nitric oxide synthase. *Biol Chem.* 384: 1343-1364.

Kolpakov, V., Gordon, D., Kulik, T.J. (1995). Nitric oxide-generating compounds inhibit total protein and collagen synthesis in cultured vascular smooth muscle cells. *Circ Res.* 76: 305-309.

Krenning, G., Zeisberg, E.M., Kalluri, R. (2010). The origin of fibroblasts and mechanism of cardiac fibrosis. *J Cell Physiol.* 225: 631-637.

Kuhn, B., del Monte, F., Hajjar, R.J., Chang, Y.S., Lebeche, D., Arab, S., Keating, M.T. (2007). Periostin induces proliferation of differentiated cardiomyocytes and promotes cardiac repair. *Nat Med.* 13: 962-969.

Laemmli, U.K. (1970). Cleavage of structural proteins during the assembly of the head of bacteriophage T4. *Nature.* 227: 680-685.

Leri, A., Kajstura, J., Anversa, P. (2002). Myocyte proliferation and ventricular remodeling. *Journal of Cardiac Failure.* 8: S518-S525.

Levy, D., Garrison, R.J., Savage, D.D., Kannel, W.B., Castelli, W.P. (1990). Prognostic implications of echocardiographically determined left ventricular mass in the Framingham Heart Study. *N Engl J Med.* 322: 1561-1566.

Li, F., Wang, X., Capasso, J.M., Gerdes, A.M. (1996). Rapid transition of cardiac myocytes from hyperplasia to hypertrophy during postnatal development. *J Mol Cell Cardiol.* 28: 1737-1746.

Loyer, X., Heymes, C., Samuel, J.L. (2008). Constitutive nitric oxide synthases in the heart from hypertrophy to failure. *Clin Exp Pharmacol Physiol.* 35: 483-488.

Lu, S., Xu, D. (2013). Cold stress accentuates pressure overload-induced cardiac hypertrophy and contractile dysfunction: role of TRPV1/AMPK-mediated autophagy. *Biochem Biophys Res Commun.* 442: 8-15.

MacLellan, W.R., Schneider, M.D. (2000). Genetic dissection of cardiac growth control pathways. *Annu Rev Physiol.* 62: 289-319.

Maillet, M., van Berlo, J.H., Molkentin, J.D. (2013). Molecular basis of physiological heart growth: fundamental concepts and new players. *Nat Rev Mol Cell Biol.* 14:38-48.

Maron, B.J., McKenna, W.J., Danielson, G.K., Kappenberger, L.J., Kuhn, H.J., Seidman, C.E., Shah, P.M., Spencer, W.H. 3rd, Spirito, P., Ten, Cate, F.J., Wigle, E.D. (2003). American College of Cardiology/European Society of Cardiology Clinical Expert Consensus Document on Hypertrophic Cardiomyopathy. A report of the American College of Cardiology Foundation Task Force on Clinical Expert Consensus Documents and the European Society of Cardiology Committee for Practice Guidelines. *Eur Heart J.* 24: 1965-1991.

Massion, P.B., Balligand, J.L. (2007). Relevance of nitric oxide for myocardial remodeling. *Curr Heart Fail Rep.* 4: 18-25.

Massion, P.B., Feron, O., Dessy, C., Balligand, J.L. (2003). Nitric oxide and cardiac function: ten years after, and continuing. *Circ Res.* 93: 388-398.

Massion, P.B., Dessy, C., Desjardins, F., Pellat, M., Havaux, X., Belge, C., Moulin, P., Guiot, Y., Feron, O., Janssens, S., Balligand, J.L. (2004). Cardiomyocyte-restricted overexpression of endothelial nitric oxide synthase (NOS3) attenuates beta-adrenergic stimulation and reinforces vagal inhibition of cardiac contraction. *Circulation.* 110: 2666-2672.

McMullen, J.R., Shioi, T., Zhang, L., Tarnavski, O., Sherwood, M.C., Kang, P.M., Izumo, S. (2003). Phosphoinositide 3-kinase(p110alpha) plays a critical role for the induction of physiological, but not pathological, cardiac hypertrophy. *Proc Natl Acad Sci. USA.* 100: 12355-12360.

Meneghini, A., Ferreira, C., Abreu, L.C., Ferreira, M., Ferreira, Filho, C., Valenti, V.E., Murad, N. (2008). Cold stress effects on cardiomyocytes nuclear size in rats: light microscopic evaluation. *Rev Bras Cir Cardiovasc.* 23: 530-533.

Mescher, A. (2013). *Junqueira's Basic Histology: Text and Atlas, Thirteenth Edition*, 2013, Kindle Ed.

Miethke, A., Feussner, M., Planitzer, G., Richter, H., Gutschmann, M., Gossrau, R. (2003). Localization of NOS-1 in the sarcolemma region of a subpopulation of atrial cardiomyocytes including myoendocrine cells and NOS-3 in vascular and endocardial endothelial cells of the rat heart. *Acta Histochem.* 105: 43-55.

Mihl, C., Dassen, W.R.M., Kuipers, H. (2008). Cardiac remodelling: concentric versus eccentric hypertrophy in strength and endurance athletes. *Neth Heart J.* 16: 129-133.

Moreno, H.Jr., Piovesan Nathan, L., Pereira Costa, S.K., Metze, K., Antunes, E., Zatz, R., De Nucci, G. (1995). Enalapril does not prevent the myocardial ischemia caused by the chronic inhibition of nitric oxide synthesis. *Eur J Pharmacol.* 287: 93-96.

Neuss, M., Crow, M.T., Chesley, A., Lakatta, E.G. (2001). Apoptosis in cardiac disease: what is it—how does it occur? *Cardiovasc Drugs Ther.* 15: 509-525.

Nishida, C.R., Ortiz de Montellano, P.R. (1998). Electron transfer and catalytic activity of nitric oxide synthases. Chimeric constructs of the neuronal, inducible, and endothelial isoforms. *J Biol Chem.* 273: 5566-5571.

Pasumarthi, K.B., Nakajima, H., Nakajima, H.O., Soonpaa, M.H., Field, L.J. (2005). Targeted expression of cyclin D2 results in cardiomyocyte DNA synthesis and infarct regression in transgenic mice. *Circ Res.* 96: 110-118.

Paz, Y., Frolkis, I., Pevni, D., Shapira, I., Yuhas, Y., Iaina, A., Wollman, Y., Chernichovski, T., Nesher, N., Locker, C., Mohr, R., Uretzky, G. (2003).

Effect of tumor necrosis factor-alpha on endothelial and inducible nitric oxide synthase messenger ribonucleic acid expression and nitric oxide synthesis in ischemic and nonischemic isolated rat heart. *J Am Coll Cardiol.* 42: 1299-1305.

Pechanova, O., Bernatova, I., Pelouch, V., Babal, P. (1999). L-NAME-induced protein remodeling and fibrosis in the rat heart. *Physiol Res.* 48: 353-362.

Pechanova, O., Bernatova, I., Pelouch, V., Simko, F. (1997). Protein remodelling of the heart in NO-deficient hypertension: the effect of captopril. *J Mol Cell Cardiol.* 29: 3365-3374.

Pelliccia, A., Maron, B. J., De Luca, R., Di Paolo, F.M., Spataro, A., Culasso, F. (2002). Remodeling of left ventricular hypertrophy in elite athletes after long-term deconditioning. *Circulation.* 105: 944-949.

Petrovic, V., Buzadzic, B., Korac, A., Vasilijevic, A., Jankovic, A., Micunovic, K., Korac, B. (2008). Antioxidative defence alterations in skeletal muscle during prolonged acclimation to cold: role of L-arginine/NO-producing pathway. *J Exp Biol.* 211: 114-120.

Petrovic, V., Korac, A., Buzadzic, B., Korac, B. (2005). The effects of L-arginine and L-NAME supplementation on redox-regulation and thermogenesis in interscapular brown adipose tissue. *J Exp Biol.* 208: 4263-4271.

Pinsky, D.J., Patton, S., Mesaros, S., Brovkovich, V., Kubaszewski, E., Grunfeld, S., Malinski, T. (1997). Mechanical transduction of nitric oxide synthesis in the beating heart. *Circ Res.* 81: 372-379.

Rajiv, C., Vinereanu, D., Fraser, A.G. (2004). Tissue Doppler imaging for the evaluation of patients with hypertrophic cardiomyopathy. *Curr Opin Cardiol.* 19: 430-436.

Regula, K.M., Kirshenbaum, L.A. (2005). Apoptosis of ventricular myocytes; a means to an end. *J Mol Cell Cardiol.* 38: 3-13.

- Rossi, M.A.** (2001). Connective tissue skeleton in the normal left ventricle and in hypertensive left ventricular hypertrophy and chronic chagasic myocarditis. *Med Sci Monit.* 7: 820-832.
- Rubart, M., Field, L.J.** (2006). Cardiac regeneration: repopulating the heart. *Annu Rev Physiol.* 68: 29-49.
- Sabahh, H.N., Sharov, V.G.** (1998). Apoptosis in heart failure. *Prog Cardiovasc Dis.* 40: 549-562.
- Saha, S.K., Ohinata, H., Kuroshima, A.** (1996). Effects of acute and chronic inhibition of nitric oxide synthase on brown adipose tissue thermogenesis. *Jpn J Physiol.* 46: 375-382.
- Saraste, A., Pulkki, K., Kallajoki, M., Heikkilä, P., Laine, P., Mattila, S., Nieminen, M.S., Parvinen, M., Voipio-Pulkki, L.M.** (1999). Cardiomyocyte apoptosis and progression of heart failure to transplantation. *Eur J Clin Invest.* 29: 380-386.
- Sarkar, S., Chawla-Sarkar, M., Young, D., Nishiyama, K., Rayborn, M.E., Hollyfield, J.G., Sen, S.** (2004). Myocardial Cell Death and Regeneration during Progression of Cardiac Hypertrophy to Heart Failure. *J Biol Chem.* 279: 52630-52642.
- Schmidt, H.H., Pollock, J.S., Nakane, M., Förstermann, U., Murad, F.** (1992). Ca²⁺/calmodulin-regulated nitric oxide synthases. *Cell Calcium.* 13: 427-434.
- Schulz, R., Rassaf, T., Massion, P.B., Kelm, M., Balligand, J.L.** (2005). Recent advances in the understanding of the role of nitric oxide in cardiovascular homeostasis. *Pharmacol Ther.* 108: 225-256.
- Sears, C.E., Ashley, E.A., Casadei, B.** (2004). Nitric oxide control of cardiac function: is neuronal nitric oxide synthase a key component? *Philos Trans R Soc Lond B Biol Sci.* 359: 1021-1044.
- Sharif-Naeini, R., Folgering, J.H., Bichet, D., Duprat, F., Delmas, P., Patel, A., Honoré, E.** (2010). Sensing pressure in the cardiovascular system: Gq-

coupled mechanoreceptors and TRP channels. *J Mol Cell Cardiol.* 48:83-89.

Sheehan, F., Redington, A. (2008). The right ventricle: anatomy, physiology and clinical imaging. *Heart.* 94: 1510-1515.

Sheth, T., Nair, C., Muller, J., Yusuf, S. (1999). Increased winter mortality from acute myocardial infarction and stroke: the effect of age. *J Am Coll Cardiol.* 33: 1916-1919.

Simko, F, Luptak, I., Matuskova, J., Krajcirovicova, K., Sumbalova, Z., Kucharska, J., Gvozdjakova, A., Simko, J., Babal, P., Pechanova, O., Bernatova, I. (2005). L-arginine fails to protect against myocardial remodelling in L-NAME-induced hypertension. *Eur J Clin Invest.* 35: 362-368.

Simon, M.A., Pinsky, M.R. (2011). Right ventricular dysfunction and failure in chronic pressure overload. *Cardiol Res Pract.* 568095 doi:10.4061/2011/568095.

Soonpaa, M.H., Field, L.J. (1998). Survey of studies examining mammalian cardiomyocyte DNA synthesis. *Circ Res.* 83: 15-26.

Sosunov, A.A., Hassall, C.J., Loesch, A., Turmaine, M., Burnstock, G. (1995). Ultrastructural investigation of nitric oxide synthase-immunoreactive nerves associated with coronary blood vessels of rat and guinea-pig. *Cell Tissue Res.* 280: 575-582.

Spann, J.F.Jr., Buccino, R.A., Sonnenblick, E.H., Braunwald, E. (1967). Contractile state of cardiac muscle obtained from cats with experimentally produced ventricular hypertrophy and heart failure. *Circ Res.* 21: 341-354.

Stephen, M.J., Poindexter, B.J., Moolman, J.A., Sheikh-Hamad, D., Bick, R.J. (2009). Do binucleate cardiomyocytes have a role in myocardial repair? Insights using isolated rodent myocytes and cell culture. *Open Cardiovasc Med J.* 3: 1-7.

Sun, Z. (2010). Cardiovascular responses to cold exposure. *Front Biosci. (Elite Ed).* 2: 495-503.

Swoap, S.J., Overton, J.M., Garber, G. (2004). Effect of ambient temperature on cardiovascular parameters in rats and mice: a comparative approach. *Am J Physiol Regul Integr Comp Physiol.* 287: R391-R396.

Takimoto, E., Champion, H.C., Li, M., Ren, S., Rodriguez, E.R., Tavazzi, B., Lazzarino, G., Paolocci, N., Gabrielson, K.L., Wang, Y., Kass, D.A. (2005). Oxidant stress from nitric oxide synthase-3 uncoupling stimulates cardiac pathologic remodeling from chronic pressure load. *J Clin Invest.* 115: 1221-1231.

Takimoto, Y., Aoyama, T., Tanaka, K., Keyamura, R., Yui, Y., Shigetake, S., (2002). Augmented Expression of Neuronal Nitric Oxide Synthase in the Atria Parasympathetically Decreases Heart Rate During Acute Myocardial Infarction in Rats. *Circulation.* 105: 490-496.

Toldo, S., Bogaard, H.J., Van Tassell, B.W., Mezzaroma, E., Seropian, I.M., Robati, R., Salloum, F.N., Voelkel, N.F., Abbate, A. (2011). Right ventricular dysfunction following acute myocardial infarction in the absence of pulmonary hypertension in the mouse. *PLoS One.* 6: e18102.

Tsutsui, M., Tanimoto, A., Tamura, M., Mukae, H., Yanagihara, N., Shimokawa, H., Otsuji, Y. (2015). Significance of nitric oxide synthases: Lessons from triple nitric oxide synthases null mice. *J Pharmacol Sci.* 127: 42-52.

Umar, S., van der Laarse, A. (2010). Nitric oxide and nitric oxide synthase isoforms in the normal, hypertrophic, and failing heart. *Mol Cell Biochem.* 333: 191-201.

Van Berlo, J.H., Maillet, M., Molkentin, J.D. (2013). Signaling effectors underlying pathologic growth and remodeling of the heart. *J Clin Invest.* 123: 37-45.

Van Empel, V.P., De Windt, L.J. (2004). Myocyte hypertrophy and apoptosis: a balancing act. *Cardiovasc Res.* 63: 487-499.

Van Wolferen, S.A., Marcus, J.T., Boonstra, A., Marques, K.M.,

- Bronzwaer, J.G., Bronzwaer, J.G., Spreeuwenberg, M.D., Postmus, P.E., Vonk-Noordegraaf, A.** (2007). Prognostic value of right ventricular mass, volume, and function in idiopathic pulmonary arterial hypertension. *Eur Heart J.* 28: 1250-1257.
- Vescovo, G., Harding, S.E., Jones, S.M., Dalla Libera, L., Pessina, A.C., Poole-Wilson, P.A.** (1989). Comparison between isomyosin pattern and contractility of right ventricular myocytes isolated from rats with right cardiac hypertrophy. *Basic Res Cardiol.* 84: 536-543.
- Voelkel, N.F., Natarajan, R., Drake, J.I., Bogaard, H.J.** (2011). Right Ventricle in Pulmonary Hypertension. *Comprehensive Physiology*: John Wiley & Sons, Inc. 525-540.
- Vonk Noordegraaf, A., Naeije, R.** (2008) Right ventricular function in scleroderma-related pulmonary hypertension. *Rheumatology (Oxford).* 47: 42-43.
- Webster, K., Bishopric, N.** (2003). Apoptosis inhibitors for heart disease. *Circulation.* 108: 2954.
- Weibel, E.R.** (1981). *Stereological Methods. Vol. 1. Practical Methods for Biological Morphometry.* *J Microsc.* 121: 131-132.
- Wilcox, J.N., Subramanian, R.R., Sundell, C.L., Tracey, W.R., Pollock, J.S., Harrison, D.G. et al.** (1997). Expression of multiple isoforms of nitric oxide synthase in normal and atherosclerotic vessels. *Arterioscler Thromb Vasc Biol,* 17: 2479-2488.
- Wood, R.D., Shivji, M.K.** (1997). Which DNA polymerases are used for DNA-repair in eukaryotes? *Carcinogenesis.* 18: 605-610.
- Xu, K.Y., Huso, D.L., Dawson, T.M., Bredt, D.S., Becker, L.C.** (1999). Nitric oxide synthase in cardiac sarcoplasmic reticulum. *Proc Natl Acad Sci U S A.* 96: 657-662.
- Xu, K.Y., Kuppusamy, S.P., Wang, J.Q., Li, H., Cui, H., Dawson, T.M., Huang, P.L., Burnett, A.L., Kuppusamy, P., Becker, L.C.** (2003). Nitric

oxide protects cardiac sarcolemmal membrane enzyme function and ion active transport against ischemia-induced inactivation. *J Biol Chem.* 278: 41798-41803.

Zhang, P., Xu, X., Hu, X., van Deel, E.D., Zhu, G., Chen, Y. (2007). Inducible nitric oxide synthase deficiency protects the heart from systolic overload-induced ventricular hypertrophy and congestive heart failure. *Circ Res.* 100: 1089-1098.

Ziolo, M.T., Kohr, M.J., Wang, H. (2008). Nitric oxide signaling and the regulation of myocardial function. *J Mol Cell Cardiol.* 45: 625-32.

Zuo, X.R., Wang, Q., Cao, Q., Yu, Y.Z., Wang, H., Bi, L.Q., Wang, H. (2012). Nicorandil Prevents Right Ventricular Remodeling by Inhibiting Apoptosis and Lowering Pressure Overload in Rats with Pulmonary Arterial Hypertension. *PLoS ONE.* 7: e44485.

Biography

Mr Amal Abdussalam Ali A. Hmaid was born in Gharian, Libya, on January 27th 1980. She started her Bachelor studies in 1997-1998 at the Faculty of Science, Biology department, Al-jabal Al-gharbi University, Gharian, where she graduated on 2000-2001.

From 2001-2003 Mr Amal Abdussalam Ali A. Hmaid worked as a Demonstrator of biology in Al-jabal Al-gharbi University, where she taught the following courses: Animal physiology, Genetic and cell biology, Histology, Immunology, General zoology.

In 2003 she started Master studies at the Czech University of Life Sciences, University of Prague and graduated on 2007. From 2007 to 2009 she worked as Assistant lecturer at the faculty of science / Gharian, Libya. She came to Serbia at the end of September 2009 to be a PhD student with a full scholarship from the faculty of science/ Gharian paid by the Libyan government.

Прилог 1.

Изјава о ауторству

Потписани-а Amal Abdussalam Ali A. Hmaid

број индекса _____

Изјављујем

да је докторска дисертација под насловом

ULOGA NO-SINTAZNOG PUTA U STRUKTURNOM REMODELIRANJU MIOKARDA
RACOVA

(THE ROLE OF NO-SYNTHETIC PATHWAY IN STRUCTURAL REMODELING OF
RAT MYOCARDIUM)

- резултат сопственог истраживачког рада,
- да предложена дисертација у целини ни у деловима није била предложена за добијање било које дипломе према студијским програмима других високошколских установа,
- да су резултати коректно наведени и
- да нисам кршио/ла ауторска права и користио интелектуалну својину других лица.

Потпис докторанда

У Београду, _____



Прилог 2.

Изјава о истоветности штампане и електронске верзије докторског рада

Име и презиме аутора Amal Abdussalam Ali A. Hmaid

Број индекса _____

Студијски програм Biologija, modul Biologija ćelija i tkiva

Наслов рада ULOGA NO-SINTAZNOG PUTA U STRUKTURNOM REMODELIRANJU
MIOKARDA PACOVA

(THE ROLE OF NO-SYNTHETIC PATHWAY IN STRUCTURAL REMODELING OF
RAT MYOCARDIUM)

Ментори:

Dr Aleksandra Korać, redovni profesor, Univerzitet u Beogradu-Biološki fakultet

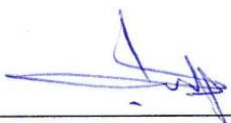
Dr Aleksandra Janković, naučni saradnik, Univerzitet u Beogradu-Institut za biološka
istraživanja „Siniša Stanković“

Потписани/а Amal Abdussalam Ali A. Hmaid

Изјављујем да је штампана верзија мог докторског рада истоветна електронској верзији коју сам предао/ла за објављивање на порталу **Дигиталног репозиторијума Универзитета у Београду**. Дозвољавам да се објаве моји лични подаци везани за добијање академског звања доктора наука, као што су име и презиме, година и место рођења и датум одбране рада. Ови лични подаци могу се објавити на мрежним страницама дигиталне библиотеке, у електронском каталогу и у публикацијама Универзитета у Београду.

Потпис докторанда

У Београду, _____



Прилог 3.

Изјава о коришћењу

Овлашћујем Универзитетску библиотеку „Светозар Марковић“ да у Дигитални репозиторијум Универзитета у Београду унесе моју докторску дисертацију под насловом:

ULOGA NO-SINTAZNOG PUTA U STRUKTURNOM REMODELIRANJU MIOKARDA PACOVA

(THE ROLE OF NO-SYNTHETIC PATHWAY IN STRUCTURAL REMODELING OF RAT MYOCARDIUM)

која је моје ауторско дело.

Дисертацију са свим прилозима предао/ла сам у електронском формату погодном за трајно архивирање.

Моју докторску дисертацију похрањену у Дигитални репозиторијум Универзитета у Београду могу да користе сви који поштују одредбе садржане у одабраном типу лиценце Креативне заједнице (Creative Commons) за коју сам се одлучио/ла.

1. Ауторство
2. Ауторство - некомерцијално
- 3. Ауторство – некомерцијално – без прераде**
4. Ауторство – некомерцијално – делити под истим условима
5. Ауторство – без прераде
6. Ауторство – делити под истим условима

(Молимо да заокружите само једну од шест понуђених лиценци, кратак опис лиценци дат је на полеђини листа).

Потпис докторанда

У Београду, _____